



FACILITY FORM 608

N66 37286  
(ACCESSION NUMBER)

116  
(PAGES)

CR-72069  
(NASA CR OR TMX OR AD NUMBER)

(THRU)

1  
(CODE)

06  
(CATEGORY)

# ELECTROCHEMICAL CHARACTERIZATION OF SYSTEMS FOR SECONDARY BATTERY APPLICATION

by

M. Shaw and A. H. Remanick

GPO PRICE \$ \_\_\_\_\_

CFSTI PRICE(S) \$ \_\_\_\_\_

Hard copy (HC) 3.00

Microfiche (MF) 1.00

ff 653 July 65

prepared for

NATIONAL AERONAUTICS AND SPACE ADMINISTRATION

CONTRACT NO. NAS 3-8509

FIRST QUARTERLY REPORT  
MAY-JULY 1966

WHITTAKER CORPORATION  
NARMCO RESEARCH AND DEVELOPMENT DIVISION  
3540 Aero Court  
San Diego, California 92123

#### NOTICE

This report was prepared as an account of Government sponsored work. Neither the United States, nor the National Aeronautics and Space Administration (NASA), nor any person acting on behalf of NASA:

- A.) Makes any warranty or representation, expressed or implied, with respect to the accuracy, completeness, or usefulness of the information contained in this report, or that the use of any information, apparatus, method, or process disclosed in this report may not infringe privately owned rights; or
- B.) Assumes any liabilities with respect to the use of, or for damages resulting from the use of any information, apparatus, method or process disclosed in this report.

As used above, "person acting on behalf of NASA" includes any employee or contractor of NASA, or employee of such contractor, to the extent that such employee or contractor of NASA, or employee of such contractor prepares, disseminates, or provides access to, any information pursuant to his employment or contract with NASA, or his employment with such contractor.

Requests for copies of this report should be referred to

National Aeronautics and Space Administration  
Scientific and Technical Information Division  
Attention: USS-A  
Washington, D. C. 20546

FIRST QUARTERLY REPORT

ELECTROCHEMICAL CHARACTERIZATION OF SYSTEMS  
FOR SECONDARY BATTERY APPLICATION

May - July, 1966

by

M. Shaw and A. H. Remanick

prepared for

NATIONAL AERONAUTICS AND SPACE ADMINISTRATION

August 17, 1966

CONTRACT NAS 3-8509

Technical Management  
Space Power Systems Division  
National Aeronautics and Space Administration  
Lewis Research Center, Cleveland, Ohio  
Mr. Robert B. King

NARMCO RESEARCH AND DEVELOPMENT DIVISION  
OF  
WHITTAKER CORPORATION  
3540 Aero Court  
San Diego, California 92123

## TABLE OF CONTENTS

	<u>Page</u>
Abstract	i
Summary	ii
I. Introduction	1
II. Interpretation of Cyclic Voltammograms	5
III. Results	12
A. Material Purification and Characterization	12
1. Solvent Purification and Characterization	12
2. Solute Purification and Characterization	19
B. Conductance	21
C. Analysis of Cyclic Voltammograms	23
D. Sweep Index - A Figure of Merit	80
E. Nature and Compatibility of Cathodes	83
IV. Experimental	86
A. Material Purification and Characterization	86
1. Distillation of Solvents	86
2. Vapor Phase Chromatography	87
3. Solution Preparation	87
B. Cyclic Voltammetric Measurements	90
1. Electrochemical Cell	90
2. Instrumentation	93
3. Measurement Procedure	95
V. Reference	99

## LIST OF FIGURES

<u>Figure</u>		<u>Page</u>
1.	Vapor Phase Chromatogram, Butyrolactone, Head Fraction	14
2.	Vapor Phase Chromatogram, MCB Propylene Carbonate	17
 <u>Cyclic Voltammograms</u>		
3.	Ag in Acetonitrile-LiClO <sub>4</sub>	37
4.	Cu in Acetonitrile-LiClO <sub>4</sub>	38
5.	Ag in Dimethylformamide-LiBF <sub>4</sub>	39
6.	Cu in Dimethylformamide-LiBF <sub>4</sub>	40
7.	Ni in Dimethylformamide-LiBF <sub>4</sub>	41
8.	Ag in Dimethylformamide-LiPF <sub>6</sub>	42
9.	Cu in Dimethylformamide-LiPF <sub>6</sub>	43
10.	Cu in Propylene carbonate-LiBF <sub>4</sub>	44
11.	Cu in Butyrolactone-LiClO <sub>4</sub>	45
12.	Cu in Butyrolactone-LiClO <sub>4</sub>	46
13.	Cu in Butyrolactone-LiClO <sub>4</sub>	47
14.	Ag in Butyrolactone-LiClO <sub>4</sub>	48
15.	Ag in Dimethylformamide-LiAlCl <sub>4</sub>	49
16.	Cu in Dimethylformamide-LiAlCl <sub>4</sub>	50
17.	Ag in Acetonitrile-LiPF <sub>6</sub>	51
18.	Cu in Acetonitrile-LiPF <sub>6</sub>	52
19.	Ag in Acetonitrile-LiBF <sub>4</sub>	53

<u>Figure</u>		<u>Page</u>
20.	Ag in Acetonitrile-LiBF <sub>4</sub>	54
21.	Cu in Acetonitrile-LiBF <sub>4</sub>	55
22.	Ni in Acetonitrile-LiBF <sub>4</sub>	56
23.	Cu in Dimethylformamide-LiCl	57
24.	Ag in Dimethylformamide-LiCl	58
25.	Ag in Propylene carbonate-LiAlCl <sub>4</sub>	59
26.	Ag in Propylene carbonate-LiAlCl <sub>4</sub>	60
27.	Cu in Propylene carbonate-LiAlCl <sub>4</sub>	61
28.	Cu in Propylene carbonate-LiAlCl <sub>4</sub>	62
29.	Ni in Propylene carbonate-LiAlCl <sub>4</sub>	63
30.	Ag in Dimethylformamide-AlCl <sub>3</sub>	64
31.	Ag in Dimethylformamide-AlCl <sub>3</sub>	65
32.	Cu in Dimethylformamide-AlCl <sub>3</sub>	66
33.	Ag in Butyrolactone-LiCl	67
34.	Cu in Butyrolactone-LiCl	68
35.	Cu in Butyrolactone-LiCl	69
36.	Ni in Butyrolactone-LiCl	70
37.	Ag in Acetonitrile-LiCl	71
38.	Ag in Acetonitrile-LiCl	72
39.	Ag in Propylene carbonate-AlCl <sub>3</sub>	73
40.	Ag in Propylene carbonate-AlCl <sub>3</sub>	74
41.	Cu in Propylene carbonate-AlCl <sub>3</sub>	75
42.	Silver oxide in Dimethylformamide-LiPF <sub>6</sub>	76

<u>Figure</u>		<u>Page</u>
43.	Copper oxide in Dimethylformamide-LiPF <sub>6</sub>	77
44.	Copper oxide in Dimethylformamide-LiPF <sub>6</sub>	78
45.	Nickel oxide in Dimethylformamide-LiPF <sub>6</sub>	79
46.	Measuring Cell for Cyclic Voltammetry	91
47.	Working Electrode Detail	92
48.	Block Diagram of Instrumentation	94

#### LIST OF TABLES

<u>Table</u>		<u>Page</u>
I.	Conductance Measurements (30°C)	22
II.	Electrochemical Systems Screened	24
III.	Sweep Index - Anodic	81
IV.	Sweep Index - Cathodic	82
V.	Reactions Involving Silver Electrode	84
VI.	Reactions Involving Copper Electrode	85
VII.	Vapor Phase Chromatography Conditions	88

# ELECTROCHEMICAL CHARACTERIZATION OF SYSTEMS FOR SECONDARY BATTERY APPLICATION

by

M. Shaw and A. H. Remanick

## ABSTRACT

Fifty-one electrochemical systems comprising silver, copper, and nickel in fluoride- or chloride-containing solvents such as butyrolactone, propylene carbonate, acetonitrile, and dimethylformamide, have been evaluated in a molecular level screening program using multi-sweep cyclic voltammetry. Chemical characterization of materials is in progress.

## SUMMARY

A program has been initiated involving the molecular level screening of electrochemical systems suitable for use in non-aqueous high energy density batteries. The term, molecular level, refers to those factors that determine the initial availability of electrochemical energy at the electrode-solution interface, contrasted with those factors at the plate level which determine the practical operation of the battery.

Solvent and solute purification and characterization studies were initiated. The solvents were purified by fractional distillation and characterized by vapor phase chromatography. Commercially available grades of solutes were dried and used without further analysis. Further characterization of the solutes is in progress.

Screening of the electrochemical systems was performed using the method of multisweep cyclic voltammetry. Silver, copper, and nickel electrodes were screened in butyrolactone, dimethylformamide, acetonitrile, and propylene carbonate solutions of  $\text{LiCl}$ ,  $\text{LiClO}_4$ ,  $\text{AlCl}_3$ ,  $\text{LiF}$ ,  $\text{LiPF}_6$  and  $\text{LiBF}_4$ , representing 51 electrochemical systems. With few exceptions, the cathodic reaction involved reduction of a solid product formed during the anodic sweep. In many cases this product was soluble in the solution under test. In nearly all cases, nickel gave extremely poor performance, most of the time due to failure to form an anodic reaction product.

An arbitrary parameter, the sweep index, serves as a relative figure of merit which can be assigned to any anodic or cathodic reaction, and gives an overall numerical comparison of the electrochemical systems in terms of reaction rate, electrode polarization, and coulombic efficiency.

## I. INTRODUCTION

The large number of electrochemical systems that can be considered for possible application in non-aqueous high energy density batteries, together with the variability of plate fabrication and its consequent effect on cell performance, involves the screening of thousands of combinations. Previous work (Ref. 1) has indicated that 30 solvent-solute systems exist having sufficient conductance to be considered as electrolytes for high energy density batteries. Using these electrolytes, the screening of 10 cathode materials comprising plates fabricated according to four types of binders, five variations of mix ratio, three sintering temperatures, three sintering times, and three values of plate compression, involves the testing of 162,000 combinations. This does not consider other determining factors of plate fabrication. It is apparent that a logical and systematic screening procedure is required to choose from the many electrode-electrolyte combinations those having the most promise for development into practical high energy density batteries.

The screening problem can be resolved by considering that even though the performance of any battery depends on a multitude of factors, they can all be grouped into the following:

### Molecular Level Factors

These are the kinetic factors related to the electrode processes that determine the initial availability of energy.

### Plate Level Factors

These are the structural factors necessary to the practical operation of the battery.

In essence, the initial release of energy is at the molecular level of the charge-transfer reaction and transport of reactive species. If the

electrons cannot be removed from the anode at a useable rate, and at the same time be taken up at the cathode at a useable rate, the system warrants no further consideration. The magnitude of the reaction rate constant, number of electrons involved in the charge transfer reaction, mass transfer effects, and magnitude of energy loss, are those factors at the molecular level which initially determine the availability of energy. An adequate molecular level screening procedure in addition to measuring these parameters should also furnish data on

actual reaction potential	charge-discharge efficiency
voltage stability	reaction complexity
anodic efficiency	side reactions
cathodic efficiency	solvent decomposition
	surface inhibition

Molecular level screening chooses those systems having the most desirable electrochemical properties. Whether these systems have any promise in an actual battery, can only be determined by a plate level screening program, since performance is greatly dependent on

plate porosity	pasting techniques
binder type	molding techniques
vehicle type	sintering conditions
mix ratio	material compatibility
surface availability	electrolyte volume
inert additives	resistivity
separator characteristics	cell case characteristics
cell fit	grid type

In order to properly screen an electrode-electrolyte combination, it is necessary to do so in the absence of such considerations as method of plate preparation, additives, separators, etc. In other words, the

screening must be done under conditions distinguishing those factors that determine the efficiency at the molecular level of the reaction from those imposed upon it by the requirements of plate composition. If this is not done, or if the screening is performed solely at the plate level, then an attempt to determine optimum plate conditions for those couples that do not possess the basic electrochemical requirements represents a wasted and futile effort. In addition, the elimination of desirable electrochemical couples is made possible because of the unfortunate choice of mix ratio, particle size, binder, or other variations. Preliminary screening at the molecular level permits the systematic and rapid elimination of the electrochemically-undesirable systems, so that a more thorough investigation of the promising systems can be made at the plate level.

#### Choice of a Molecular Level Screening Technique

The voltage sweep technique (also variously known as sweep voltammetry, triangular voltage sweep, linear potential scan voltammetry) is particularly suited to the electrochemical characterization of electrode-electrolyte systems in a molecular level screening program. Inherent in this single technique is the ability to obtain information as to the extent of electrode polarization, reaction potential, anodic and cathodic efficiency, charge-discharge efficiency, reaction complexity, solvent decomposition, surface passivation, and separation of individual discharge steps with their relative efficiency. Although the instrumentation is complex, the technique is simple and rapid - necessary requirements for a screening technique.

The measuring technique used in these studies will be referred to as Cyclic Voltammetry, inasmuch as it involves the characterization of systems for secondary battery application, so that a single voltammogram will exhibit both the anodic and cathodic reactions.

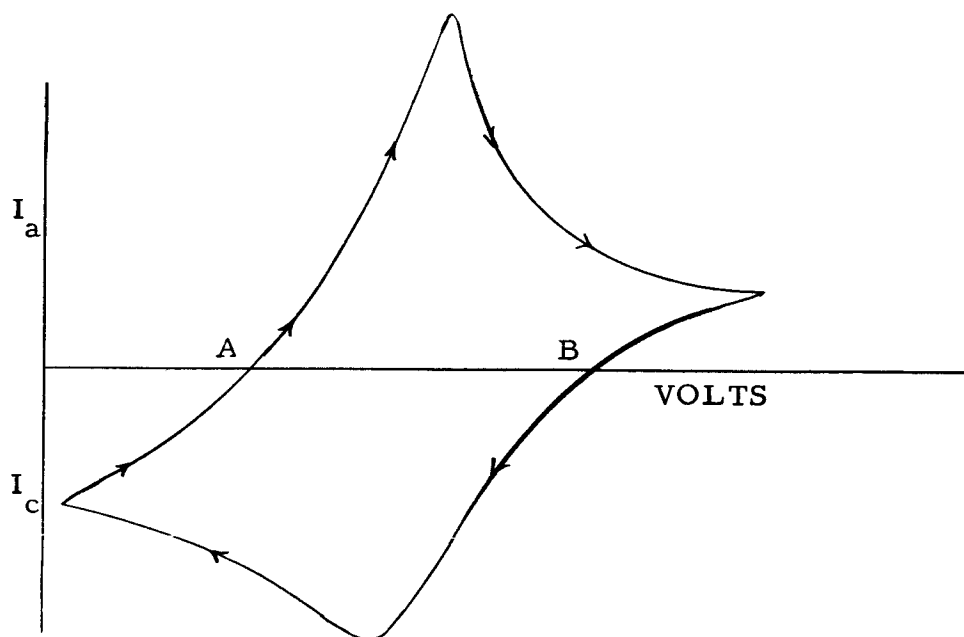
Simply described, linear sweep cyclic voltammetry is a procedure by which the voltage is varied continuously in a linear manner in an unstirred solution using a stationary microelectrode. Basically, a linearly varying voltage over a given range is applied between the working and reference electrodes. This voltage is a triangular function of time and is supplied by a function generator. Since the voltage applied to the cell varies linearly with time, the X-axis corresponds to either voltage or time units. Variations of the current flowing between the working and counterelectrodes are followed by means of a suitable recorder. The current-voltage (current-time) curve is characterized by peaks resulting from the opposing effects of increasing rate of electron transfer and depletion of the electroactive species. With appropriate instrumentation, the sweep rate (rate at which the applied voltage changes) can be varied over any desired range. This allows interpretation of the curves in terms of both reaction and diffusion rates at various applied voltages and scan rates. The processes can be separated as to type by comparison of the area under the current-time plots as a function of sweep rate. Information regarding the mechanism of the various processes can be derived from the slope of the current rise. Integration of the areas enclosed by the peaks gives a measure of depth of material conversion, while comparison of the anodic and cathodic peak areas gives the charge-discharge efficiency. Decomposition of the solvent is made evident by the appearance of peaks due to solvent oxidation or reduction.

## II. INTERPRETATION OF CYCLIC VOLTAMMOGRAMS

Cyclic voltammetry has been extensively used in electroanalysis and the determination of reaction mechanisms for the oxidation and reduction of soluble species, both organic and inorganic. Mathematical relationships have been derived relating the electrode kinetic parameters of such systems. Nicholson and Shain (Ref. 2) review developments in this area, and have extended the theory to include additional kinetic cases (Refs. 2-5). Mathematical relationships, relating peak potential and peak current as a function of sweep rate in characterization of the reaction kinetics, have been developed for the mercury electrode only. Cyclic voltammetric data have been qualitatively analyzed for platinum electrodes in the case of the electro-oxidation of organic compounds (Refs. 6-14).

The theoretical derivation of kinetic relationships in the case of consumable electrodes, or electrodes forming insoluble oxidation products, as for those systems of interest to battery application, is an almost impossible task. The changing nature of the electrode surface, and the formation of semiconducting layers make even a qualitative analysis more difficult than for the soluble species - platinum systems. Nevertheless, the cyclic voltammetric method serves as a valuable tool for the rapid screening of electrochemical systems in evaluating their possible use in non-aqueous battery systems, as past work in this laboratory has proven.

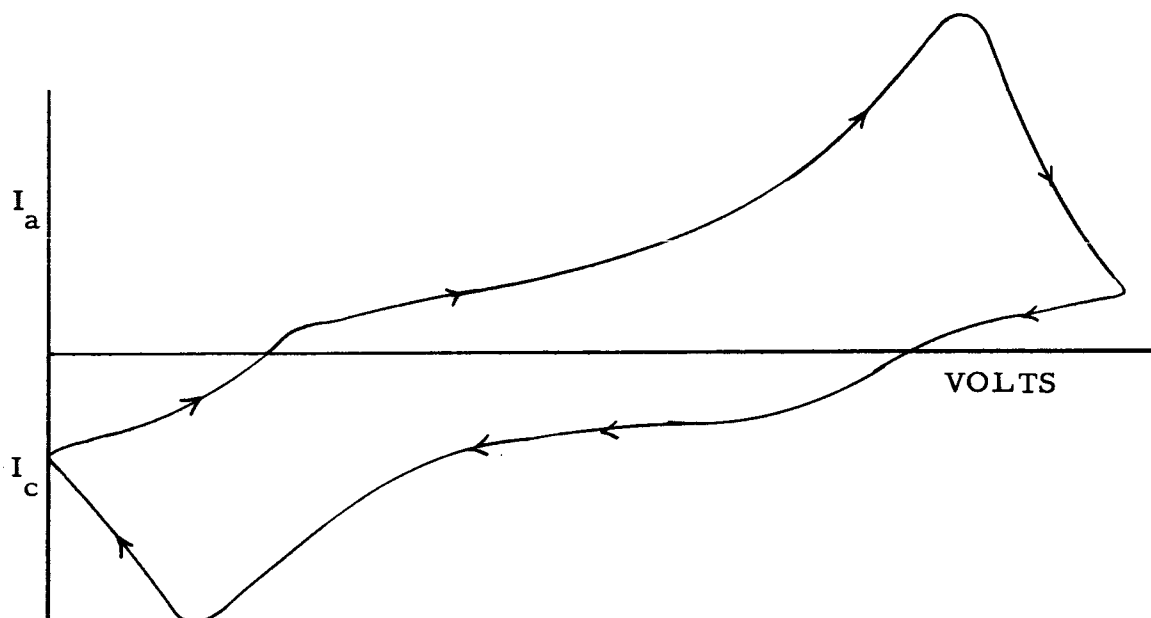
The sweep curves will take different shapes according to the type of polarization present, and the rate at which the potential is scanned. In the case of concentration polarization where the electrode reaction is diffusion limited (mass transfer process) the curve will resemble the following at moderate sweep rates (e.g. 4 mv/sec):



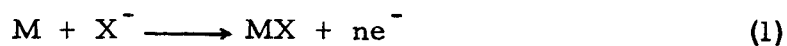
In this and all following curves,  $I_a$  is the anodic current (above the zero-current axis), and  $I_c$  is the cathodic current (below the zero-current axis). The scan is in a clockwise direction, with the potential becoming more anodic (positive) towards the right. The sweep curve indication of concentration polarization is characterized by having the peak currents at close to the same potential, and the peak currents being proportional to the bulk concentration as well as to the square root of the sweep rate. For a homogeneous reversible reaction, the peak potential (the potential corresponding to the peak current) depends only on the polarographic half-wave potential. Where a solid product is involved, however, the peak potential is a function of concentration. In addition, stirring greatly increases the current. Increasing the sweep rate has the effect of increasing the distance between points A and B at which the forward and return portions of the curve cross the zero-current axis.

If concentration polarization is accompanied by activation polarization, (charge transfer process) the peak potentials will be separated by a greater

distance, this distance increasing with increasing sweep rate. In the case of extreme activation polarization, a typical sweep curve would resemble the following:



An ideal battery plate is one which involves oxidation of the metal to an insoluble compound according to the reaction



All metals forming insoluble compounds on oxidation passivate to some extent, with the degree of passivation being dependent upon the solid state properties of the film. As  $M$  is converted to  $MX$ , either the  $X^-$  ion must migrate across the film to the metal and react with it, or the metal ion must migrate across the film to the solution to be neutralized by the  $X^-$  ion. Modern theoretical studies in fact favor the latter concept as the general case, in that the charged species migrates across the film to the solution interface by means of lattice defect vacancies present

within the film. This amounts to transfer of charged particles through a conductor (or in most cases, a semiconductor) and therefore acts similar to a resistance in series with the chemical reaction. The effective resistance of the layer (transfer resistance) can be described in terms of the average film thickness and the number of charge carriers (or defect sites) per unit volume according to

$$\eta_s = i r d \quad (2)$$

where  $\eta_s$  is the voltage loss across the film,  $i$  is the current density in amps/cm<sup>2</sup>,  $d$  is the film thickness in cms., and  $r$  is the film resistivity in ohm-cms. The film thickness is a function of time and current density according to

$$d = d_0 + \beta \int_0^t i \, dt \quad (3)$$

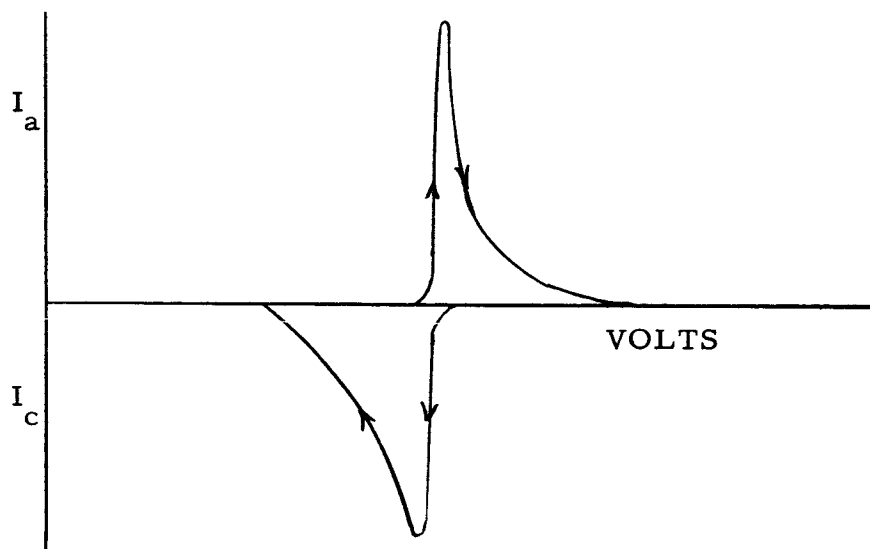
$\beta$  can be evaluated from the molar volume of the compound and the Faraday constant, and has the dimensional units, cm<sup>3</sup>/amp-sec. Ideally  $d_0$  should be zero at zero time, but the term is included since a film may be initially present. Derivation of equation (3) assumes the number of charge carriers to be constant.

Transfer resistance is a more complex parameter than solution resistance, due to the uncertain nature of the charge carriers within the film. Different phases of the same material may have differing semiconductor properties, so that the number of charge carriers may also be a function of the current density and time (total charge).

Combining equations (2) and (3) results in an expression for the polarization due to film transfer resistance

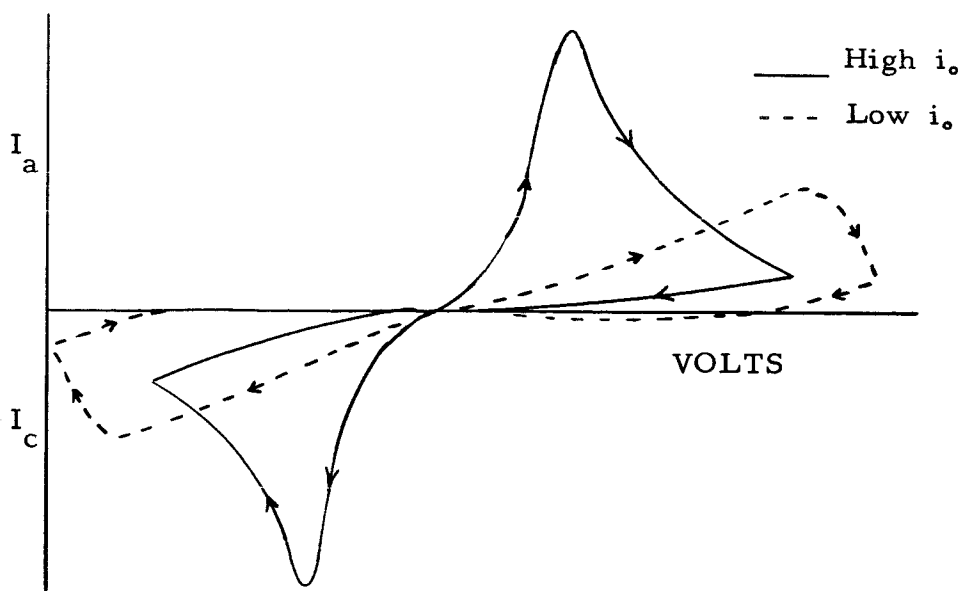
$$\eta_s = i r (d_0 + \beta \int_0^t i \, dt) \quad (4)$$

Where the current is limited by the thickness of the MX layer, the following sweep curve would be obtained



As the sweep rate is increased, the width of the peak increases. Although stirring would have no effect, a change in  $X^-$  concentration might. The coulombs under each peak however would remain equal.

In the case of a solid state reaction accompanied by activation polarization, the following curve will result in which the solid curve represents a higher exchange current than the broken curve:



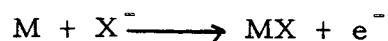
The effect of concentration polarization on the above curve is again to increase the separation of the points at which the forward and return portions of the curve cross the zero-current axis.

For small values of  $\beta \int_0^t i \, dt$ , the mass transfer and charge transfer processes control the ascending portion of the current-voltage curve. The slope of this portion of the curve will be a function of the relative contribution of these processes. In addition, because these are independent of time, the ascending portion will be independent of the sweep rate. When  $\beta \int_0^t i \, dt$  becomes large, it controls the shape of the curve. The current must then decrease in a manner such that

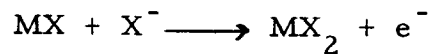
$$i \approx \frac{k}{t \left(1 + \frac{r\beta}{\sqrt{\phantom{x}}} k\right)^{1/2}} \quad (5)$$

where  $k$  is an integration constant. Equation (5) shows that the current in the descending portion of the current-voltage curve is a function of the sweep rate,  $\sqrt{\phantom{x}}$ . With increasing sweep rate, the current will increase, and in those cases where the electrode reaction is diffusion limited, the peak current is proportional to the square root of the sweep rate.

For reactions involving transfer of more than a single electron, multiple peaks will be evident under certain conditions. Thus, if the reaction  $M + 2X^- \longrightarrow MX_2 + 2e^-$  occurs as written, only one peak would be observed. However, if the reaction occurs according to



followed by



then two distinct peaks would be observed. A peak is therefore observed for each charge transfer step, with the characteristics of each peak depending upon the individual mechanism.

### III RESULTS

#### A. Material Purification and Characterization

In order to obtain meaningful results from the sweep measurements, it is important to identify all components in the materials used in the study, and to remove whenever possible, any impurities having a contributory effect on data interpretation. Since a priori, one does not know the effect of an impurity, it would be desirable to remove all impurities. In certain cases, however, such removal becomes extremely arduous, and possibly self-defeating. In such cases, if the impurity is identifiable, it may be more advisable to add known amounts of the impurity and characterize their effect on the cyclic voltammogram. The present program will nevertheless endeavor to present data derived from materials that are as pure as practically possible, and are as well-characterized as standard analysis permits. It should be emphasized that characterization of some of the materials screened during this first quarter is not complete. This has been due in part to lack of complete instrumentation (e.g. appropriate columns for vapor phase chromatography), and to the fact that some commercially available materials are of doubtful composition due to inherent instability. Until these materials are thoroughly characterized, interpretation of the sweep data will be qualified until repeat measurements are made for those systems of immediate interest.

The following sections detail the purification and/or characterization schemes used in this phase of the work.

##### 1. Solvent Purification and Characterization

The solvents studied during this period were dimethylformamide, butyrolactone, acetonitrile, and propylene carbonate. Inspection

of the literature indicated that a reasonable purification-characterization scheme was fractional distillation through an efficient column followed by vapor phase chromatography (VPC). The present stage of this purification-characterization scheme, together with some storage stability data for each solvent is given below.

a. Butyrolactone

Matheson, Coleman and Bell, b.p. 91-93°C/17 mm

This material showed water ( $\sim 0.1$  mole %) as the only impurity by VPC analysis on a polyethylene glycol (PEG) 1540 column. The butyrolactone was fractionally distilled through a 3-foot column at 80°C/10 mm. Four cuts were taken, the first two comprising about 10% of the total volume. VPC's of the latter two fractions showed no impurities. VPC of the first fraction, however, (Figure 1) showed two additional impurities (0.2 mole % and 0.3 mole %) close to the main peak. These impurities were also present in the second fraction to a lesser extent. Inspection of Figure 1 indicated that the type of resolution afforded by the PEG column would only allow determination of those impurities in concentrations of greater than about 0.05 mole %. Although the possibility existed that the supposedly pure main fraction contained 0.05 mole % of unknown impurities, it was evident these impurities were readily concentrated in the head cuts. Therefore, until other VPC columns are received and the resolution of the impurities improved, a relatively large head cut will be taken to insure removal of the unknown impurities from the main fraction of distilled butyrolactone. VPC analysis

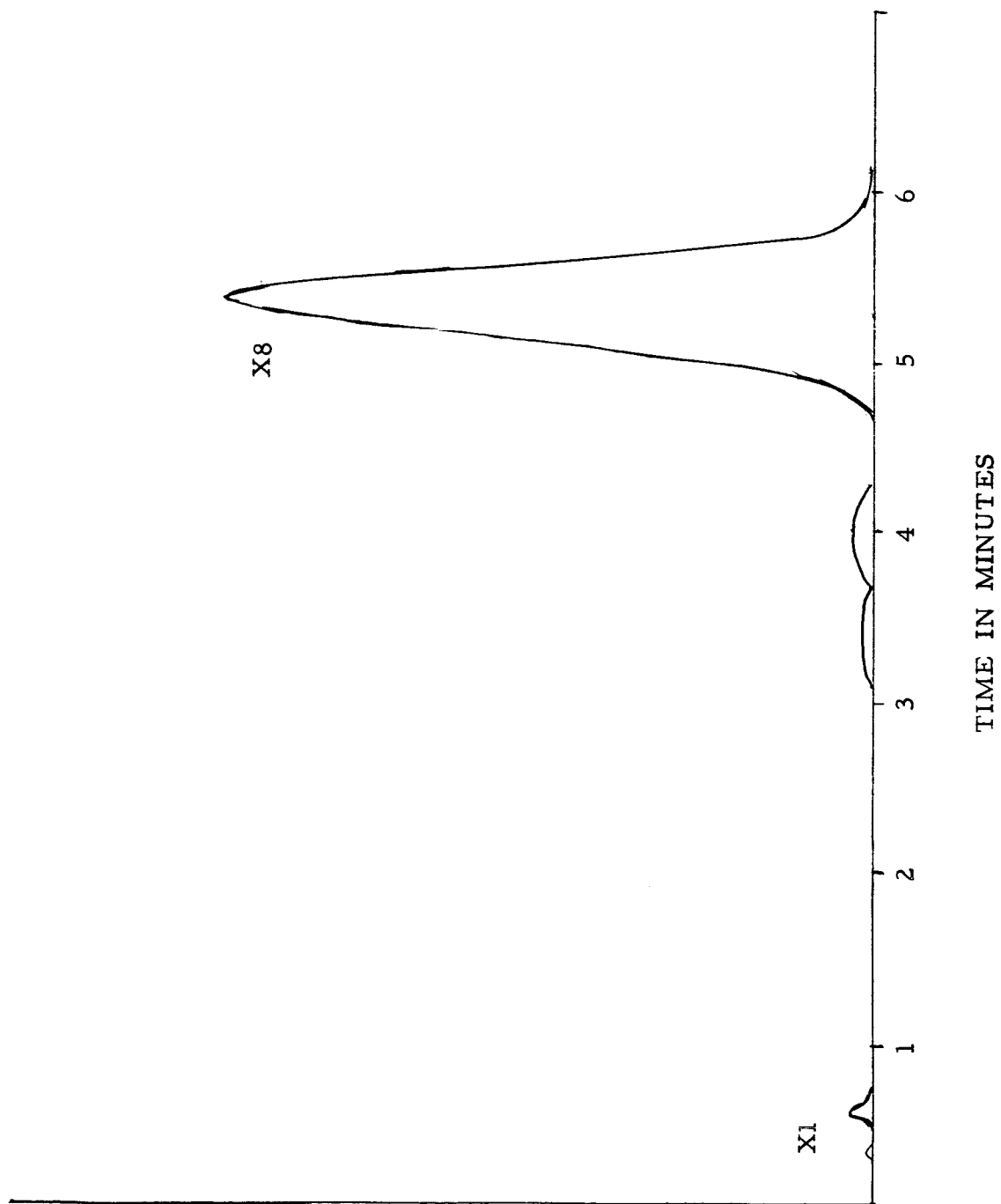


Figure 1 Vapor Phase Chromatogram, Butyrolactone, Head Fraction

of butyrolactone (main fraction) stored in glass bottles showed no change after two weeks.

b. Dimethylformamide

Matheson, Coleman and Bell. Spectroquality grade

This material was subjected to VPC analysis on a PEG 1540 column. No impurities were detected under conditions where as little as 0.01 mole % water would have been evident. Distillation of dimethylformamide at 80°C/40 mm yielded material showing no impurities of any of the fractions by VPC analysis. It therefore appeared unnecessary to distill dimethylformamide, and subsequent solution preparation was accomplished using "as received" material.

c. Acetonitrile

Matheson, Coleman and Bell, b.p. 80.5-82.5°C

This material was distilled at 80°C through a 3-foot column. VPC analysis on a PEG 1540 column was not successful (with respect to resolution of water) since the large acetonitrile peak obscured possible small quantities of water. Furthermore, suspected impurities such as acrylonitrile and propionitrile were not indicated. In order to facilitate measurements, a middle fraction of acetonitrile was used for solution preparation.

Recently, another grade of acetonitrile has been received (Matheson, Coleman and Bell, chromatquality). VPC analysis of this specific lot by Matheson, Coleman and Bell

on 3, 3' - iminodipropionitrile column showed acrylonitrile (0.15%) as the only impurity. Since no information concerning the resolution of water on this column was indicated, complete characterization of acetonitrile will only be made when a VPC column capable of determining trace amounts of water is found.

d. Propylene Carbonate

Matheson, Coleman and Bell, b. p. 108-110°/10 mm

This was subjected to VPC analysis on a PEG 1540 column (Ref. 15). The material showed five peaks in addition to the air peak (Figure 2). The first peak probably contained both air and carbon dioxide, but resolution of these components under the conditions employed was not possible. The second peak (probably propylene oxide) was 0.22 to 0.25 mole %. The third peak, identified as water by peak enhancement techniques, was 0.02 to 0.03 mole %. The fourth peak, as yet unexplained, was usually 0.015 to 0.02 mole %. The fifth peak, tentatively identified as propanediol by boiling point considerations, usually comprised 0.16 to 0.25 mole %. The sixth peak corresponded to propylene carbonate. The indicated variation was between various lots of "as received" propylene carbonate. Distillation of propylene carbonate at 109°/10 mm. followed by VPC analysis indicated that the impurities corresponding to the fourth and fifth peaks were removed. The amount of propylene oxide was reduced to 0.01 - 0.02 mole %, while the amount of water was 0.015 - 0.025 mole %. The variations in the amount of these impurities did not

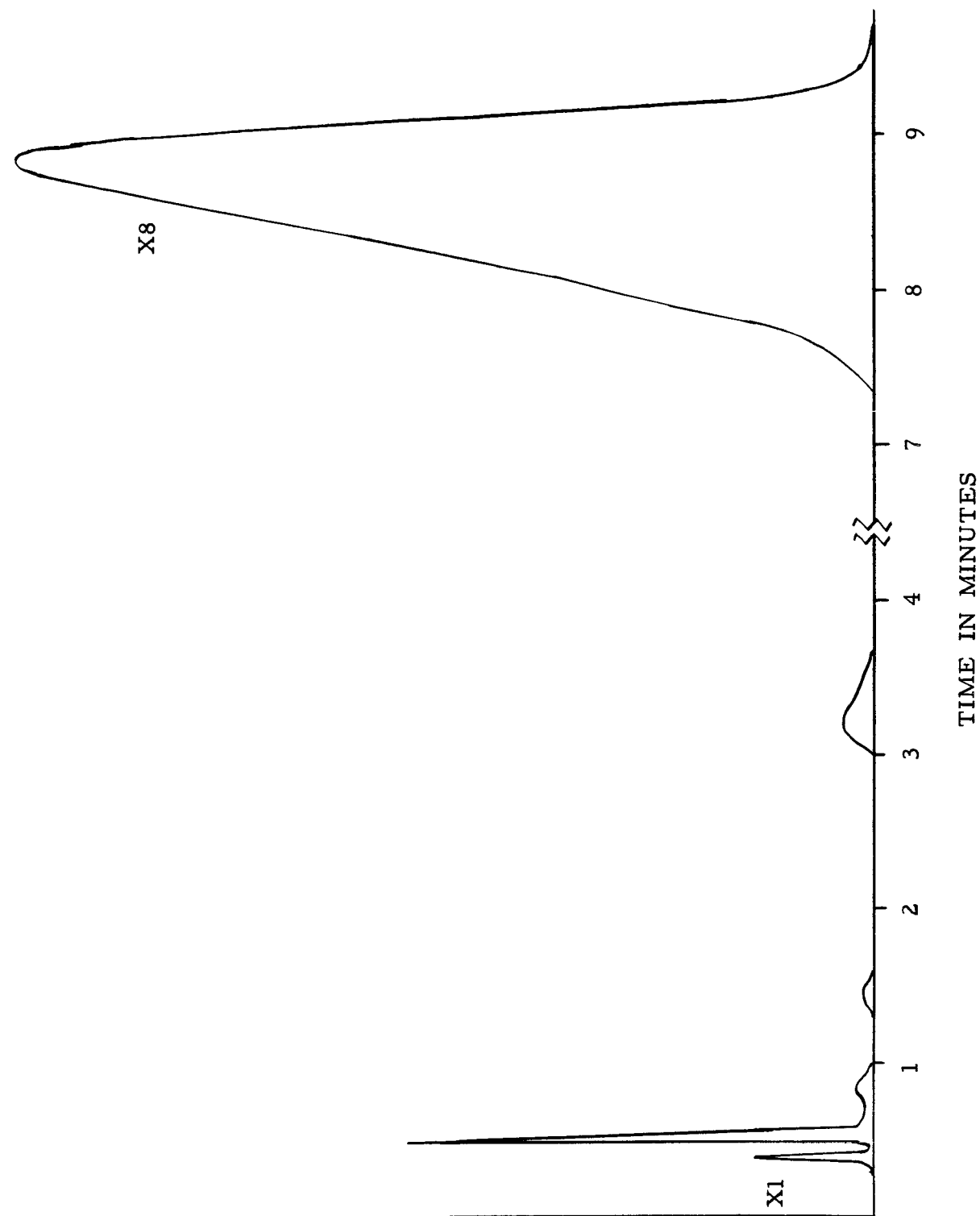


Figure 2 Vapor Phase Chromatogram, MCB Propylene Carbonate

occur between samples obtained in a single batch distillation (neglecting the head cuts which were discarded) but were obtained between the main cuts of separate distillations. Alteration of such factors as reflux ratio (100:1 to 25:1) produced no change (within analytical limits) in the amounts of propylene oxide or water. It therefore appears that some unobserved variation in distillation technique produces a small change in the amounts of residual impurities.

It is interesting to note that the amount of water in certain samples apparently showed a small increase (beyond analytical limits) with respect to the "as received" material. This fact of "reverse" concentration cannot be explained at this time.

Some preliminary data were obtained on the storage stability of distilled propylene carbonate. It appears that a marked decrease (0.019 mole % to less than 0.01 mole %) occurs in the amount of propylene oxide, whereas only a small decrease (0.028 mole % to 0.025 mole %) in the amount of water occurs. The decrease in propylene oxide may be attributed to a simple vapor phase transition. Since the change in water content was within analytical limits, no definitive statements with respect to the stability of propylene carbonate can be made at this time. On the other hand, it is rather difficult to envision any reasonable chemical scheme which would increase the amount of water upon storage at room temperature. Therefore, any increase in the amount of water on standing would probably be due to improper storage.

## 2. Solute Purification and Characterization

The purification of the inorganic solutes during this initial phase of the program was largely confined to the elimination of water. Investigation of cationic and anionic impurities was not performed at this time. As will become evident, however, most of the solutes used during this quarter could be obtained in reasonable purities without detailed purification. Characterization of these salts will be detailed in a later report.

- a. Lithium fluoride (J. T. Baker, Reagent grade, 0.1% sodium, 0.2% potassium as the main impurities) was dried at 110°C for 48 hours. Under these conditions there is some possibility of hydrolysis (by trace moisture) to lithium hydroxide and hydrogen fluoride. The hydroxide was not expected to interfere with the measurements. Since the lithium fluoride-hydrogen fluoride complex is unstable even at room temperature, contamination due to hydrogen fluoride is not expected.
- b. Magnesium fluoride (Research Inorganic Chemical Co., 99%) was dried at 110°C for 48 hours. The primary impurity expected was magnesium oxide which is essentially insoluble in organic solvents. Since hydrogen fluoride (possibly formed by hydrolysis) does not form a complex with magnesium fluoride, no acidic contamination is expected.
- c. Lithium fluoride-magnesium fluoride mixture was prepared from an equimolar mixture of the dried salts by dry mixing.
- d. Lithium chloride (J. T. Baker reagent grade, 0.2% sodium, 1.0% water as the primary impurities) was dried at 110°C

for 48 hours. Possible hydrolysis under these conditions would leave a small amount of lithium oxide in the material. It was felt that the lithium oxide, because of its insolubility, would not affect the electrochemical reaction (except to act as a partial water scavenger for the solvents).

- e. Magnesium chloride (Research Inorganic Chemical Co., 98%) was dried at 125°C for 48 hours. This temperature was chosen since the literature indicated complete dehydration would occur under these conditions. The major impurity was undoubtedly magnesium oxide, formed during the initial dehydration of the hexahydrate by the manufacturer and during removal of trace moisture in this laboratory. No deleterious effects were expected from the introduction of this material into the solution.
- f. Magnesium chloride-lithium chloride mixture was prepared from equimolar quantities of dried salts by dry mixing.
- g. Aluminum chloride (Matheson, Coleman and Bell - anhydrous reagent grade) was slowly heated to 105°C to volatilize trace amounts of water and/or to react the water with aluminum chloride to yield alumina and hydrogen chloride. Both of these materials would be expected to appear in the electrolyte, the former because of its insolubility in organic solvents and the latter by simple volatilization under the conditions specified.
- h. Lithium chloride-aluminum chloride was prepared in situ from dried salts (see Experimental section).

- i. Lithium perchlorate (Research Inorganic Chemical Co., anhydrous) was dried at 160°C for 72 hours. It is suspected that these conditions did not afford complete removal of water (Ref. 16).
- j. Lithium hexafluorophosphate (Ozark Mahoning, unspecified grade) was used in the "as received" conditions. No purification was attempted at this time since the critical evaluation of data obtained using this solute is expected to be obtained from lithium hexafluorophosphate prepared in situ. However, for the initial screening purposes, it was useful to have some measure of effect of this salt in the electrochemical systems. In addition to lithium fluoride and water, the salt may have contained anions corresponding to partial hydrolysis of the hexafluorophosphate moiety. Purification by simple heating would be expected to remove some of these materials, but would lower the hexafluorophosphate content by dissociation of the salt to lithium fluoride and phosphorous pentafluoride.
- k. Lithium tetrafluoroborate (Ozark Mahoning - unspecified grade) was used in the "as received" conditions for reasons similar to those described for the hexafluorophosphate salt.

B. Conductance

As part of the screening program previously outlined, it was felt that electrolytes having a conductance of less than  $5 \times 10^{-4} \text{ ohm}^{-1} \text{ cm}^{-1}$  would be of little value for future cell preparation. Therefore, conductance measurements were made on all solutions. Those solutions showing conductivity below the indicated limit (except for lithium chloride) were not subjected to electrochemical screening.

Furthermore, investigation of the literature (Ref. 1) indicated some of the systems initially considered for screening would possess insufficient conductance. No solutions were prepared for these systems. The conductance of all systems investigated is given in Table I

TABLE I CONDUCTANCE MEASUREMENTS (30°C)

<u>Electrolyte</u>	<u>Conductance*</u>
AN-LiF	$1.4 \times 10^{-5}$
AN-MgF <sub>2</sub>	$2.6 \times 10^{-4}$
AN-LiF+MgF <sub>2</sub>	$1.0 \times 10^{-4}$
AN-LiClO <sub>4</sub>	$2.7 \times 10^{-2}$
AN-LiPF <sub>6</sub>	$2.8 \times 10^{-3}$
AN-LiBF <sub>4</sub>	$2.5 \times 10^{-3}$
AN-LiCl	$4.2 \times 10^{-4}$
BL-LiClO <sub>4</sub>	$1.1 \times 10^{-2}$
BL-LiCl	$8.2 \times 10^{-4}$
BL-AlCl <sub>3</sub>	$2.9 \times 10^{-5}$
BL-LiCl+AlCl <sub>3</sub>	$8.1 \times 10^{-4}$
DMF-LiClO <sub>4</sub>	$1.3 \times 10^{-2}$
DMF-LiPF <sub>6</sub>	$1.7 \times 10^{-2}$
DMF-LiBF <sub>4</sub>	$2.6 \times 10^{-2}$
DMF-LiCl	$1.8 \times 10^{-3}$
DMF-AlCl <sub>3</sub>	$1.5 \times 10^{-3}$
DMF-LiCl+AlCl <sub>3</sub>	$7.2 \times 10^{-3}$
PC-LiClO <sub>4</sub>	$2.8 \times 10^{-2}$
PC-LiPF <sub>6</sub>	$5.7 \times 10^{-3}$
PC-LiBF <sub>4</sub>	$2.6 \times 10^{-2}$
PC-LiCl+AlCl <sub>3</sub>	$1.6 \times 10^{-3}$

\* ohm<sup>-1</sup> - cm<sup>-1</sup>

AN= acetonitrile      DMF= dimethylformamide  
BL= butyrolactone    PC= propylene carbonate

### C. Analysis of Cyclic Voltammograms

Table II lists the 51 electrochemical systems that have been screened by the method of cyclic voltammetry during the first quarter of this program. As described in the Experimental section, triplicate measurements were made at varying sweep rates and techniques so that a few hundred curves were obtained during this period. The curves included in this report were chosen on the basis of two sweep rates, high and low (either 200 and 20 mv/sec, or 400 and 40 mv/sec) and at 30°C for nearly all cases. Each sweep curve has been given a number, preceded by the prefix CV (Cyclic Voltammogram). The zero reference voltage represents the open circuit potential of the working electrode with respect to the indicated reference electrode (either Zn or Pt). In all cases, a silver counterelectrode was used. The voltage axis units are relative to the open circuit potential equal to zero, so that voltage units are in terms of electrode polarization.

For comparative purposes the magnitude of current density is classified as follows

<u>Range</u>	<u>Relative Magnitude</u>
Less than 1 ma/cm <sup>2</sup>	very low
1 - 10 ma/cm <sup>2</sup>	low
10 - 50 ma/cm <sup>2</sup>	medium low
50 - 100 ma/cm <sup>2</sup>	medium high
100 - 300 ma/cm <sup>2</sup>	high
More than 300 ma/cm <sup>2</sup>	very high

#### 1. Acetonitrile - LiClO<sub>4</sub> (Cyclic Voltammograms start on page 37)

Figure 3 shows the cyclic voltammogram for silver in this electrolyte, recorded at 200 mv/sec. The system exhibits

TABLE II ELECTROCHEMICAL SYSTEMS SCREENED

<u>Solvent</u>	<u>Solutes</u>					
	$\frac{\text{AlCl}_3}{-}$	$\frac{\text{LiAlCl}_4}{-}$	$\frac{\text{LiBF}_4}{-}$	$\frac{\text{LiCl}}{-}$	$\frac{\text{LiClO}_4}{-}$	$\frac{\text{LiPF}_6}{-}$
Butyrolactone	-	a	-	a	a	-
Acetonitrile	-	-	a	a	a	a
Dimethylformamide	a	a	a	a	a	a, b
Propylene Carbonate	a	a	a	-	-	-

a - Ag, Cu, and Ni

b - Oxides of Ag, Cu, and Ni electrodes

a medium high anodic current density not reaching a peak in the 0.5 v. range, and a medium high cathodic peak current density.

Decreasing the sweep rate has the effect of eliminating the cathodic reaction. Thus at 20 mv/sec the cathodic peak c.d. is  $7.6 \text{ ma/cm}^2$  compared with  $67.0 \text{ ma/cm}^2$  at 200 mv/sec. At 2 mv/sec no cathodic current is evident at the same recorder sensitivity. The effect of sweep rate on anodic current is only slight, such that at 0.5 v. the anodic current densities are as follows:

<u>mv/sec</u>	<u>ma/cm<sup>2</sup></u>
200	148
20	139
2	130

Discoloration of the solution indicates that the silver oxidation product is soluble in the electrolyte. The marked effect of sweep rate on the cathodic current is understandable if the cathodic reaction represents reduction of a solid product at the electrode. If the cathodic reaction involved reduction of silver ions in solution no such pronounced effect by sweep rate would be evident, since a sufficient amount would be available for reaction. If, however, the cathodic reaction involved reduction of a solid state product, then at slower sweep rates more of the anodic product has had time to dissolve, resulting in less material available for reduction. At sufficiently slow sweeps, little or none is left at the electrode for the discharge reaction. The effect of sweep rate on the height of the cathodic peak can therefore serve as a measure of cathode solubility.

The copper electrode in acetonitrile -  $\text{LiClO}_4$  is characterized by a very high and sharp anodic peak (Figure 4). The rapid rise of anodic current to a high value indicates that the oxidation reaction has a high rate constant (very low activation polarization), such that passage of current to the extent of  $579 \text{ ma/cm}^2$  causes a polarization of less than 0.2 volts. Unfortunately, the discharge (cathodic) reaction is accompanied by excessive activation polarization, 0.9 volts polarization to pass a current density of  $193 \text{ ma/cm}^2$ . No concentration polarization is evident.

In the case of nickel, current densities are considerably below  $0.1 \text{ ma/cm}^2$ /cm current axis and not distinguishable from acetonitrile alone. No anodic (and therefore no cathodic) reaction occurs for Ni in this electrolyte.

## 2. Dimethylformamide - $\text{LiBF}_4$

Figure 5 shows the CV for silver in this electrolyte. Very high anodic and cathodic currents are obtained, with the former being larger and peaking out just at the +1.0 volt level. As for the case of Ag in acetonitrile -  $\text{LiClO}_4$ , the cathodic peak at lower sweep rates is much lower, and non-existent at 2 mv/sec, indicating that the cathodic reaction involves reduction of a solid anodic product soluble in the electrolyte. This system has a greater amount of concentration polarization than does Ag in the former electrolyte.

The CV for copper is shown in Figure 6, in which two anodic peaks occur close together, the second being accompanied by a greater degree of activation polarization. On continued cycling, these two peaks become smaller and indistinguishable. The

cathodic reaction consists of reduction of the two oxidation states, with the higher state reaction being more irreversible. Again, the cathodic reaction involves reduction of a solid anodic product, as shown by the effect of decreasing the sweep rate. Dissolution of the anodic product was observed.

Nickel in dimethylformamide -  $\text{LiBF}_4$ , (Figure 7), is characterized by a very low anodic peak current density, excessive activation polarization for the cathodic reaction, and the absence of concentration polarization.

3. Dimethylformamide -  $\text{LiPF}_6$

The CV for silver in this electrolyte is shown in Figure 8. The anodic and cathodic reactions occur at close to the same potential indicating a relatively reversible system. Since this potential is anodic to the zero reference point, the anodic scan was insufficient to permit the much larger anodic currents that certainly would have occurred. In this and other cases involving complex fluorides, the cathodic peak occurred considerably anodic to the zero reference point. The initiation of reaction just at the voltage where the scan was reversed prompted the decision to extend the scan range. Disappearance of the cathodic current with decreasing sweep rate indicated that the discharge reaction involved reduction of a solid phase material.

Figure 9 shows the cyclic voltammograms for copper at 200 and 20 mv/sec. This illustrates the effect of sweep rate on the cathodic peak height as described above, as indicating that the cathodic reaction represents discharge of the solid anodic product formed during the anodic scan. Again, oxidation product dissolution was observed, in addition to copper plating out at the counterelectrode. As before, no cathodic current was evident at 2 mv/sec.

Nickel showed current densities less than the minimum  $0.1 \text{ ma/cm}^2/\text{cm}$  current axis.

4. Propylene Carbonate -  $\text{LiBF}_4$

The CV for copper is shown in Figure 10. Again, high anodic currents are obtained, but no peak is reached in the 0.5 v range. Similar to dimethylformamide -  $\text{LiPF}_6$ , the anodic and cathodic reactions occur near the same potential.

Decreasing the sweep rate showed that discharge of a solid product was involved. The observed dissolution of the oxidation product again confirmed the effect of decreasing the sweep rate.

Silver exhibited much lower currents than copper, and resembled the CV shown in Figure 8. The effect of decreasing the sweep rate indicated reduction of a solid phase.

Nickel electrodes exhibited anodic current densities of  $8 \text{ ma/cm}^2$  (at +0.5 v.) but zero cathodic current up to -0.5 v. indicating no discharge reaction within this voltage range.

5. Dimethylformamide -  $\text{LiClO}_4$

All electrodes (Ag, Cu, Ni) gave poor performance in this electrolyte. The anodic reaction for silver initiated near the +0.5 v. level, so that only a slight amount of oxidation product was available for reduction, which occurred at a potential close to the anodic reaction. Both copper and nickel gave current densities below the acceptable minimum, with nickel showing solvent background only.

6. Butyrolactone -  $\text{LiClO}_4$

Cyclic voltammograms for copper were obtained at 400 mv/sec. These are shown in Figures 11 and 12. The anodic and cathodic

peak heights are approximately equal in Figure 11, but the cathodic peak height is more than double that of the anodic peak in Figure 12, which represents a repeat run obtained after replacing the electrode and electrolyte with fresh materials. Continued cycling resulted in greater cathodic currents with observed dissolution of oxidation product. The cathodic current eventually increased sufficiently large to overload the power amplifier. Figure 13 shows the CV for copper at the much lower sweep rate of 40 mv/sec. This CV was obtained with a third sample immediately following a 400 mv/sec sweep exhibiting a cathodic peak current density of 70 ma/cm<sup>2</sup>. The new peak of 64 ma/cm<sup>2</sup> for 40 mv/sec indicates that decreasing the sweep rate had only little effect on cathodic peak height. This, together with the observation of anodic product dissolution suggests that the cathodic peak results from the discharge of dissolved copper species.

Silver exhibited the same effect as copper. Silver dissolution is apparent, and cycling increases the cathodic current density. Such large currents were obtained at 400 mv/sec, that it was necessary to record the data at 40 mv/sec (Figure 14).

Nickel exhibited current densities less than the minimum (0.1 ma/cm<sup>2</sup>/cm).

7. Dimethylformamide - LiAlCl<sub>4</sub>

The CV for silver (Figure 15) is complex, although all peaks are reproducible. Whatever the nature of the anodic reactions, the first cathodic reaction is characterized by a sharp peak indicating a highly reversible reduction.

Copper (Figure 16) shows high currents with no anodic peak in the 0.5 v. range. Copper plating at the counterelectrode was observed indicating dissolution of anodic product. A smaller peak at 20 mv/sec and none at 2 mv/sec indicates discharge of solid anodic product.

Although nickel exhibits measureable anodic currents, no cathodic reaction was evident in this electrolyte.

8. Acetonitrile - LiPF<sub>6</sub>

Silver (Figure 17) exhibited a very high anodic current not reaching a peak in the 0.5 v. range, as well as a high cathodic current occurring close to the anodic potential. No cathodic current is evident at 20 and 2 mv/sec indicating rapid anodic product dissolution. Silver whiskers were deposited at the counterelectrode.

Copper (Figure 18) gave a very high anodic peak with minimal activation polarization. A double cathodic peak is observed, although only a single anodic peak was evident. On completion of the descending slope of the anodic peak, the current remains low and constant for the remainder of the anodic range (in the forward and reverse direction) and only increases when the cathodic reaction begins. This is indicative of the absence of any other oxidizable species, as well as the complete absence of concentration polarization. This type of anodic peak was also obtained for Cu in acetonitrile - LiClO<sub>4</sub> (Figure 4), but not for copper in other solvents, indicating a peculiarity of the copper reaction in acetonitrile.

Nickel exhibited less than the minimum current density.

9. Acetonitrile -  $\text{LiBF}_4$

Silver (Figure 19) exhibits a very high anodic current which increases proportional to the anodic voltage without reaching a peak. On the return scan of the anodic reaction, the anodic current is nearly retraced (a duplicate run showed even a closer retrace than the above figure) indicating the virtual absence of concentration polarization. Figure 20 shows the scan at 40 mv/sec, the anodic peak now being evident (because of anodic peak shift to more negative values).

In the case of copper (Figure 21), the two anodic and two cathodic peaks are observed with a very high current density for the lower oxidation state. The second oxidation peak, as well as the reduction peak corresponding to this, disappears after continued cycling. The initial anodic peak is high and sharp indicating minimal activation polarization. The discharge reaction is accompanied by a greater degree of activation polarization. The system is also characterized by negligible concentration polarization. Decreasing the sweep rate to 40 mv/sec did not change the anodic/cathodic peak heights, nor was solution discoloration evident, indicating stability of the cathode material in this electrolyte. This system is recommended for further study.

The sweep curve for nickel (Figure 22) is a typical example of extreme activation polarization for both the anodic and cathodic reactions, and the virtual absence of concentration polarization.

10. Dimethylformamide -  $\text{LiCl}$

Silver, copper, and nickel all represent poor electrodes in this electrolyte. The anodic products of both copper and nickel do

not show any discharge up to 0.5 v. negative to the open circuit voltage, even though medium low anodic currents are obtained for copper (Figure 23). Some reduction of the silver anodic product is obtained with silver (Figure 24), but this is eliminated at lower sweep rates, indicating that the discharge reaction involves reduction of a solid product, AgCl probably, which is known to be soluble in dimethylformamide.

11. Propylene Carbonate - LiAlCl<sub>4</sub>

Cyclic voltammograms for silver are shown in Figures 25 and 26. This is typical of a system having desirable electrochemical properties for secondary battery application, namely, initiation of both the charge and discharge reactions at the same potential with relatively little activation polarization, a minimal amount of concentration polarization, and 100% charge-discharge efficiency (obtained by integration of the peak areas). Sweep rate has no effect on the peak currents indicating that the reactions are independent of chloride ion diffusion, and also that the oxidation product is compatible with the electrolyte. The shift of the anodic and cathodic peaks with sweep rate is according to theory. This same system was developed by Lockheed for the Air Force as the Li-AgCl battery. The system unfortunately has a theoretical energy density of only 229 watt-hours per pound, considerably lower than the minimum 400 wh/lb based on the net theoretical value obtained with the lithium anode (the minimum set for this program).

The sweep curves for copper are shown in Figures 27 and 28 at 40 and 400 mv/sec respectively. There appear to be two separate anodic reactions (the slower sweep resolves these more clearly because of the decreased anodic peak for the lower

oxidation step). The cathodic peak may represent the reduction of the higher valence copper, since curves from triplicate runs show a second reduction with extreme activation polarization occurring at a more negative potential. Sweep measurements will be repeated for this system.

Nickel in propylene carbonate -  $\text{LiAlCl}_4$  (Figure 29) shows a very small anodic peak. Reduction of this anodic product is accompanied by extreme activation polarization and very low current.

12. Dimethylformamide -  $\text{AlCl}_3$

Although the anodic reaction for silver is accompanied by appreciable activation polarization, the reduction reaction shows little such polarization (Figures 30 and 31). Dissolution of anodic product ( $\text{AgCl}$ ) was observed, again consistent with its behaviour in dimethylformamide.

Copper (Figure 32) and nickel show low anodic peaks, with no cathodic reaction.

13. Butyrolactone -  $\text{LiCl}$

Figure 33 shows the CV for silver, and its comparison to silver in acetonitrile -  $\text{LiBF}_4$  is noted (see Figure 19), although much lower currents are obtained in the chloride case. Sweep rate has no appreciable effect on the cathodic peak current density indicating stability of  $\text{AgCl}$  in this electrolyte. No solution discoloration was observed.

Copper (Figures 34 and 35) again shows two anodic and two cathodic peaks, the anodic scan resembling that obtained for

copper in propylene carbonate -  $\text{LiAlCl}_4$  (Figures 27 and 28). Reduction of the anodic product is poor, with low current and severe activation polarization. This system also shows appreciable concentration polarization.

Nickel (Figure 36), although exhibiting a medium low cathodic current, shows no reduction reaction in this electrolyte, even at the high sweep rate of 400 mv/sec. A blue coloration was observed in the solution.

14. Butyrolactone -  $\text{LiAlCl}_4$

All electrodes, Ag, Cu, and Ni, showed current densities less than the minimum  $0.1 \text{ ma/cm}^2/\text{cm}$  current axis.

15. Acetonitrile -  $\text{LiCl}$

Silver (Figures 37 and 38) represents a fairly reversible system in this electrolyte, but with a medium low current density, probably due to the low solubility of  $\text{LiCl}$  in acetonitrile. The cathodic currents are higher than the anodic currents, but with increased cycling, the cathodic peak decreases such that after 60 cycles it is reduced to 50% of its original value recorded after 10 cycles as per normal procedure. This represents decreased charge acceptance with increased cycling. No anodic product dissolution was observed. The sweep curves are typical for a solid state reaction. Cu and Ni exhibited no reduction.

16. Propylene Carbonate -  $\text{AlCl}_3$

The sweep curves for silver are shown in Figures 39 and 40, for 400 and 40 mv/sec respectively. These curves are compared with those of Figures 25 and 26 which represent the same system but with the  $\text{AlCl}_4^-$  complex ion. Lack of this ion results in

lower peak currents (no doubt due to the lower solubility of the salt) and greater activation polarization. In essence these cyclic voltammograms point out the desirability of the addition of  $\text{AlCl}_3$  to  $\text{LiCl}$  in propylene carbonate for the  $\text{AgCl}$  cathode.

The sweep curve for copper is shown in Figure 41. Low peak currents exist for both the anodic and cathodic reactions which commence at nearly the same potential. This system exhibits negligible concentration polarization and would represent a good system if higher currents could be obtained. Curves at 2 and 200 mv/sec show lower and higher peak currents respectively. The peaks are closer together at the 2 mv/sec rate than at the 20 mv/sec rate, and are further apart at the 200 mv/sec sweep rate. This change in peak height and separation is in accordance with theory. This curve compares well with that of Figure 27 which is the CV for copper in propylene carbonate -  $\text{LiAlCl}_4$ .

Nickel showed no reduction of the anodically-formed product.

#### 17. Cyclic Voltammograms of Silver, Copper, and Nickel Oxides

Some preliminary measurements were made using Ag, Cu, and Ni wire electrodes converted to the oxides prior to screening in dimethylformamide -  $\text{LiPF}_6$ . Nickel wire was oxidized directly in air, whereas the silver and copper were anodically oxidized in KOH solution. The cyclic voltammograms shown here were recorded after a minimum of 10 cycles.

The CV for silver oxide is shown in Figure 42 and is compared with that for the silver metal (Figure 8). The primary difference is the much larger currents for the oxide electrode. The anodic curves appear identical, but the possibility exists for a 2-step reduction reaction for the oxide electrode. Similar to the

untreated silver, the AgO electrode shows no cathodic current at 2 mv/sec, consistent with the discharge of a solid anodic product soluble in the electrolyte, which was evident by solution discoloration and silver deposition at the counterelectrode.

Figures 43 and 44 show the sweep curves for copper oxide at 40 and 400 mv/sec respectively in dimethylformamide -  $\text{LiPF}_6$ . These are compared with Figure 9 for copper metal in the same electrolyte, where the voltage was scanned only  $\pm 0.5$  v. relative to the zero reference, compared with  $\pm 1.0$  v. for the oxide electrode. The 400 mv/sec sweep (Figure 44) shows at least two oxidation steps, the second not evident at the lower sweep rate (Figure 43), which shows a reverse anodic peak representative of further oxidation on the return scan of the original oxidation step. The cathodic reaction shows at least two reduction steps at the lower sweep rate, probably corresponding to the two inflections at the higher sweep rate. Also differing from the copper electrode is the extreme activation polarization accompanying the cathodic reaction of the copper oxide electrode.

The curve for nickel oxide is shown in Figure 45. This curve cannot be directly compared with nickel metal since the latter gave less than the minimum current density. It is suffice to say that the nickel oxide exhibits different curve characteristics than the untreated metal.

No significant evaluation of the data can be made at this time, but it is evident that the oxides of Ag, Cu, and Ni represent different cathodic materials than the reduced metal which becomes oxidized in halide-containing electrolytes. It is yet to be determined whether this is also true for the chlorides and fluorides of these metals, prepared independently prior to their screening by cyclic voltammetry.

Electrode - Ag  
 Electrolyte - Acetonitrile-LiClO<sub>4</sub>  
 Sweep rate - 200 mv/sec  
 Temp. - 50°C  
 Zero ref. - 1.0 v/Zn  
 CV-210

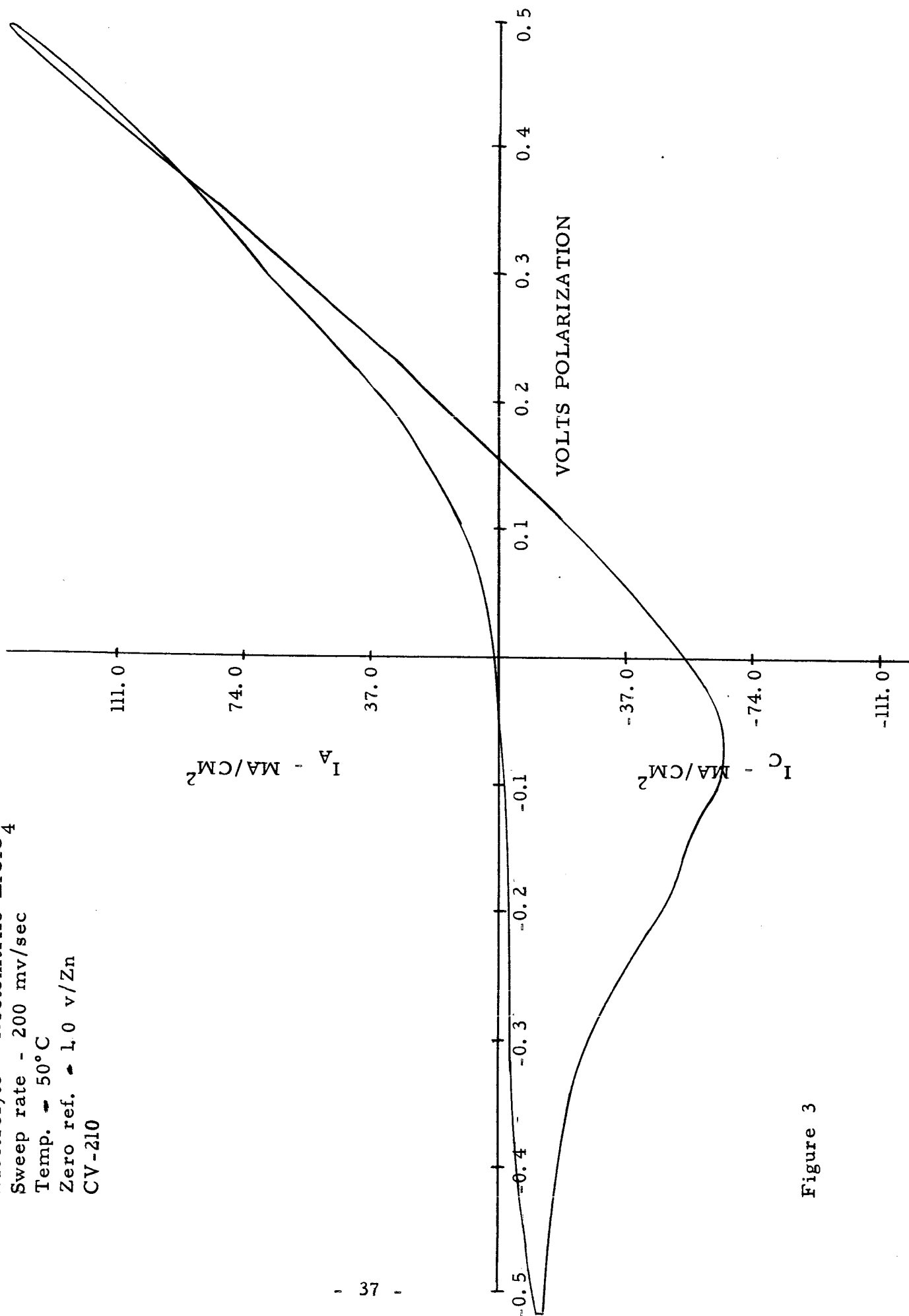


Figure 3

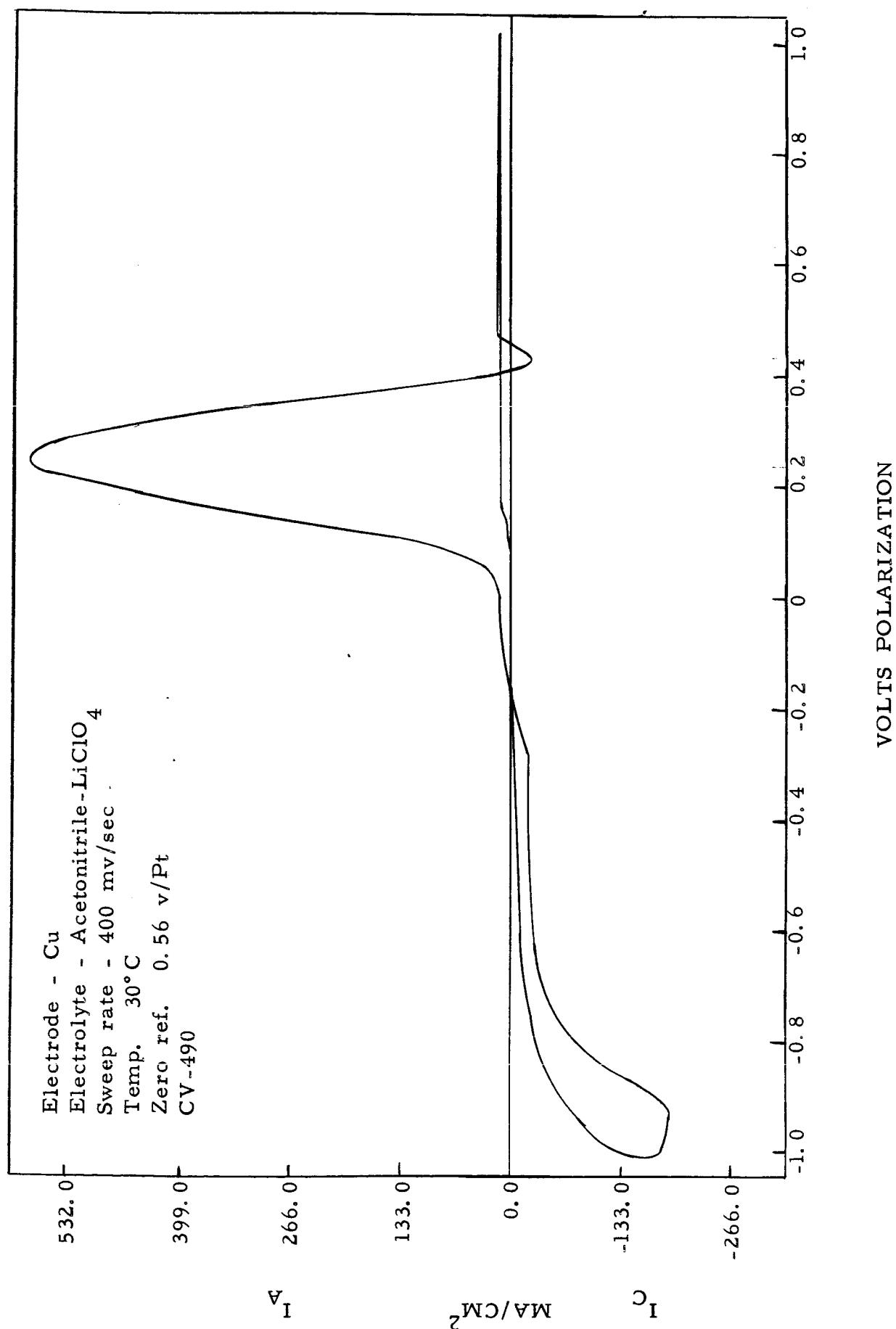


Figure 4

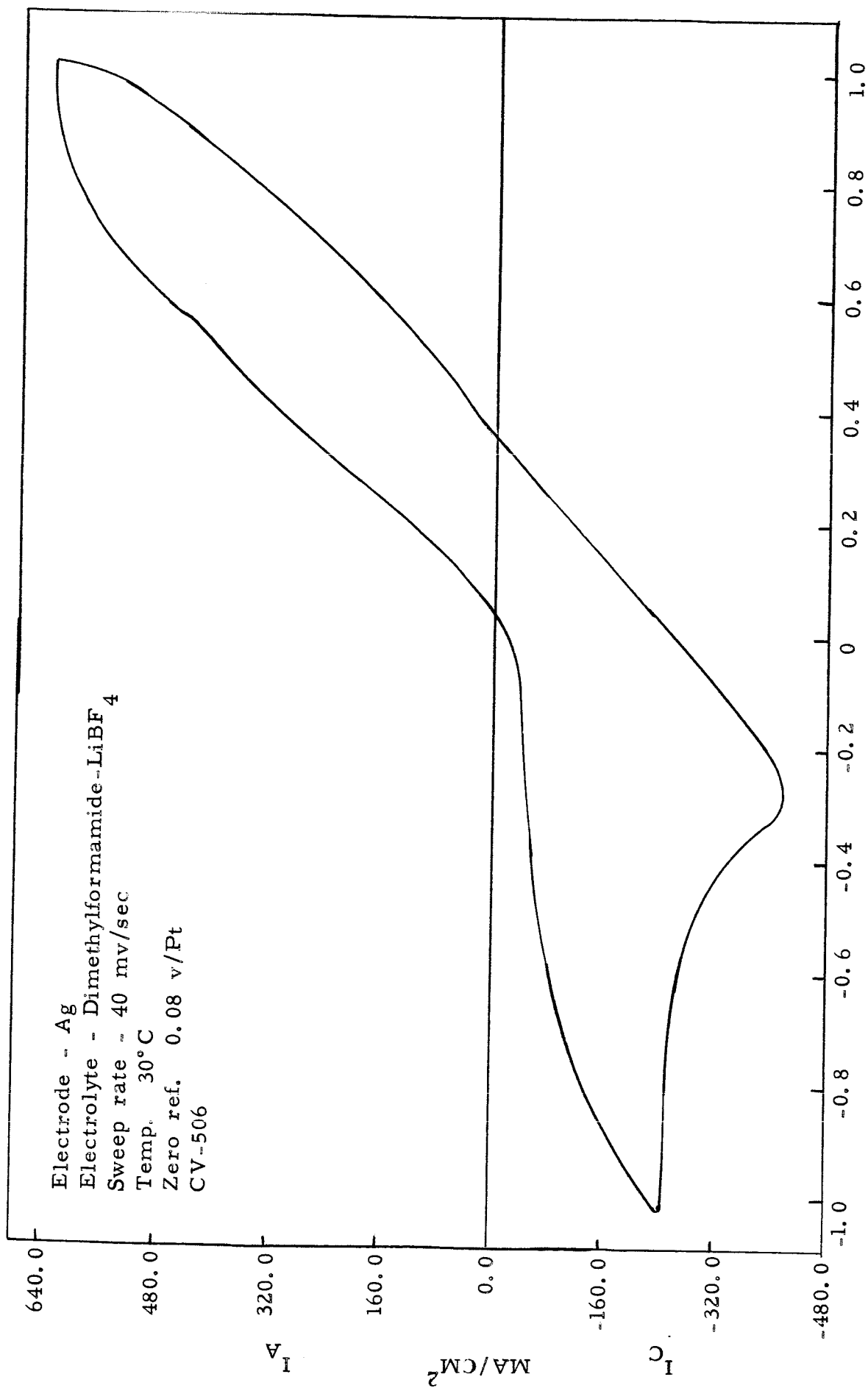


Figure 5

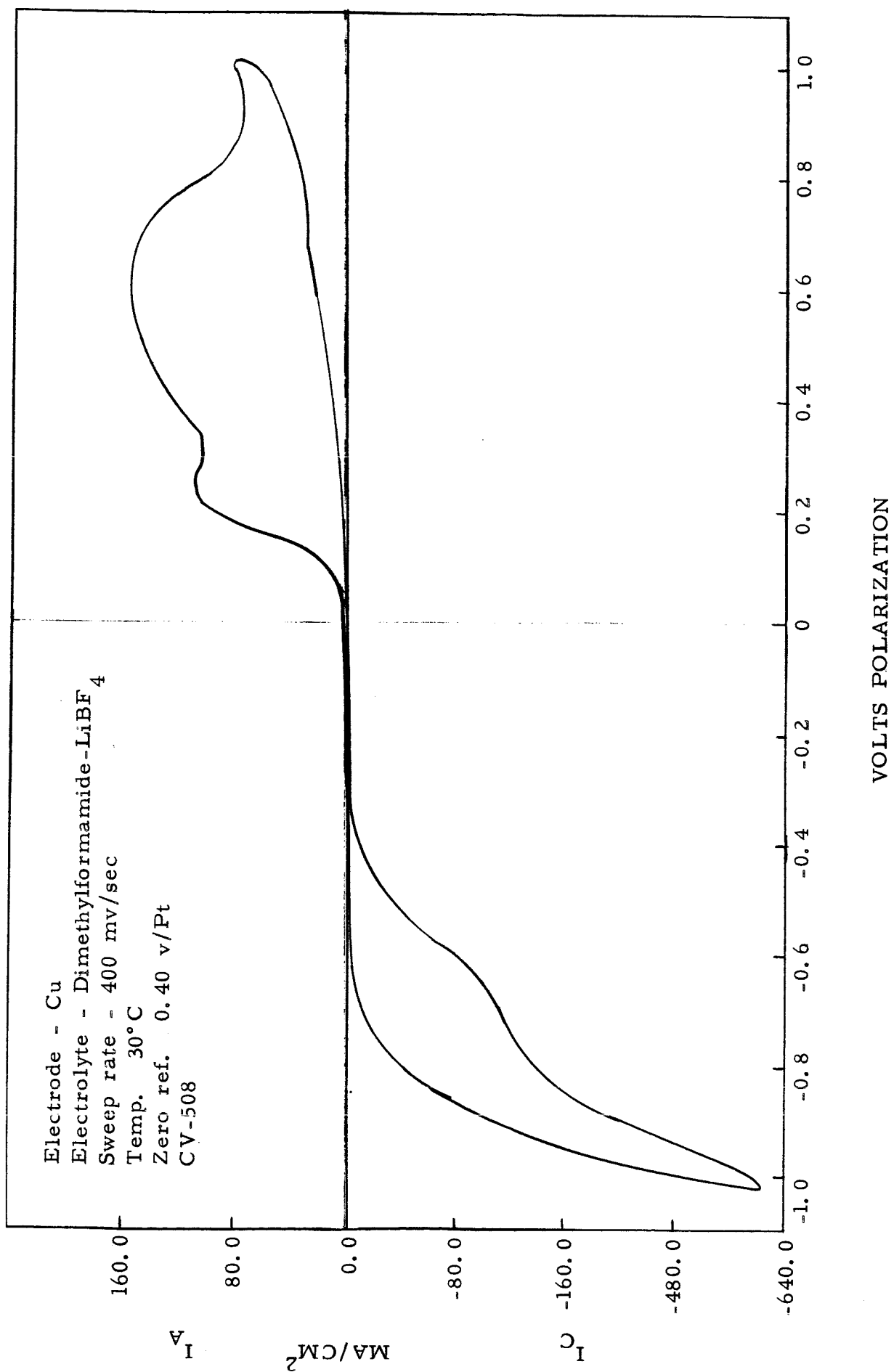


Figure 6

Electrode -- Ni

Electrolyte - Dimethylformamide-LiBF<sub>4</sub>

Sweep rate - 20 mv/sec

Temp. 30°C

Zero ref. 0.02 v/Zn

CV-266

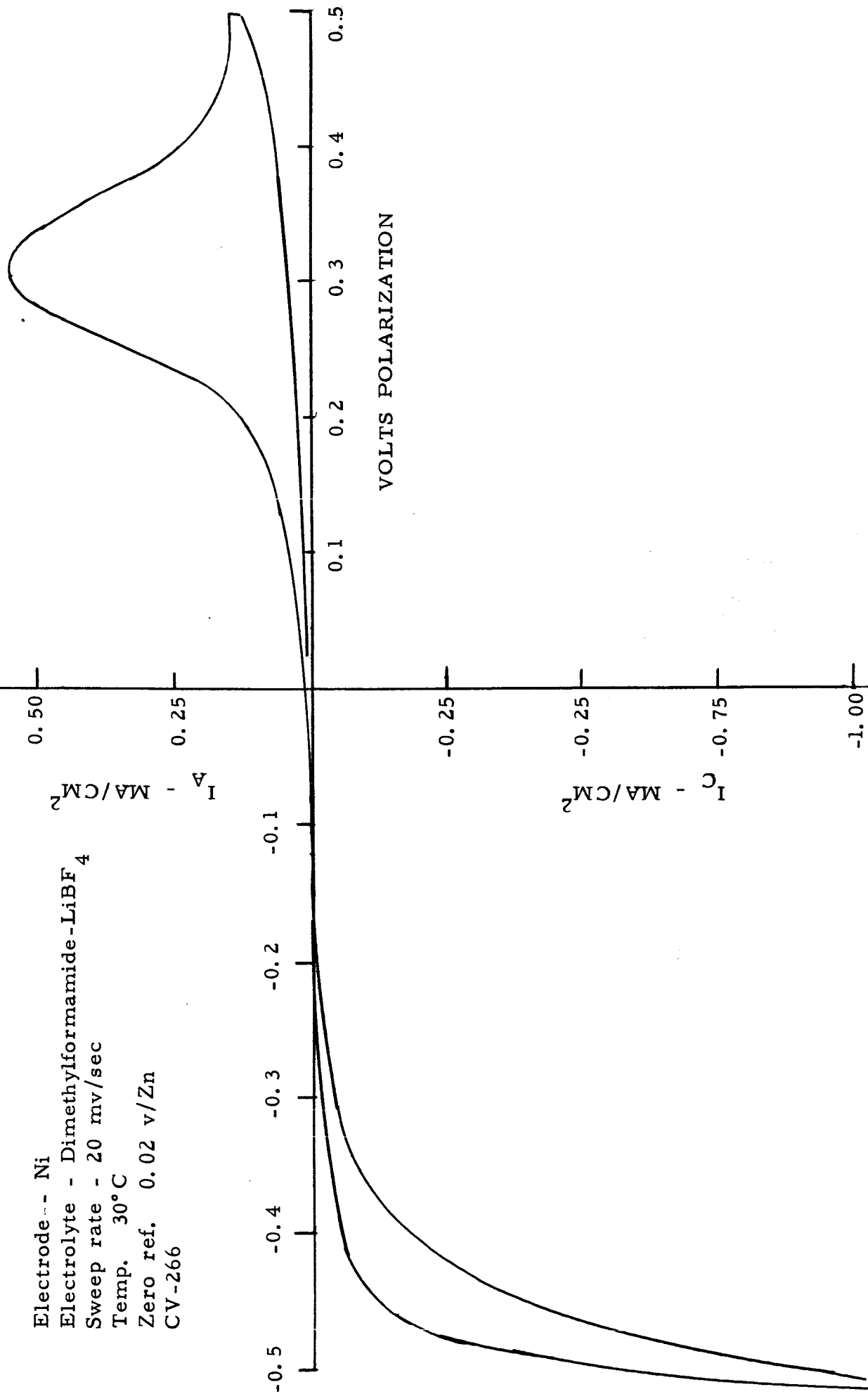


Figure 7

Electrode - Ag  
 Electrolyte - Dimethylformamide-LiPF<sub>6</sub>  
 Sweep rate - 200 mv/sec  
 Temp. 30°C  
 Zero ref. 1.14 v/Zn  
 CV-280

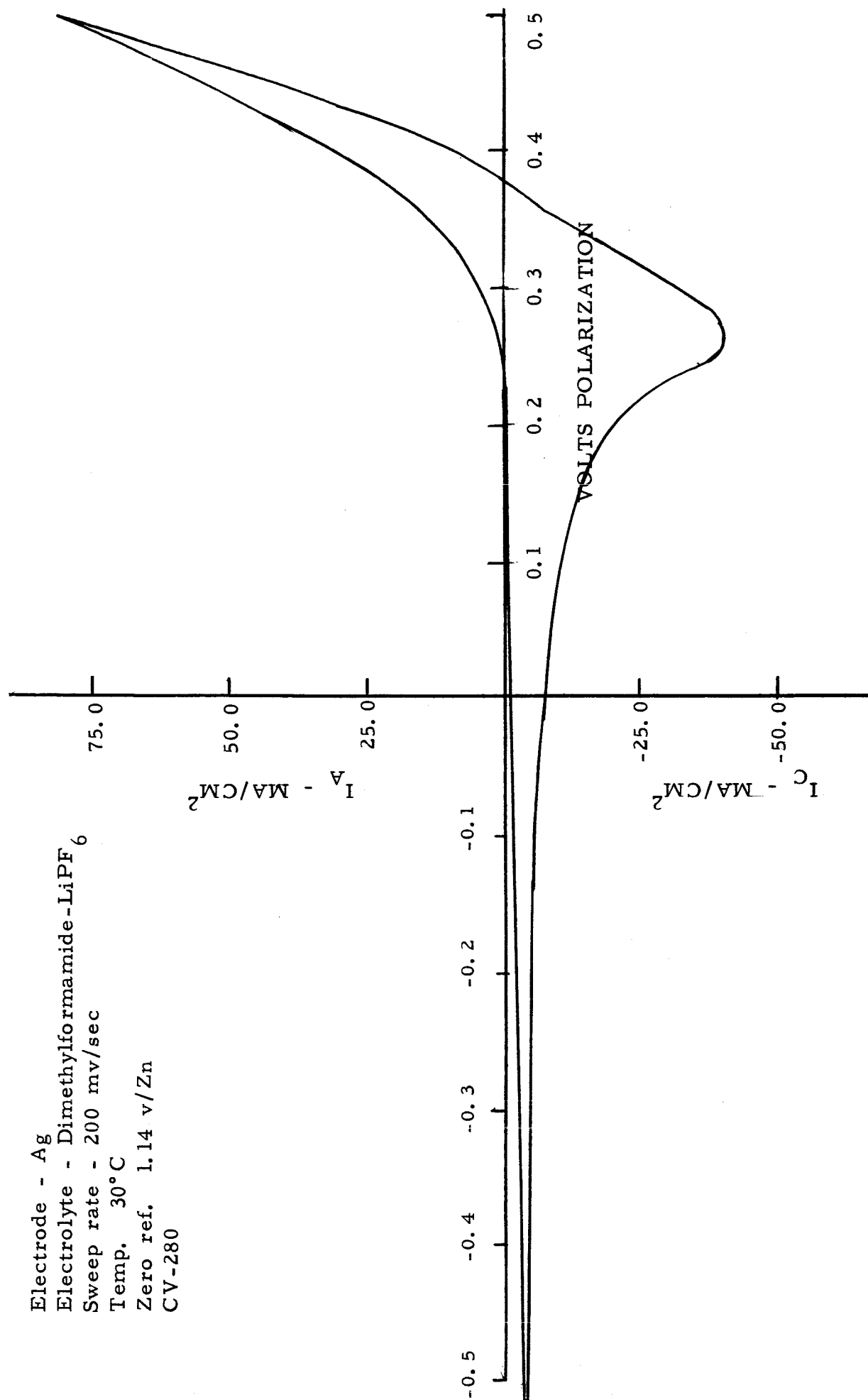


Figure 8

Electrode - Cu  
 Electrolyte - Dimethylformamide-LiPF<sub>6</sub>  
 Sweep rate - 200 mv/sec (solid curve)  
                   20 mv/sec (broken curve)  
 Temp. 50°C  
 Zero ref. 0.02 v/Zn  
 CV-302, 298

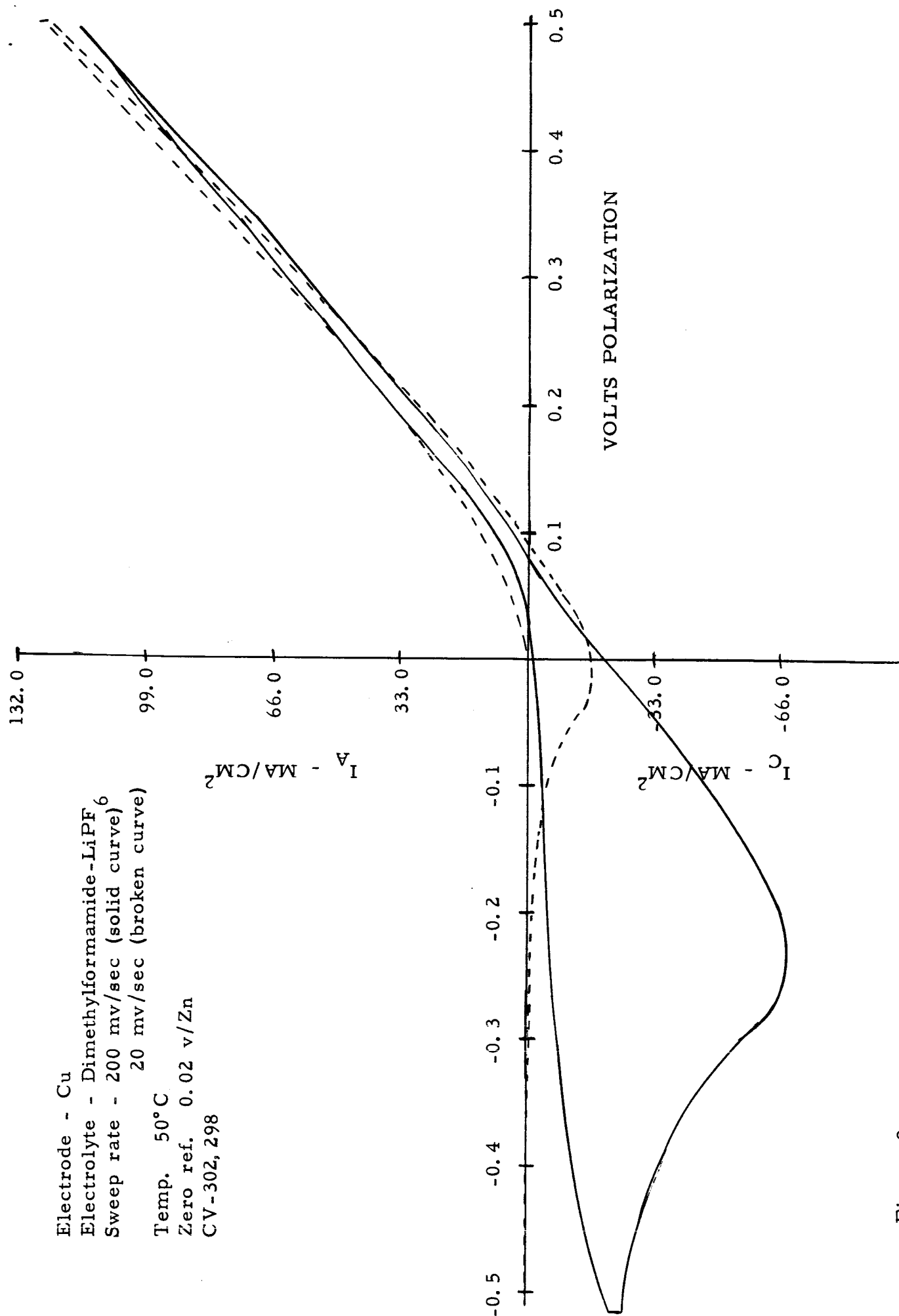


Figure 9

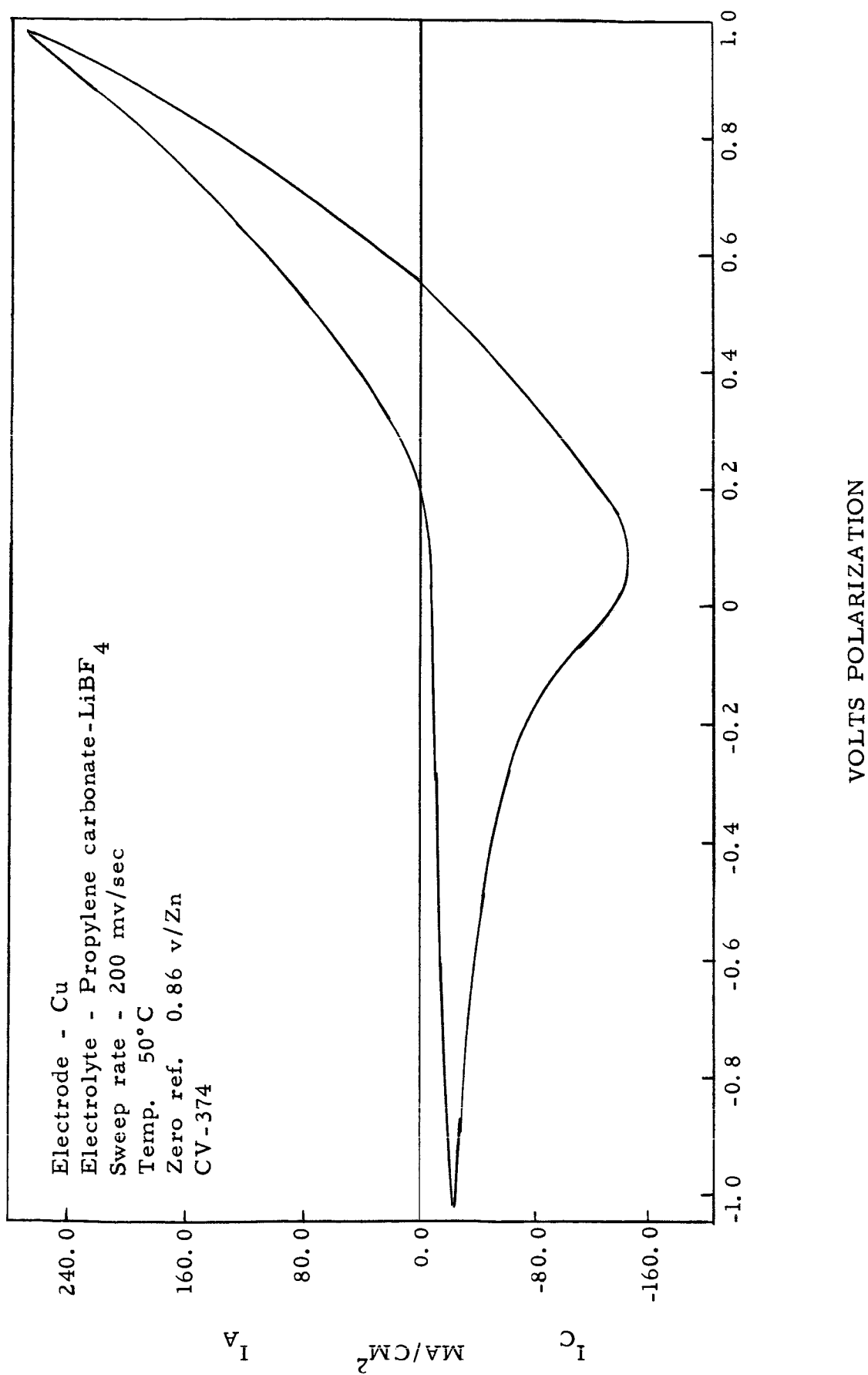


Figure 10

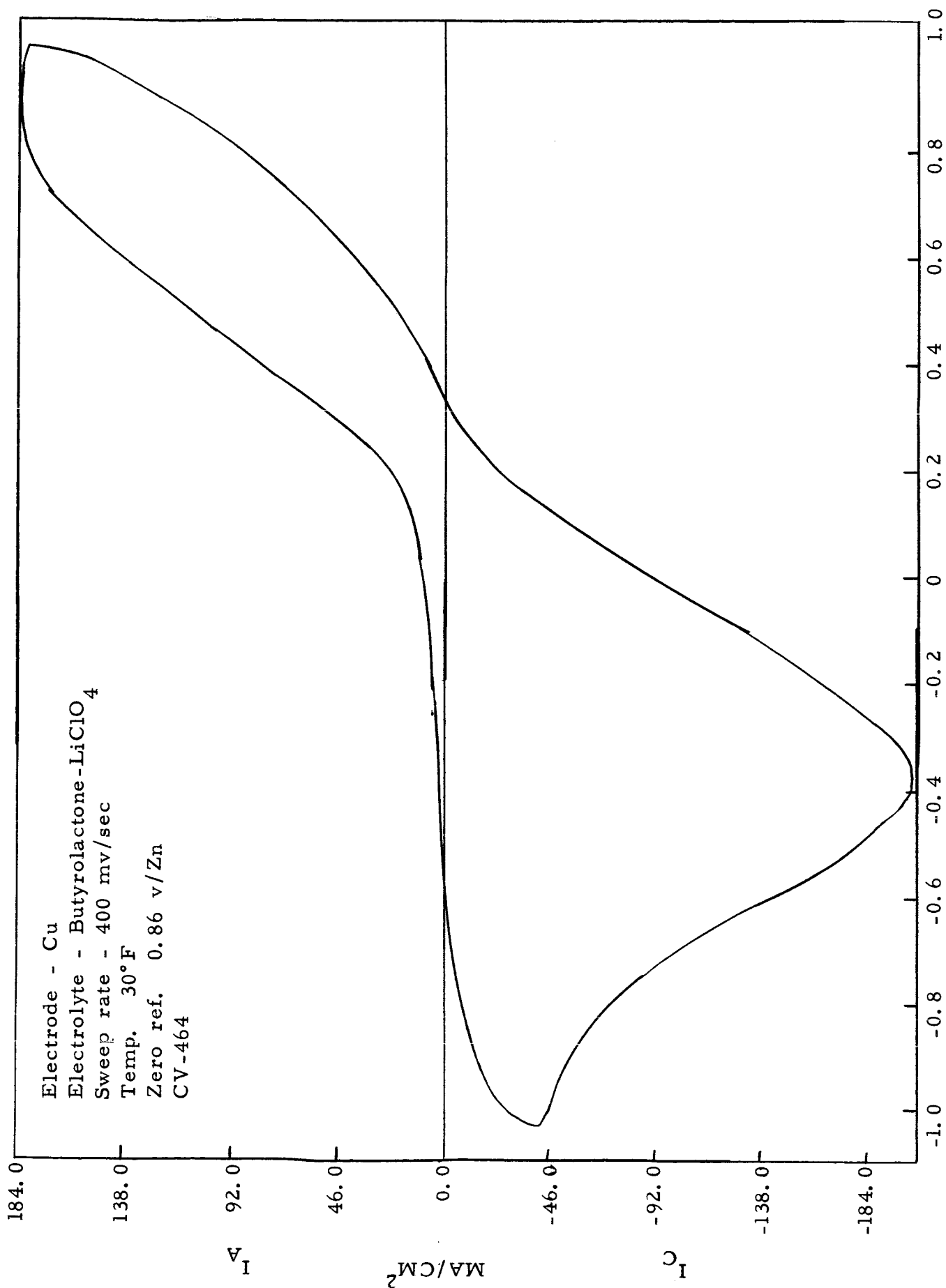


Figure 11

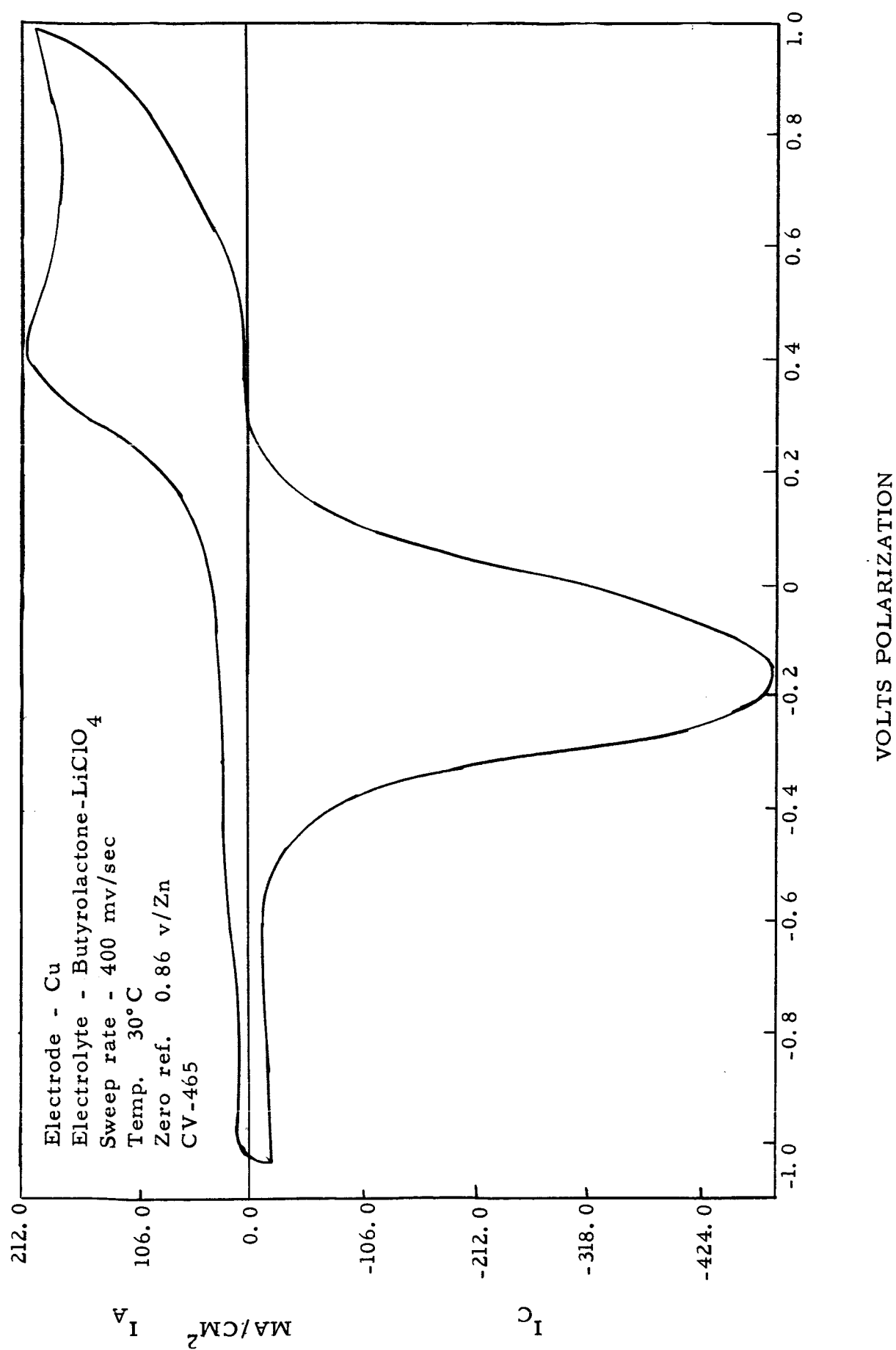


Figure 12

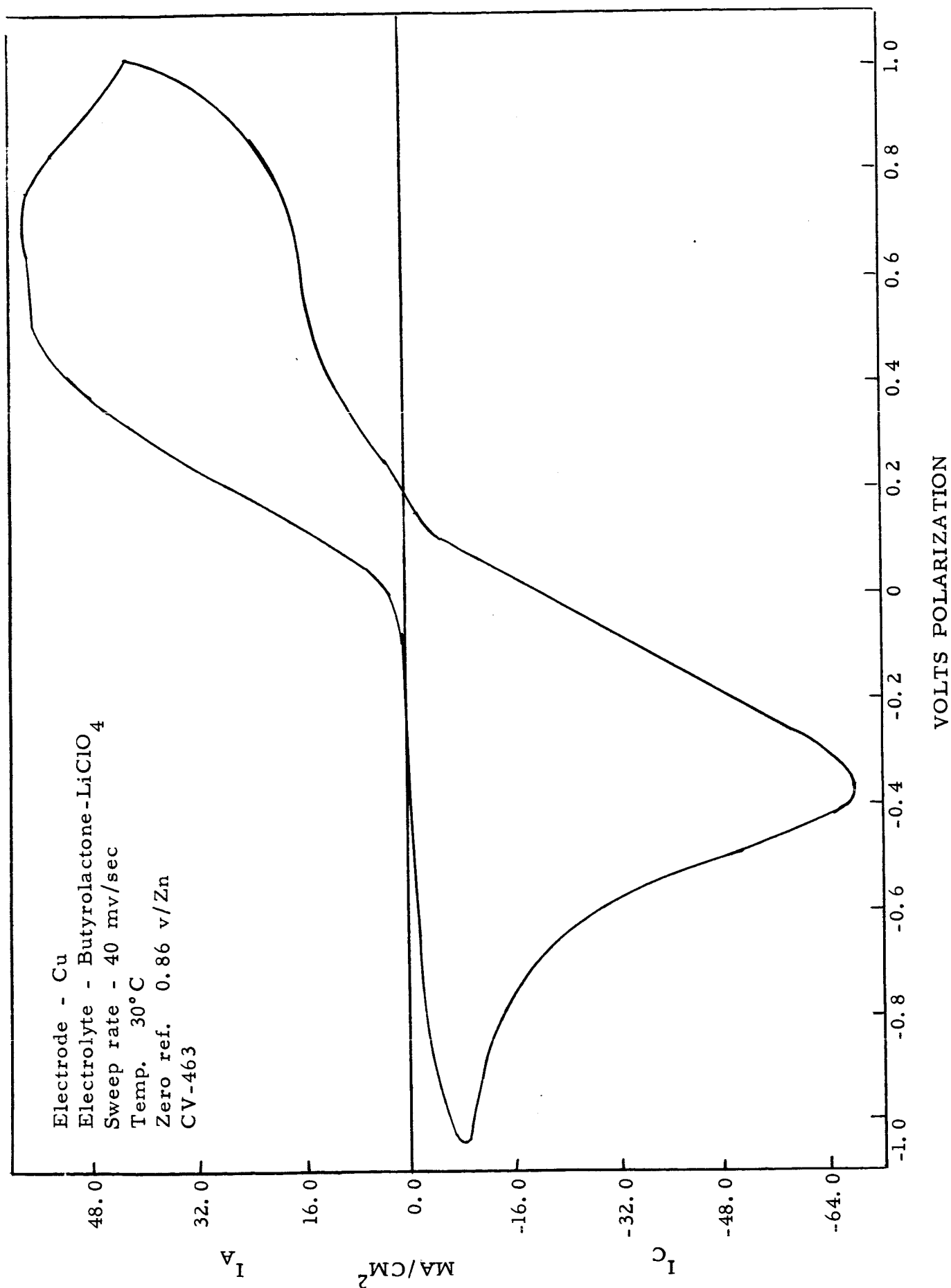


Figure 13

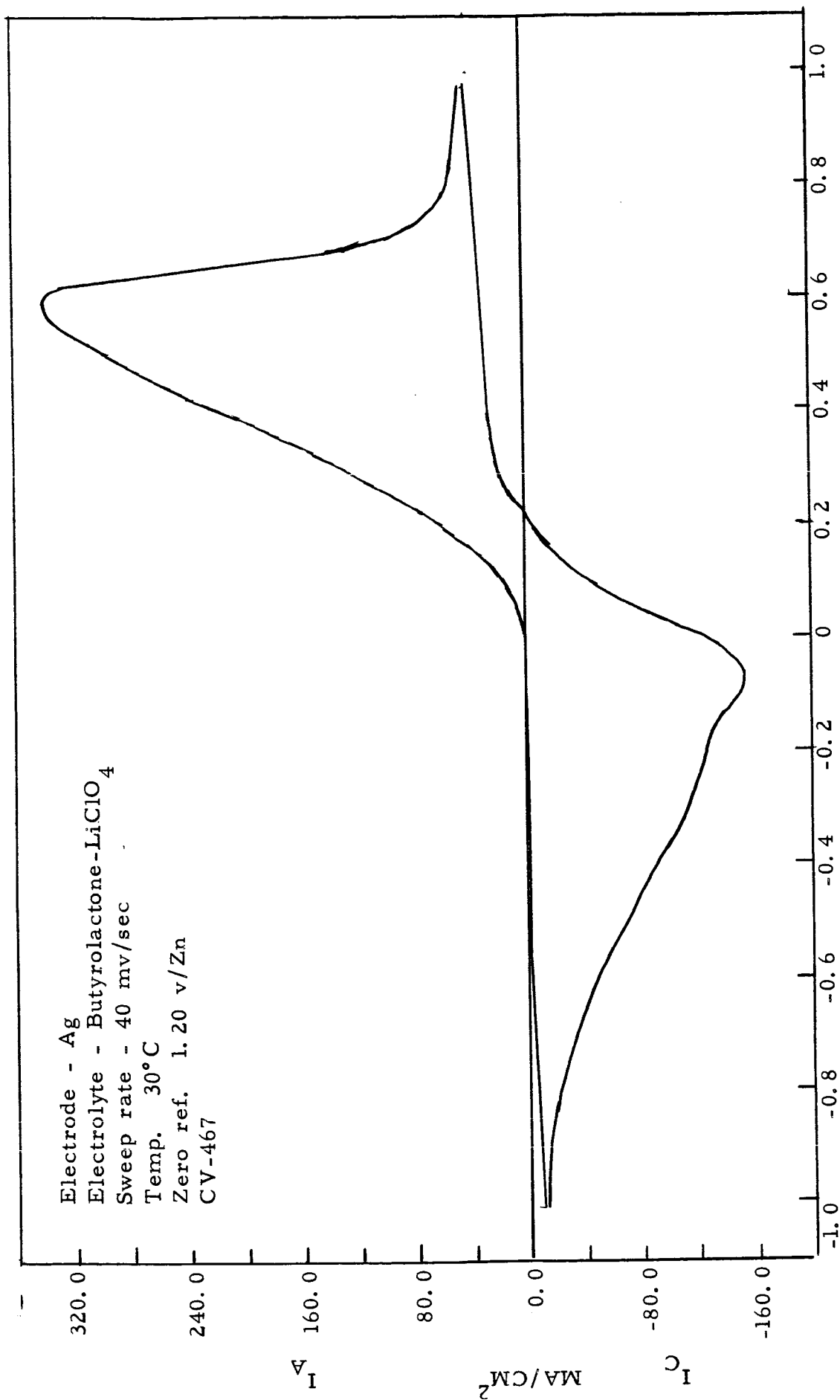


Figure 14

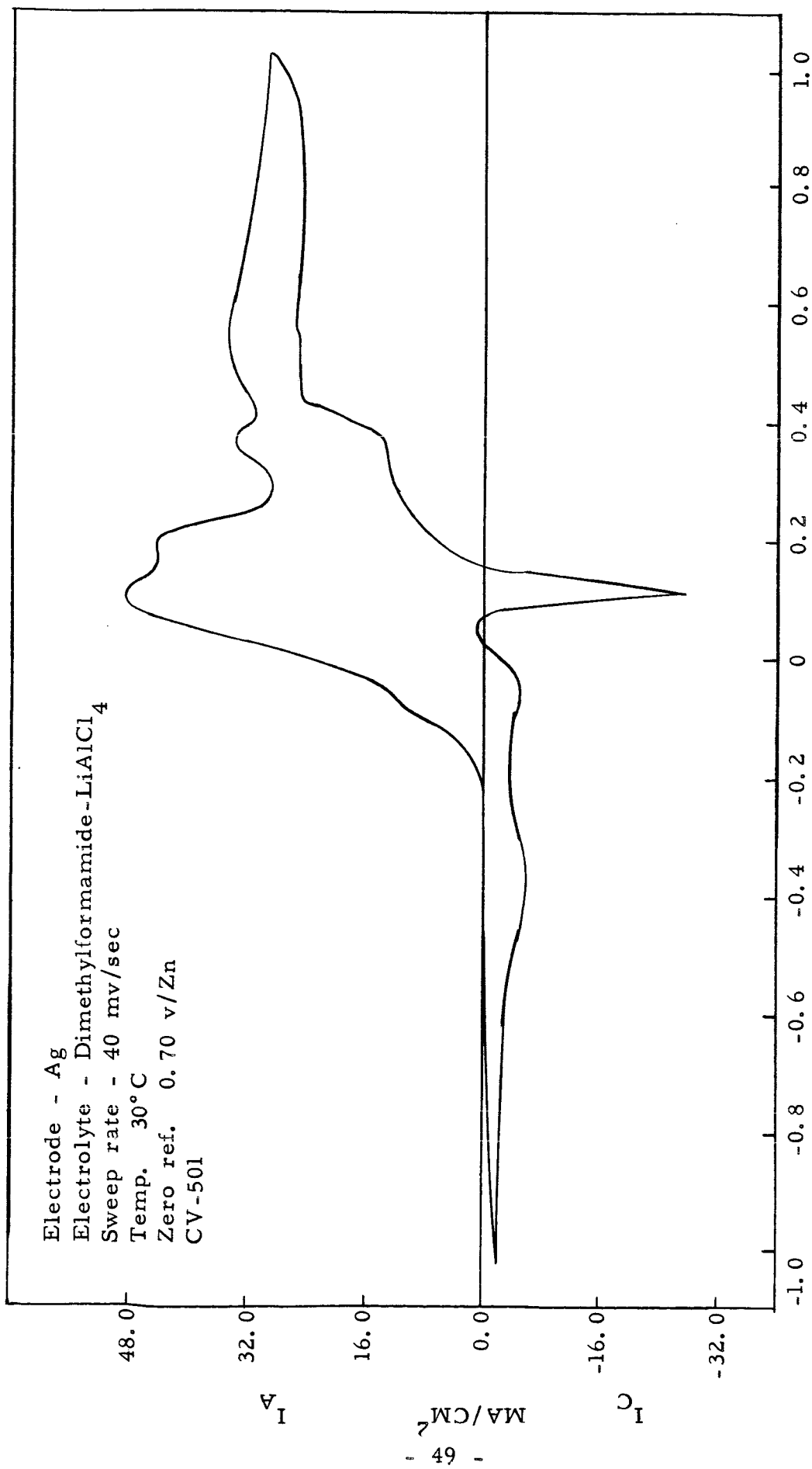


Figure 15

Electrode - Cu

Electrolyte - Dimethylformamide-LiAlCl<sub>4</sub>

Sweep rate - 200 mv/sec

Temp. 50°C

Zero ref. 1.68 v/Zn

CV-325

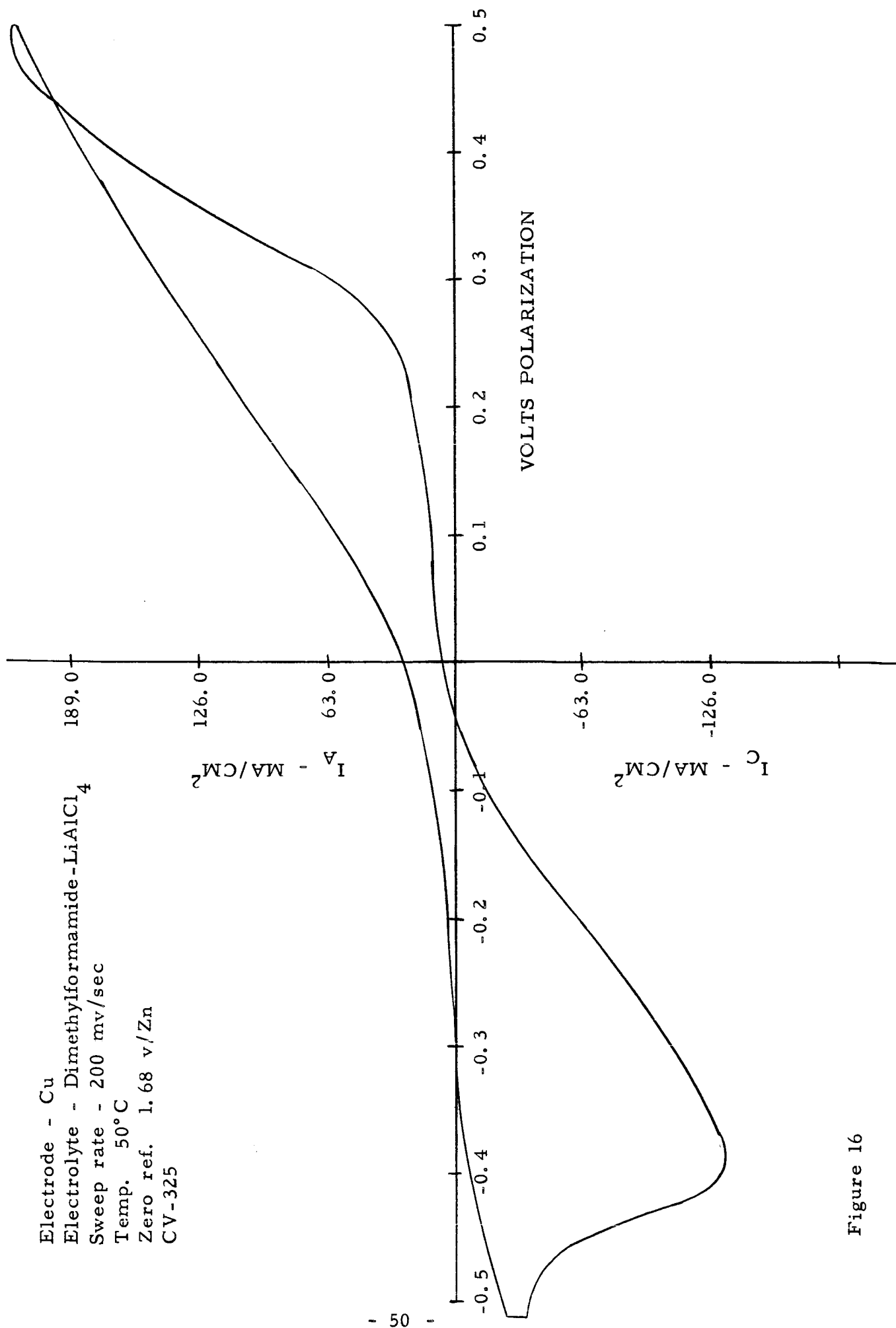


Figure 16

Electrode - Ag  
 Electrolyte - Acetonitrile-LiPF<sub>6</sub>  
 Sweep rate - 200 mv/sec  
 Temp. - 30°C  
 Zero ref. - 0.82 v/Zn  
 CV-136

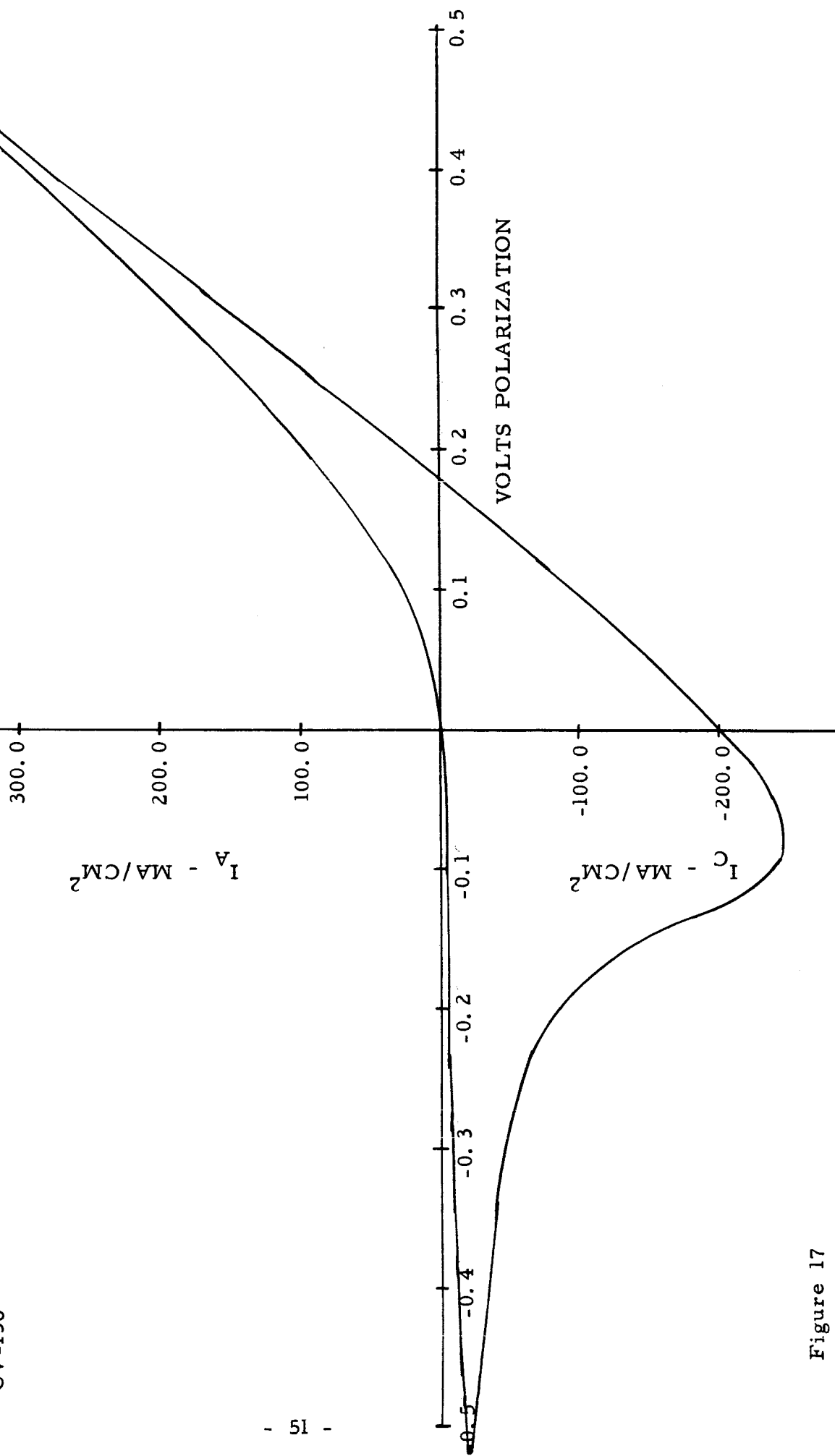


Figure 17

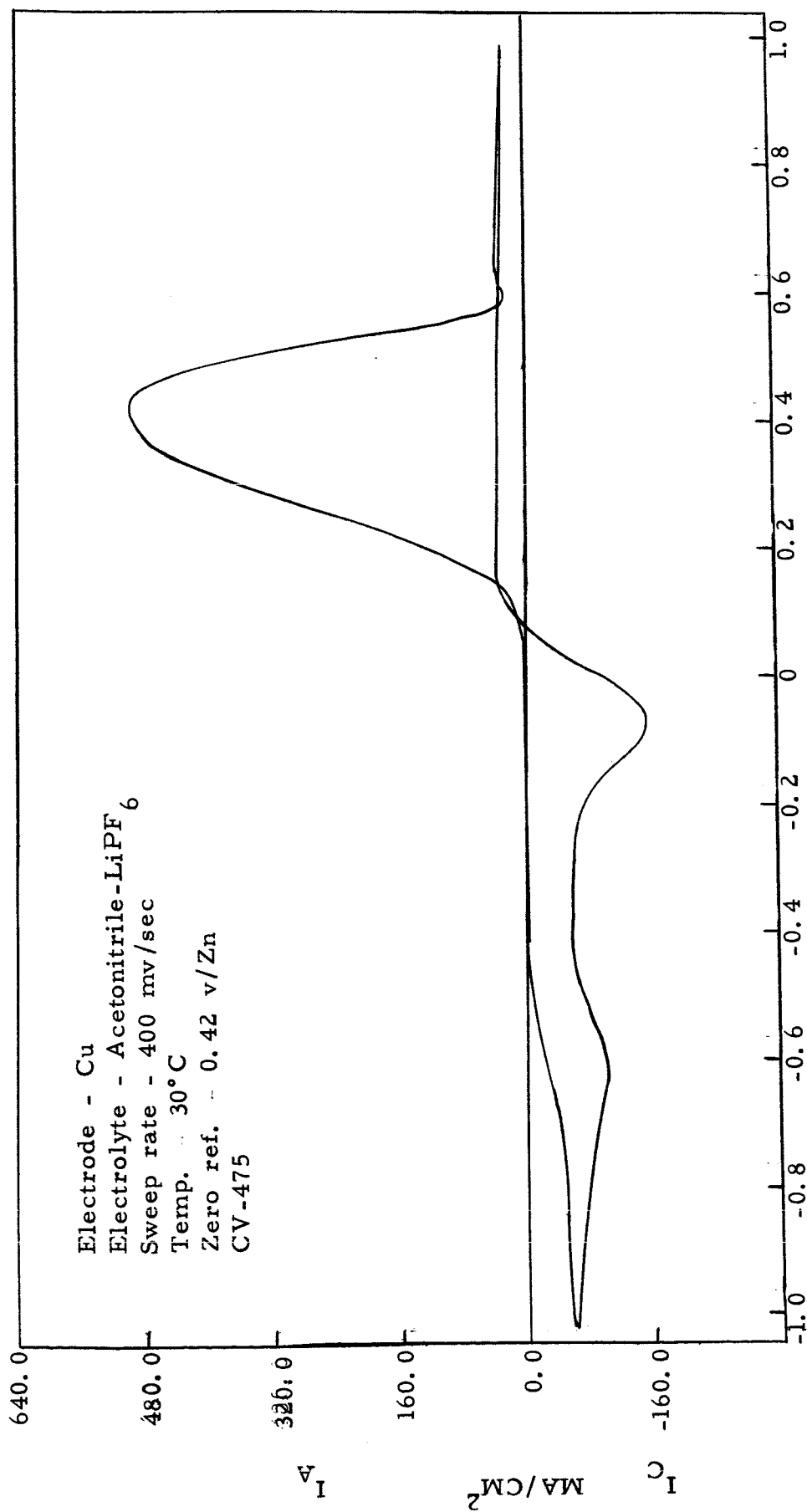


Figure 18

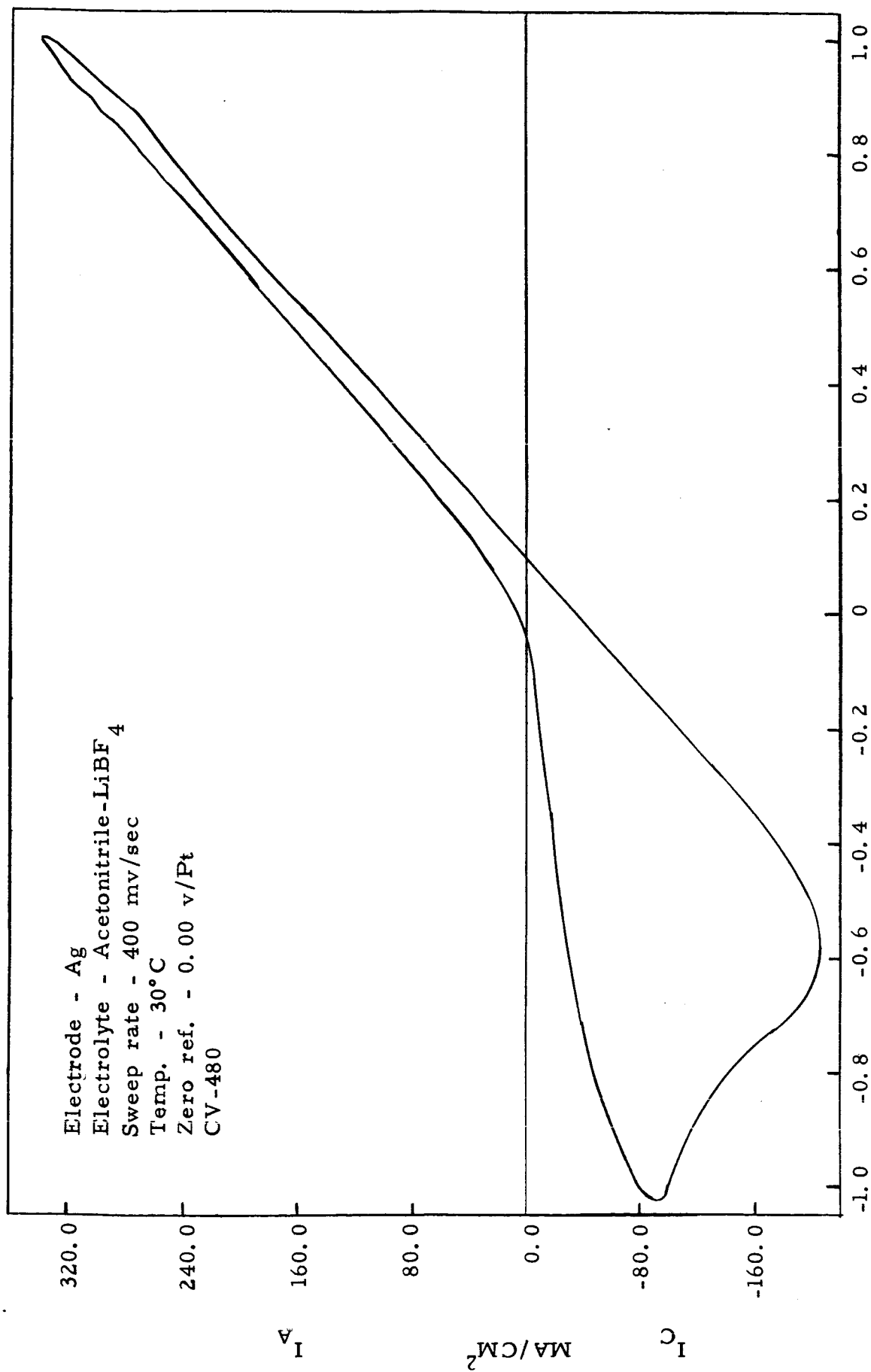


Figure 19

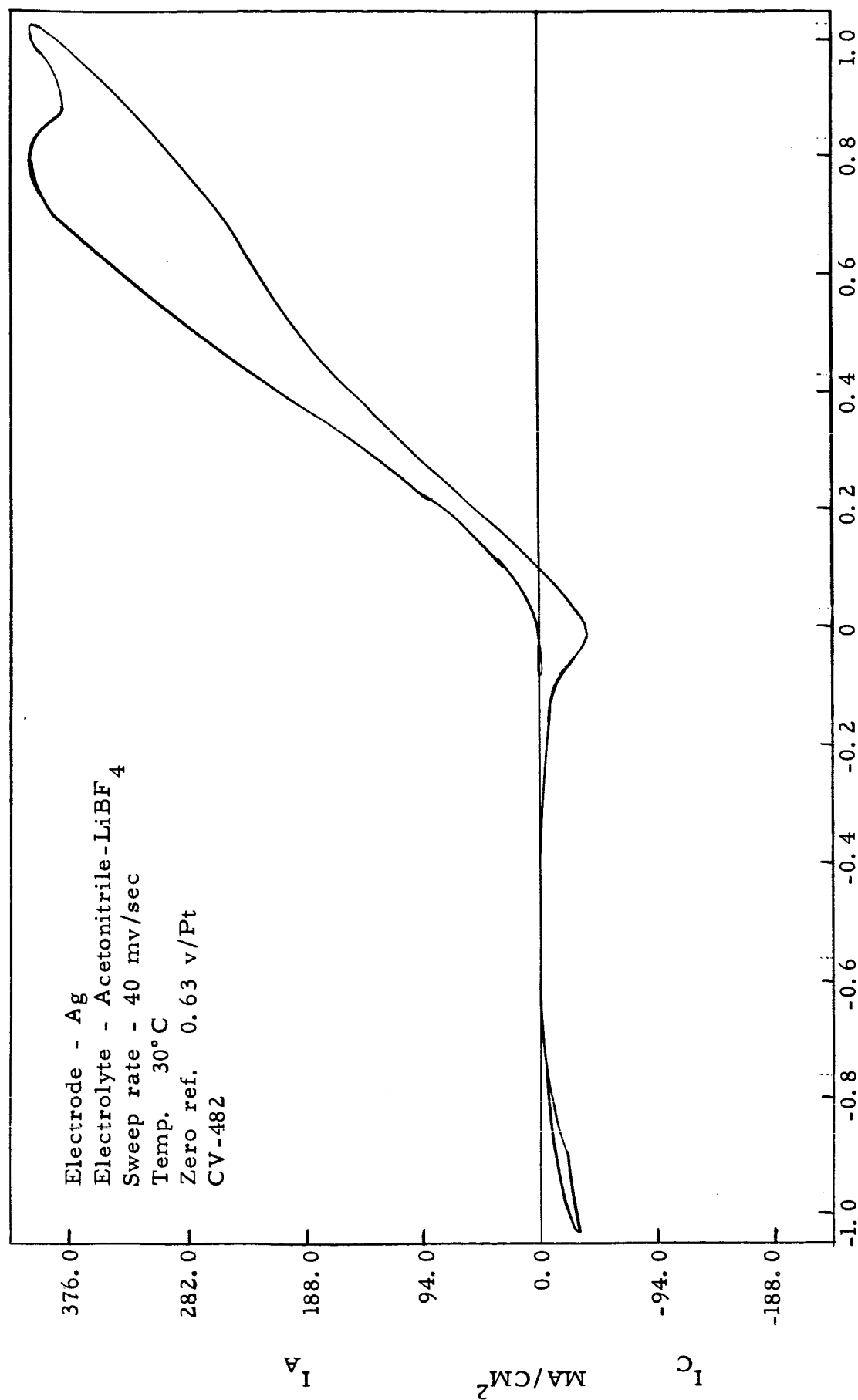


Figure 20

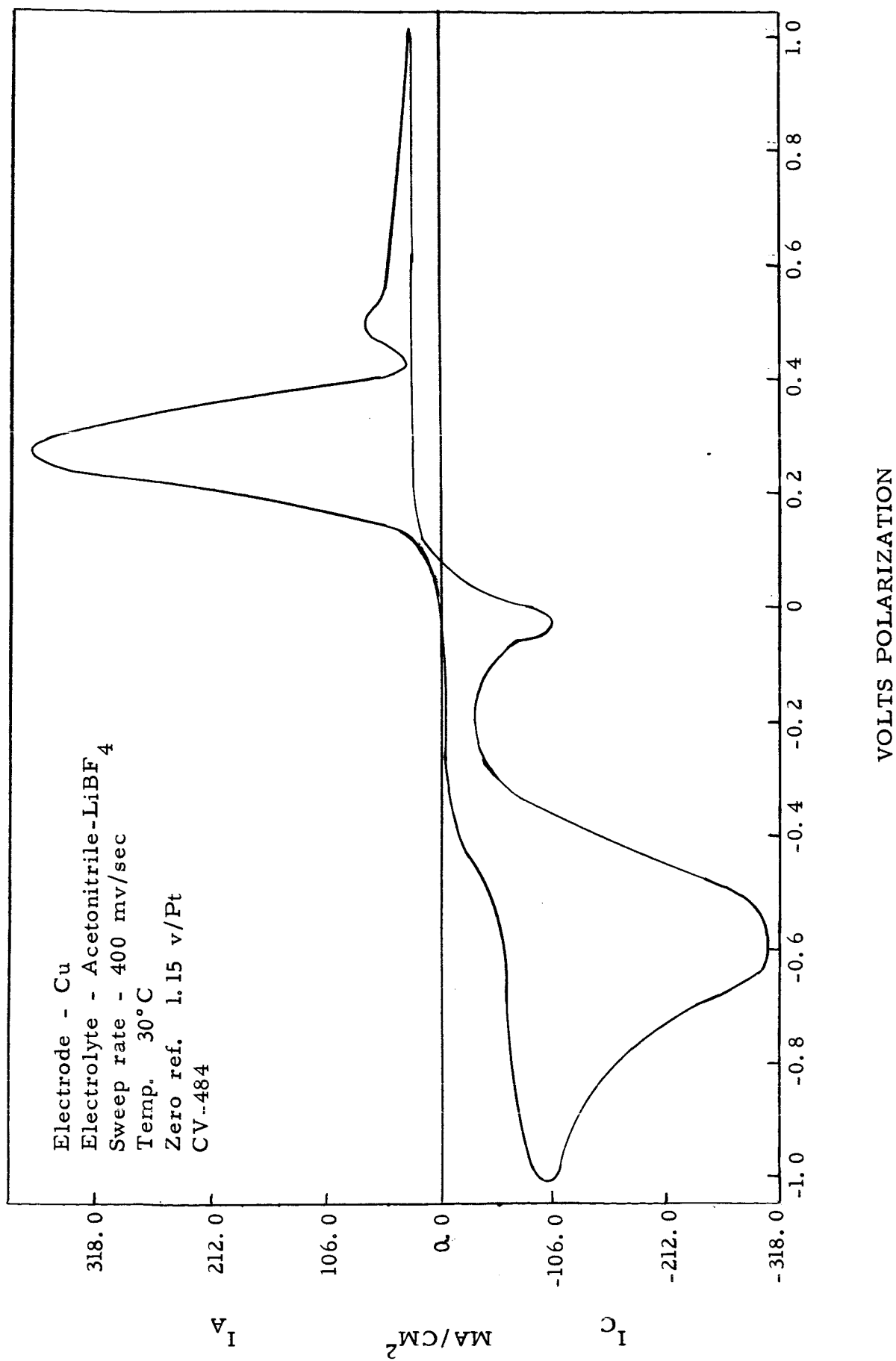


Figure 21

Electrolyte - Ni  
 Electrolyte - Acetonitrile-LiBF<sub>4</sub>  
 Sweep rate - 200 mv/sec  
 Temp. 50°C  
 Zero ref. 0.96 v/Zn  
 CV-170

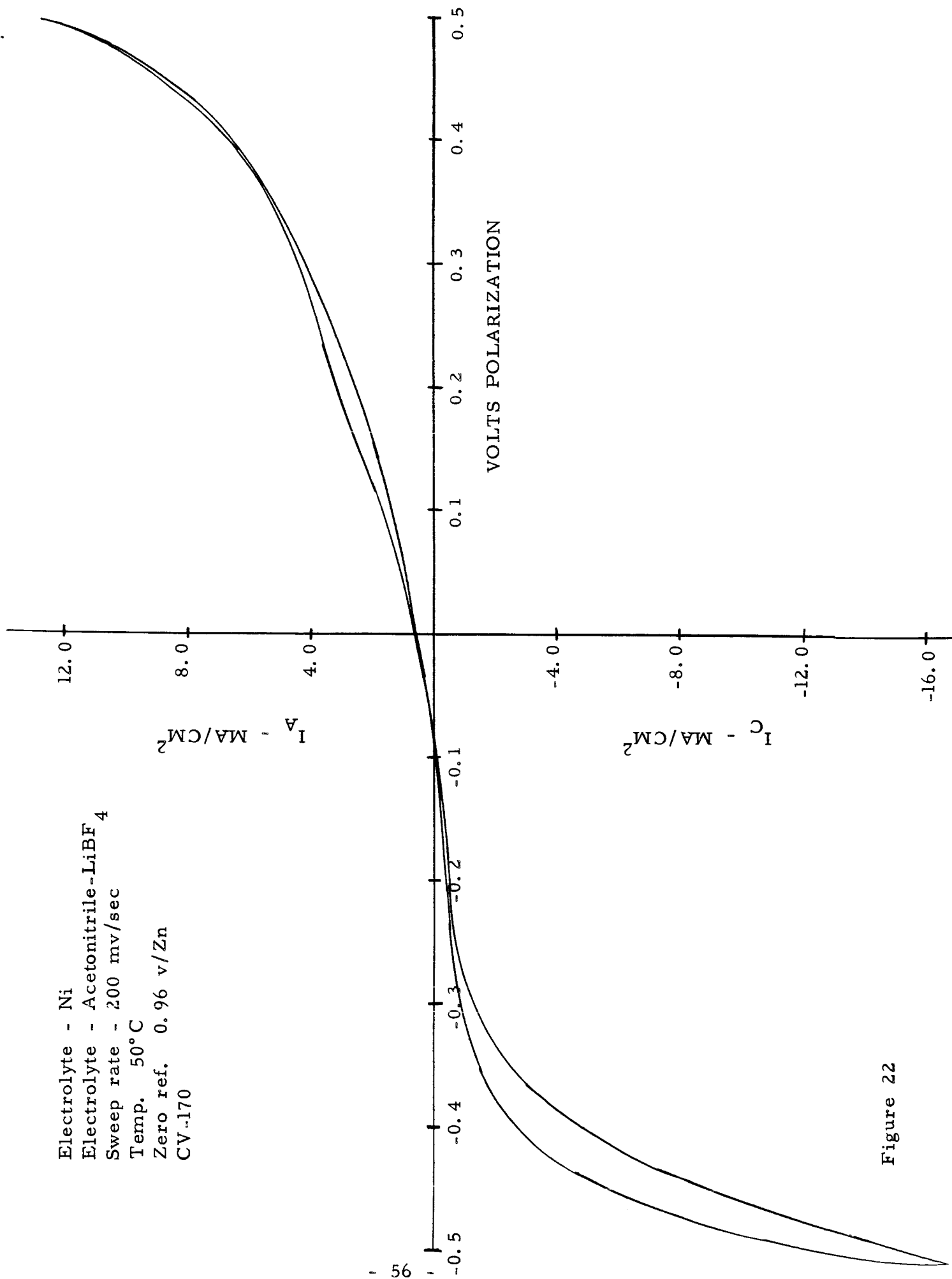


Figure 22

Electrode - Cu  
 Electrolyte - Dimethylformamide-LiCl  
 Sweep rate - 20 mv/sec  
 Temp. - 30°C  
 Zero ref. - 0.66 v/Zn  
 CV-73

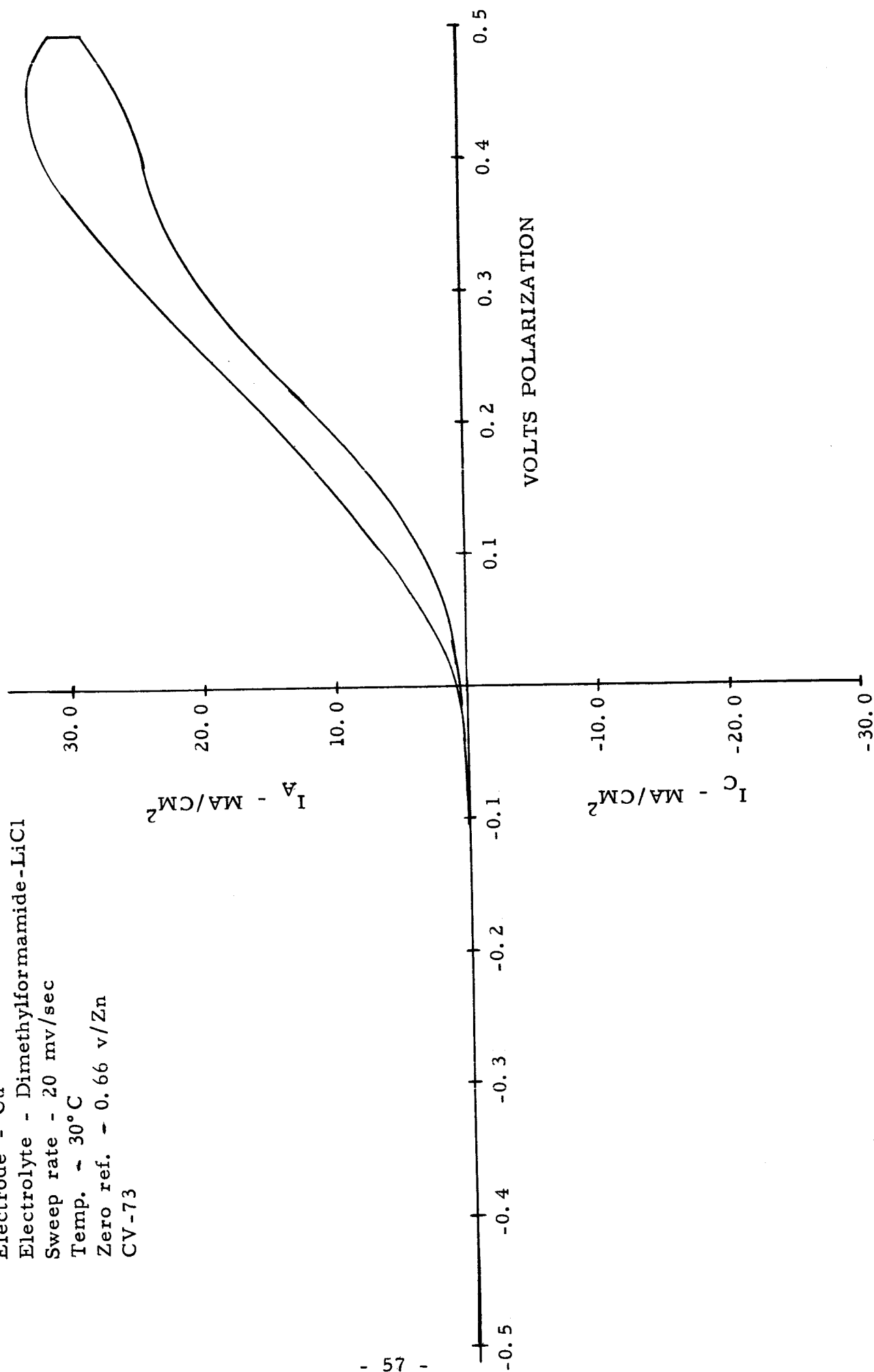


Figure 23

Electrode - Ag  
 Electrolyte - Dimethylformamide - LiCl  
 Sweep rate - 200 mv/sec  
 Temp. - 40°C  
 Zero ref. - 0.74 v/Zn  
 CV-75

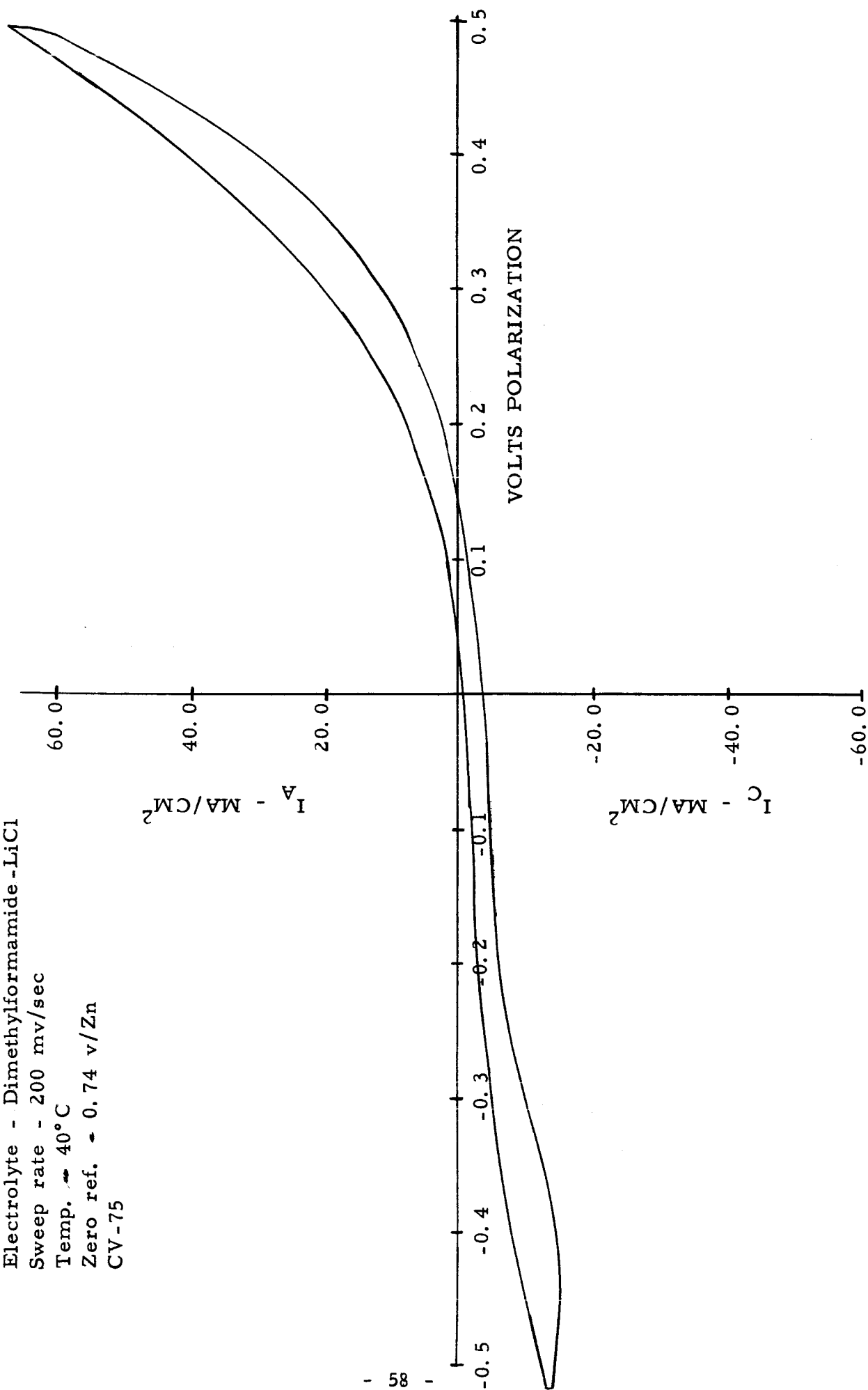


Figure 24

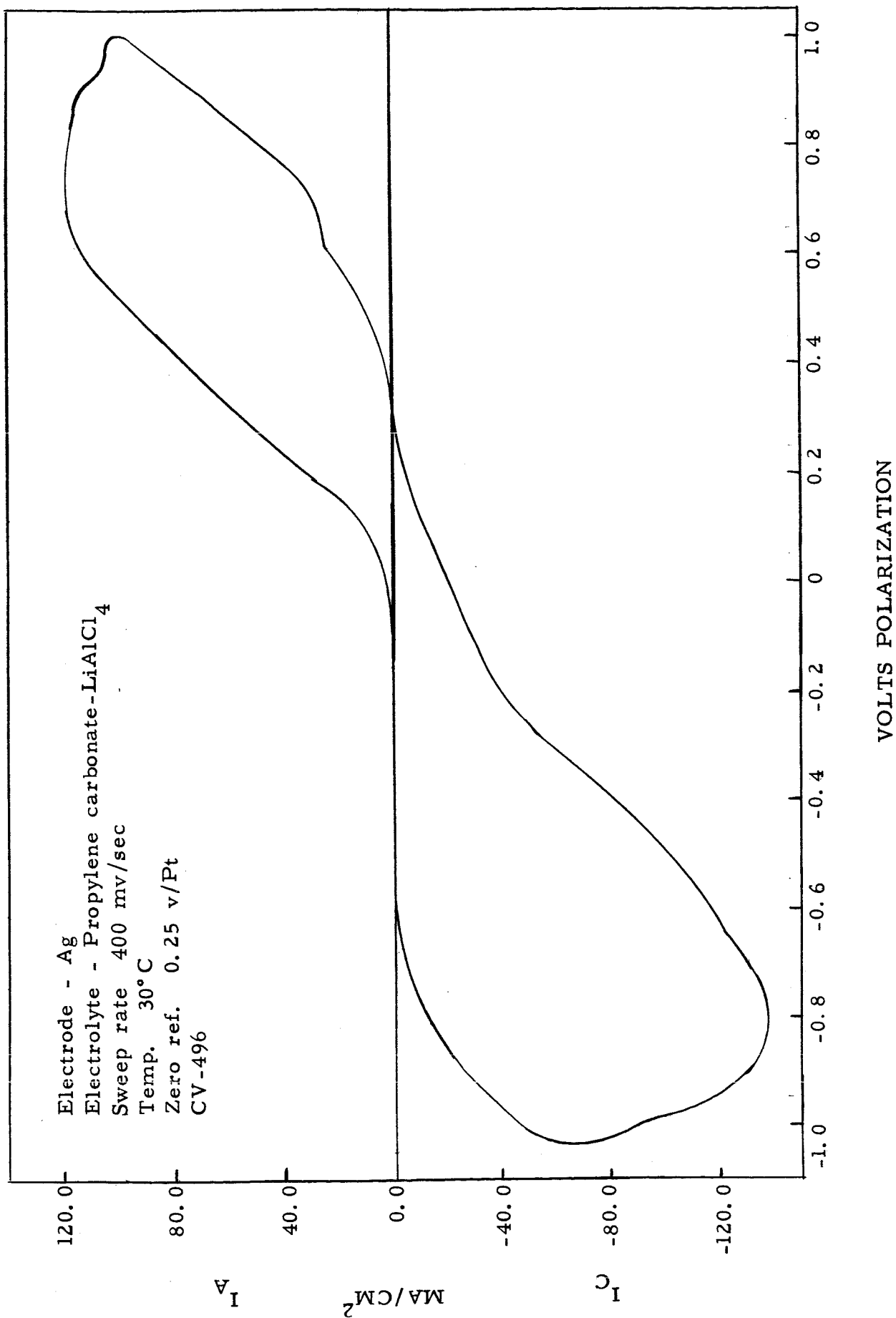
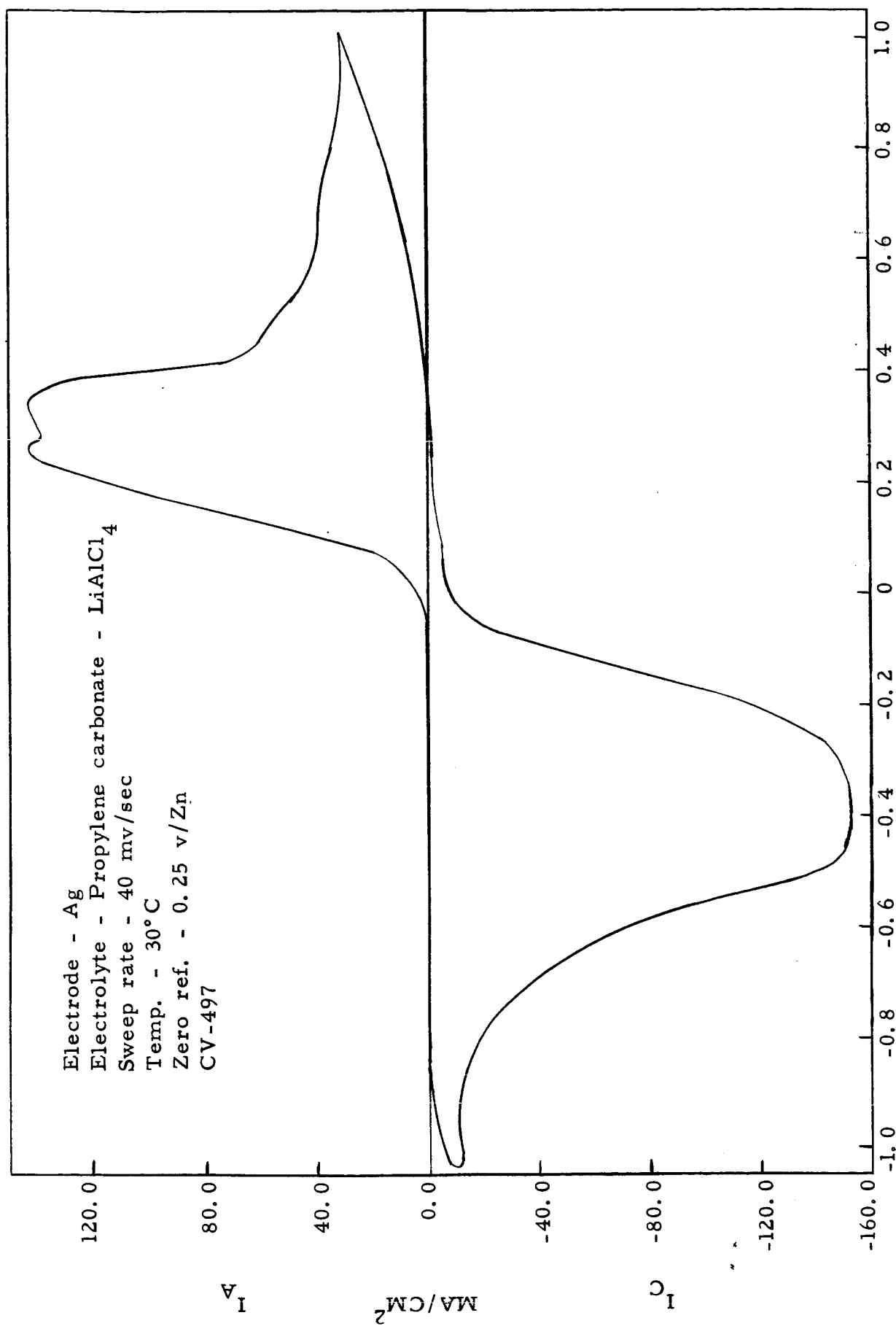


Figure 25



VOLT POLARIZATION

Figure 26

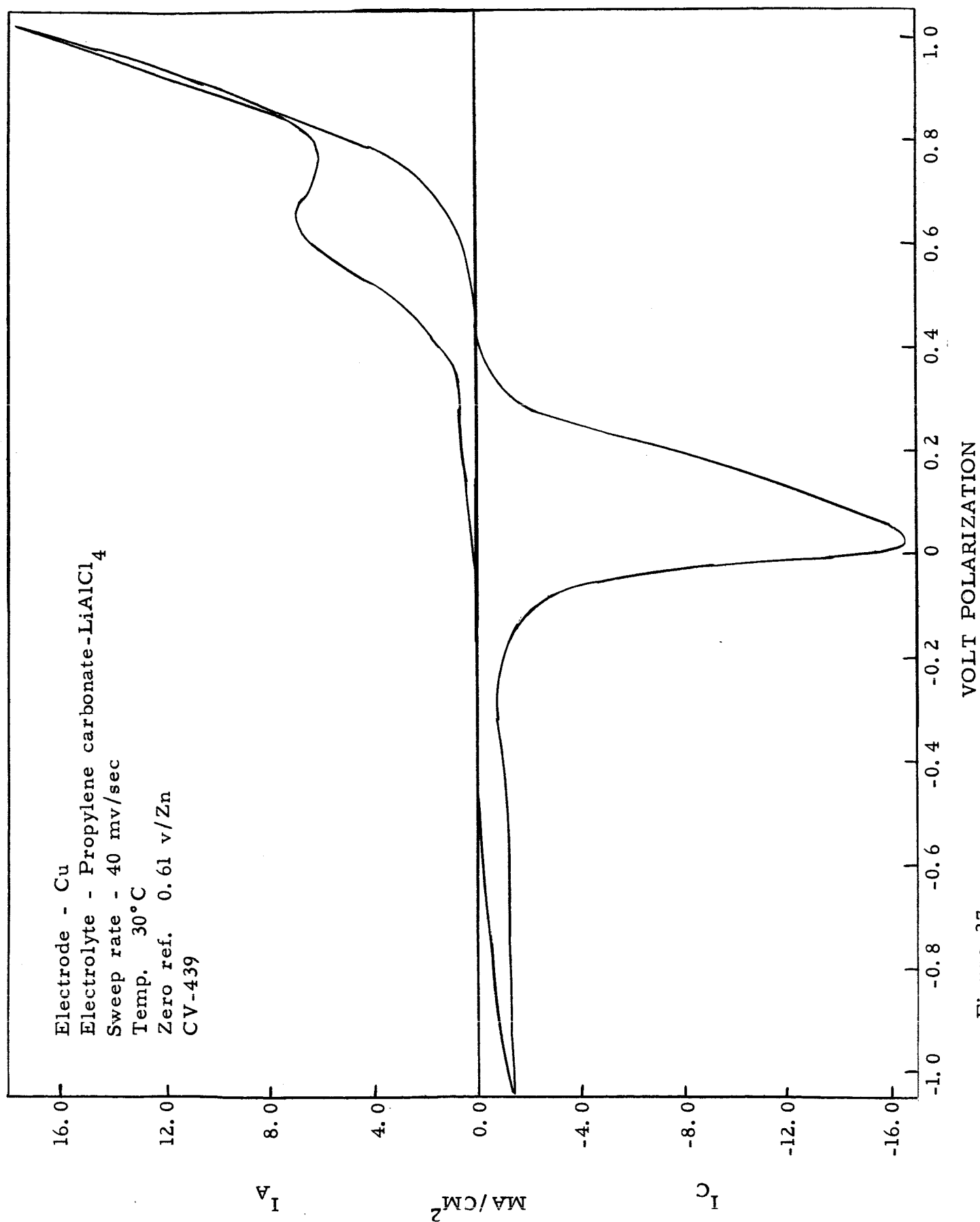
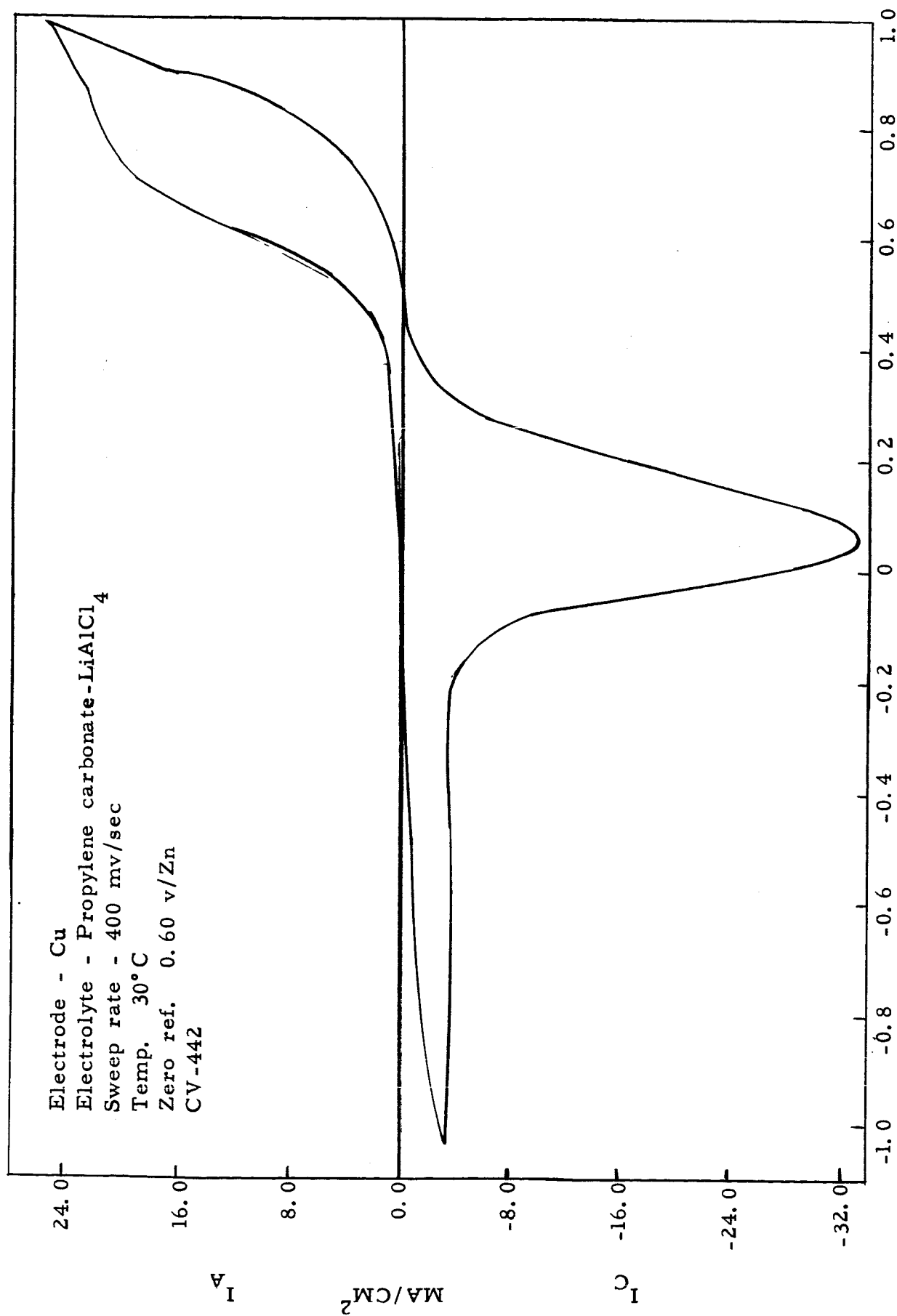


Figure 27



VOLTS POLARIZATION

Figure 28

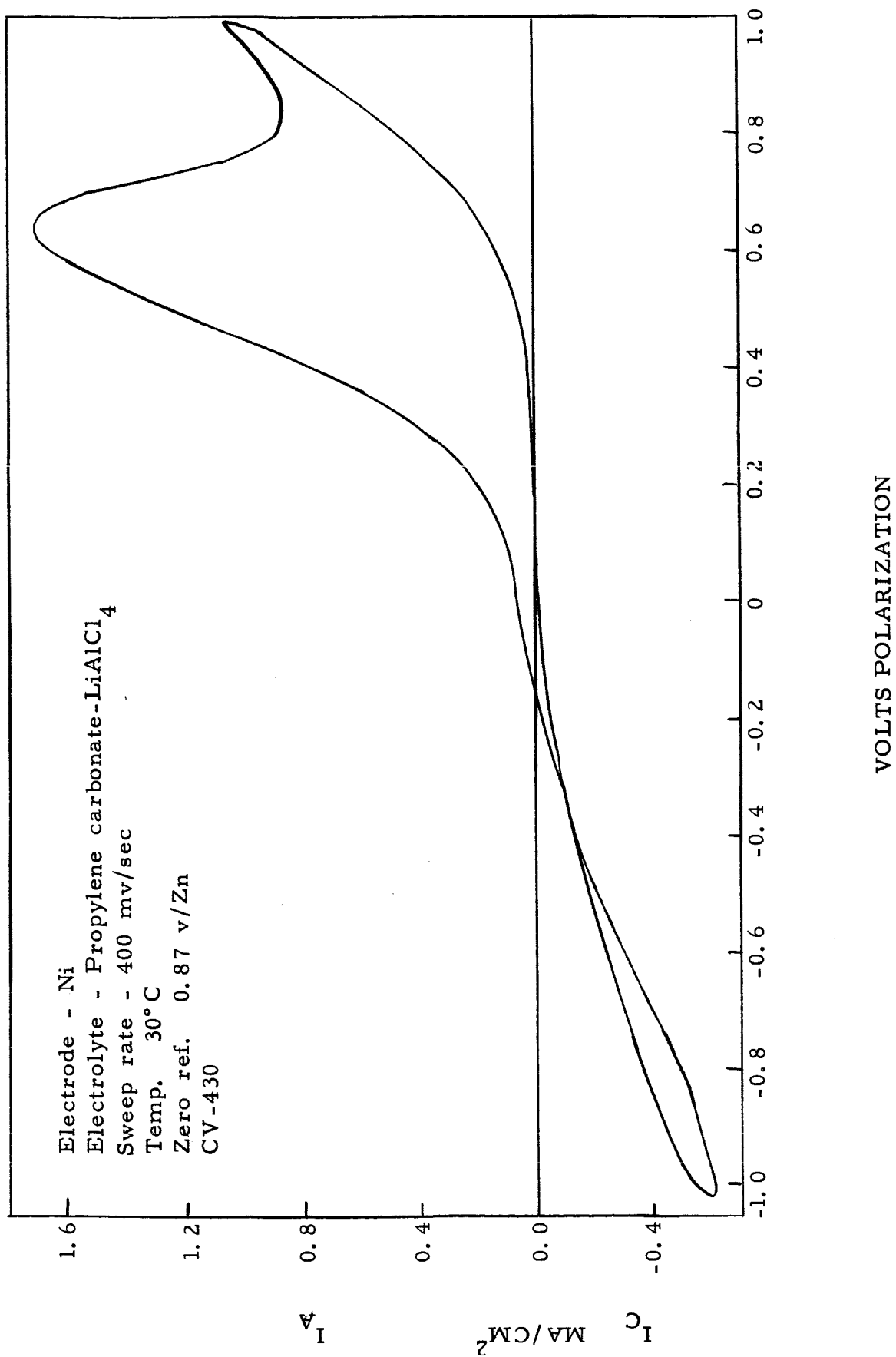


Figure 29

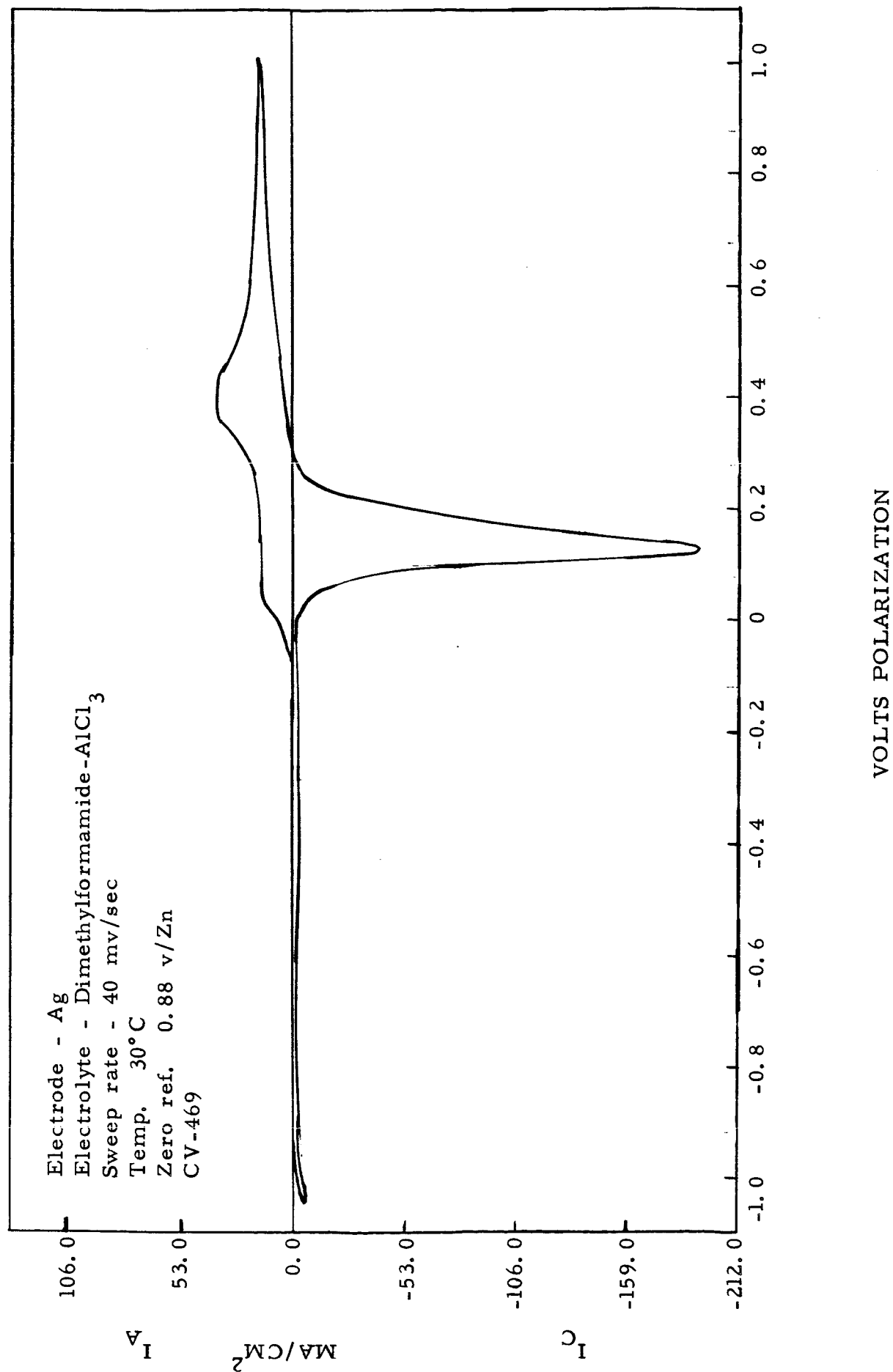


Figure 30

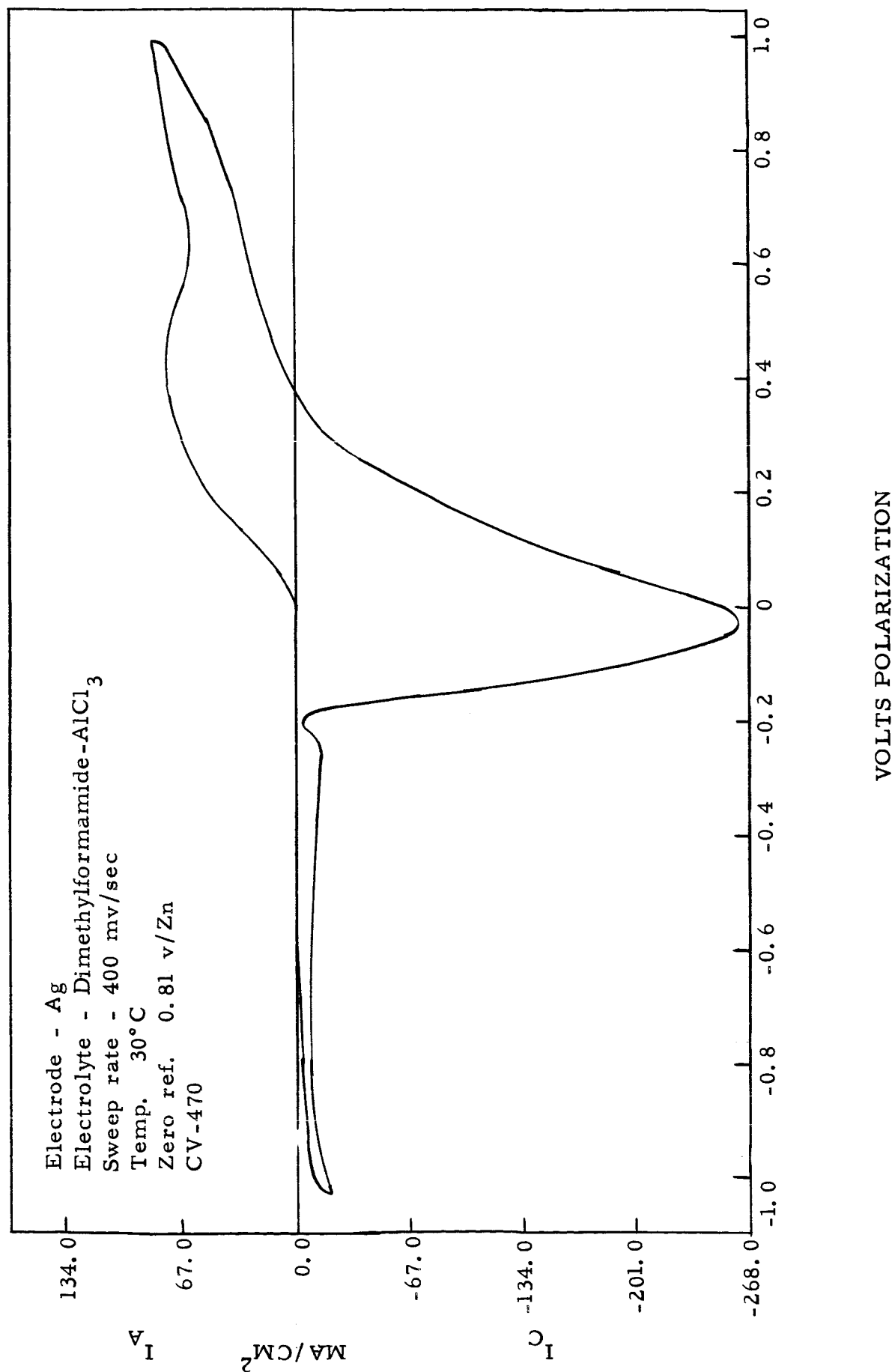


Figure 31

Electrode - Cu  
 Electrolyte - Dimethylformamide- $\text{AlCl}_3$   
 Sweep rate - 20 mv/sec  
 Temp.  $30^\circ\text{C}$   
 Zero ref. 0.66 v/Zn  
 CV-99

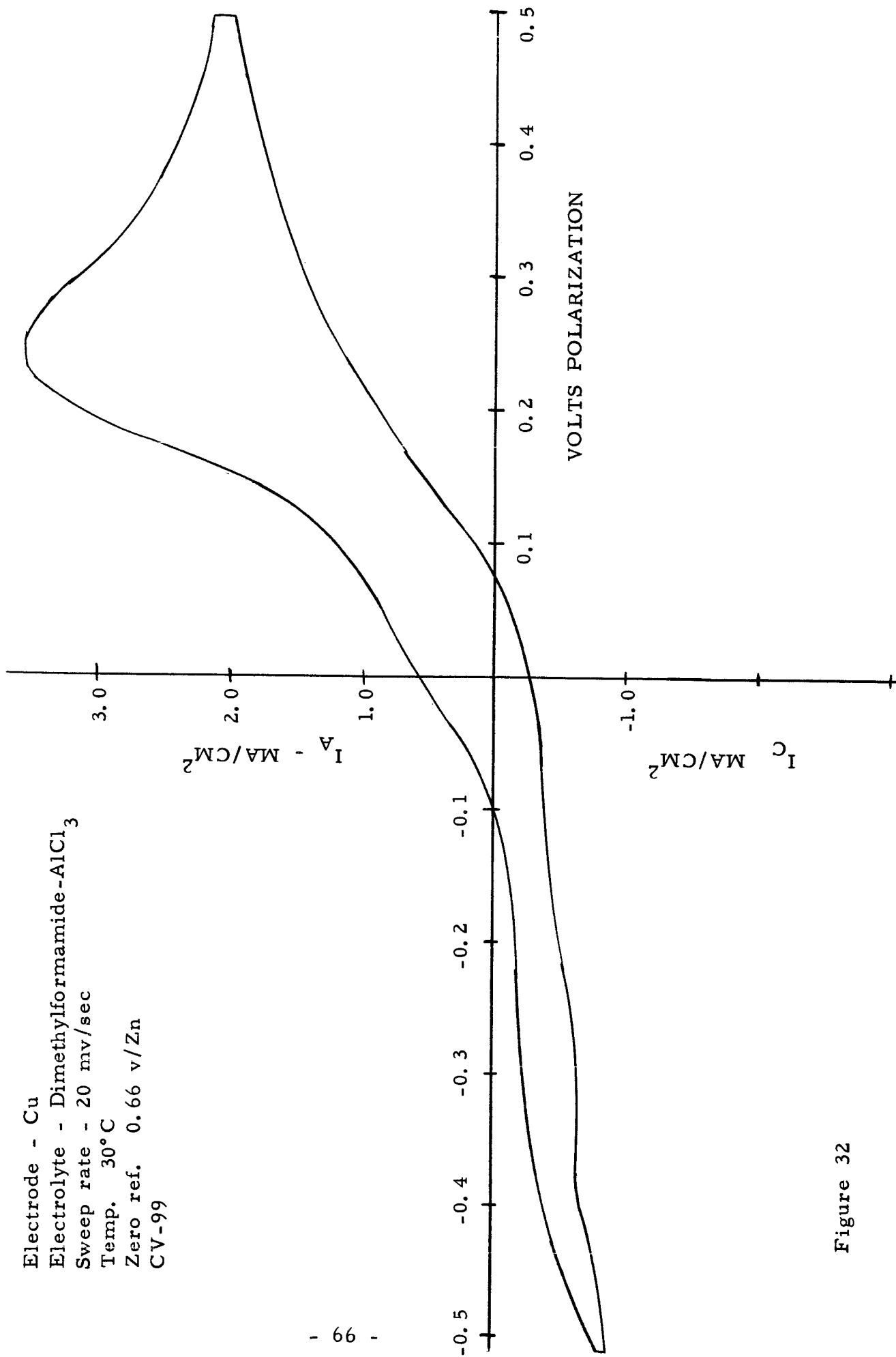


Figure 32

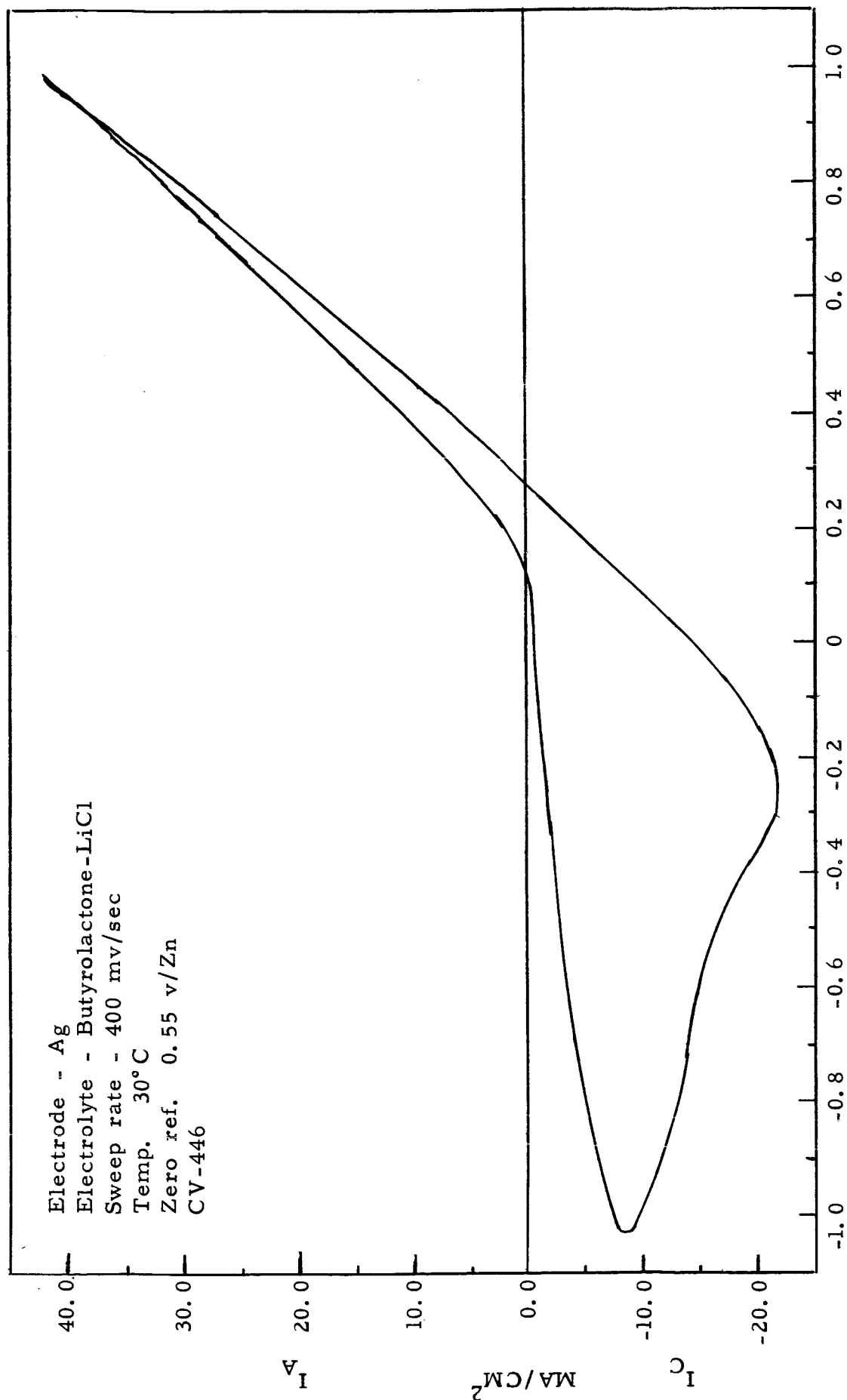


Figure 33

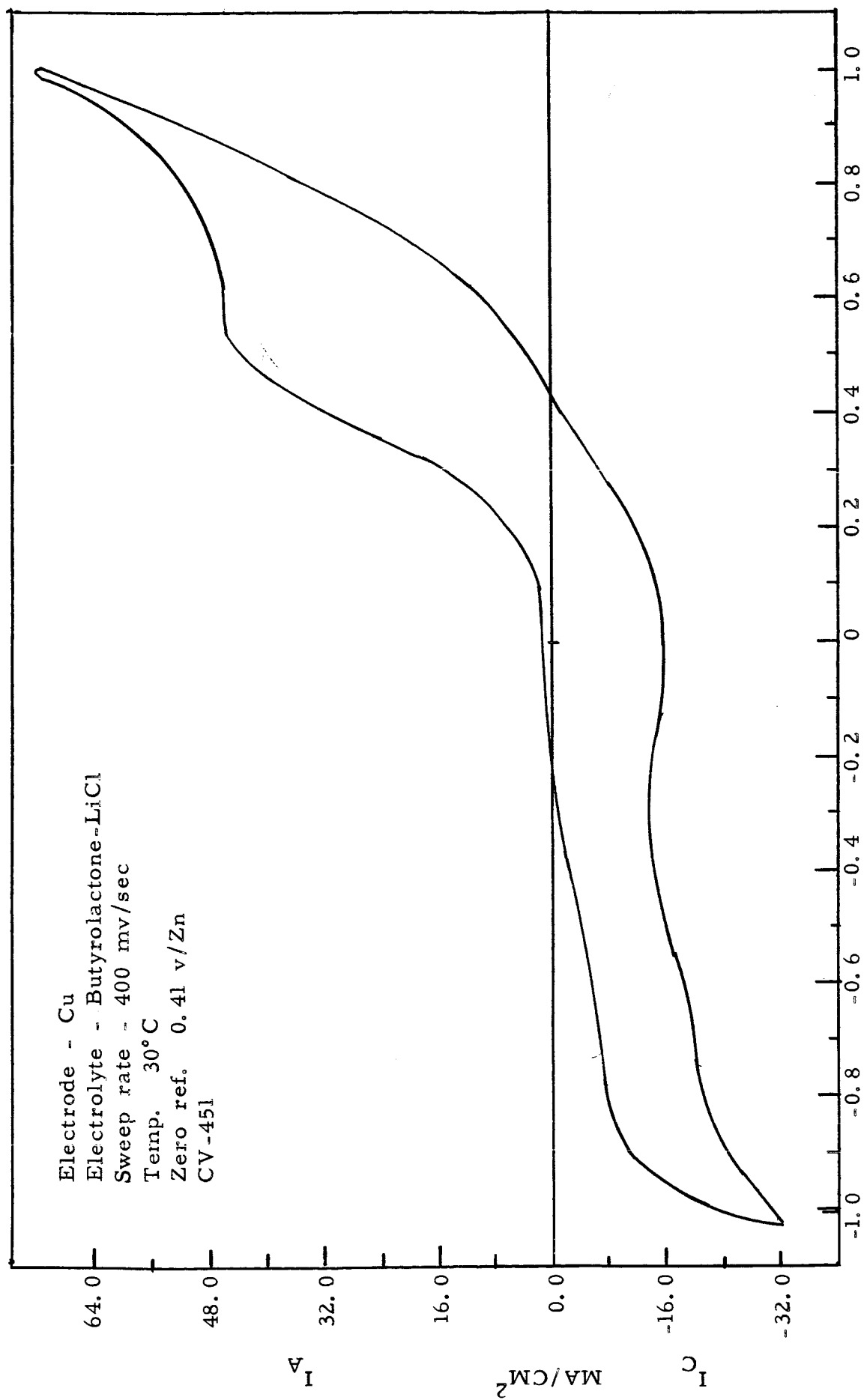


Figure 34

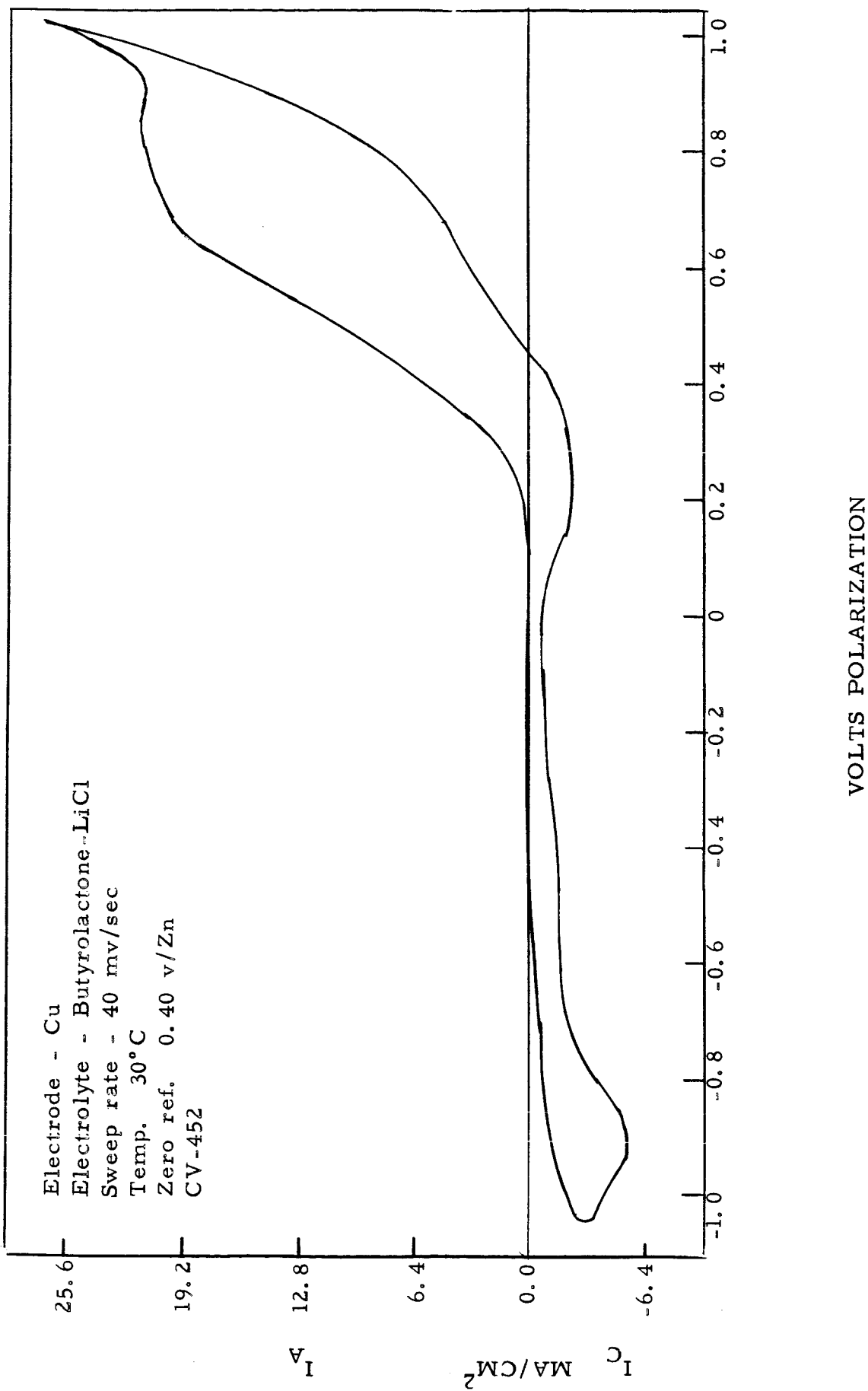


Figure 35

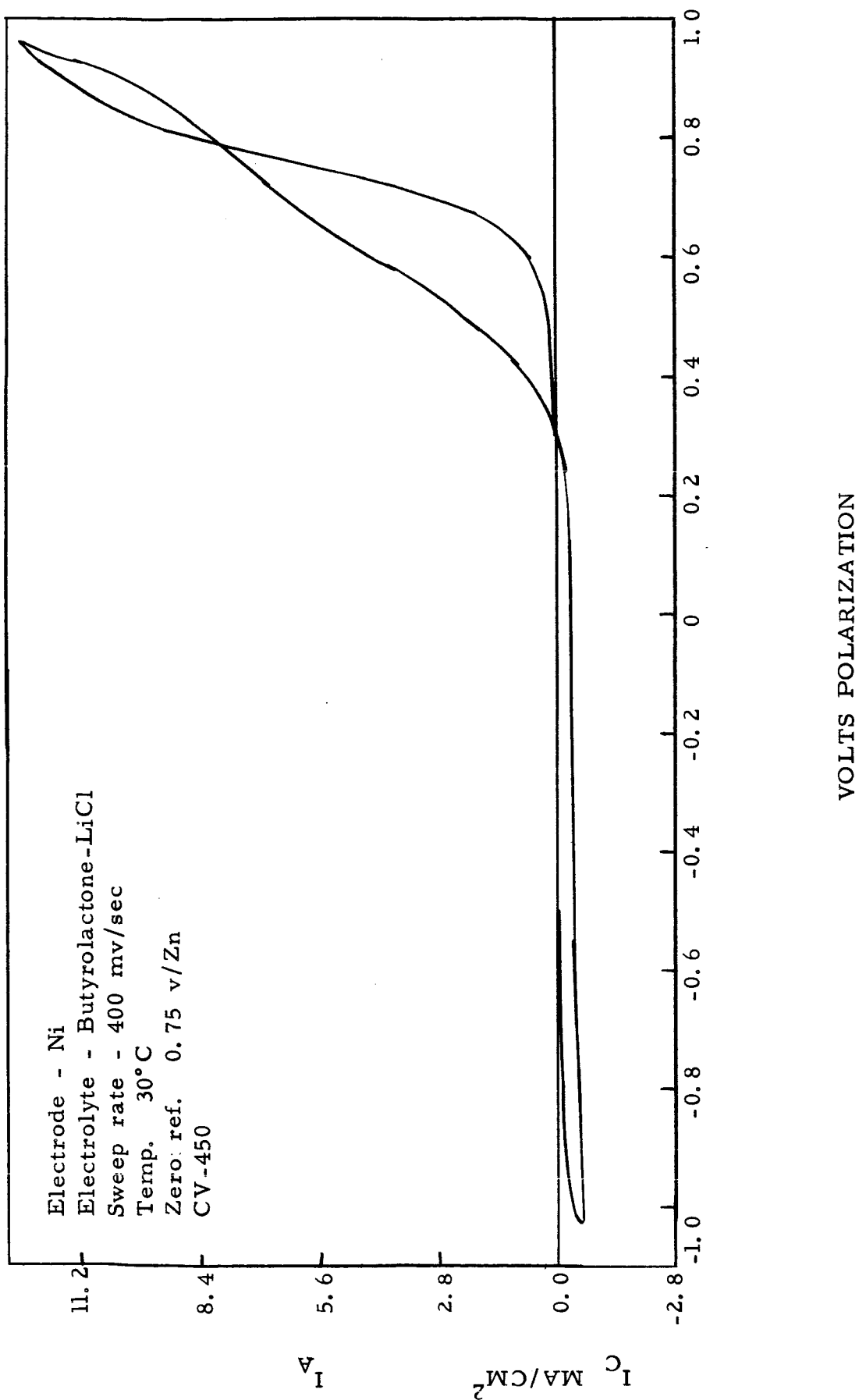


Figure 36

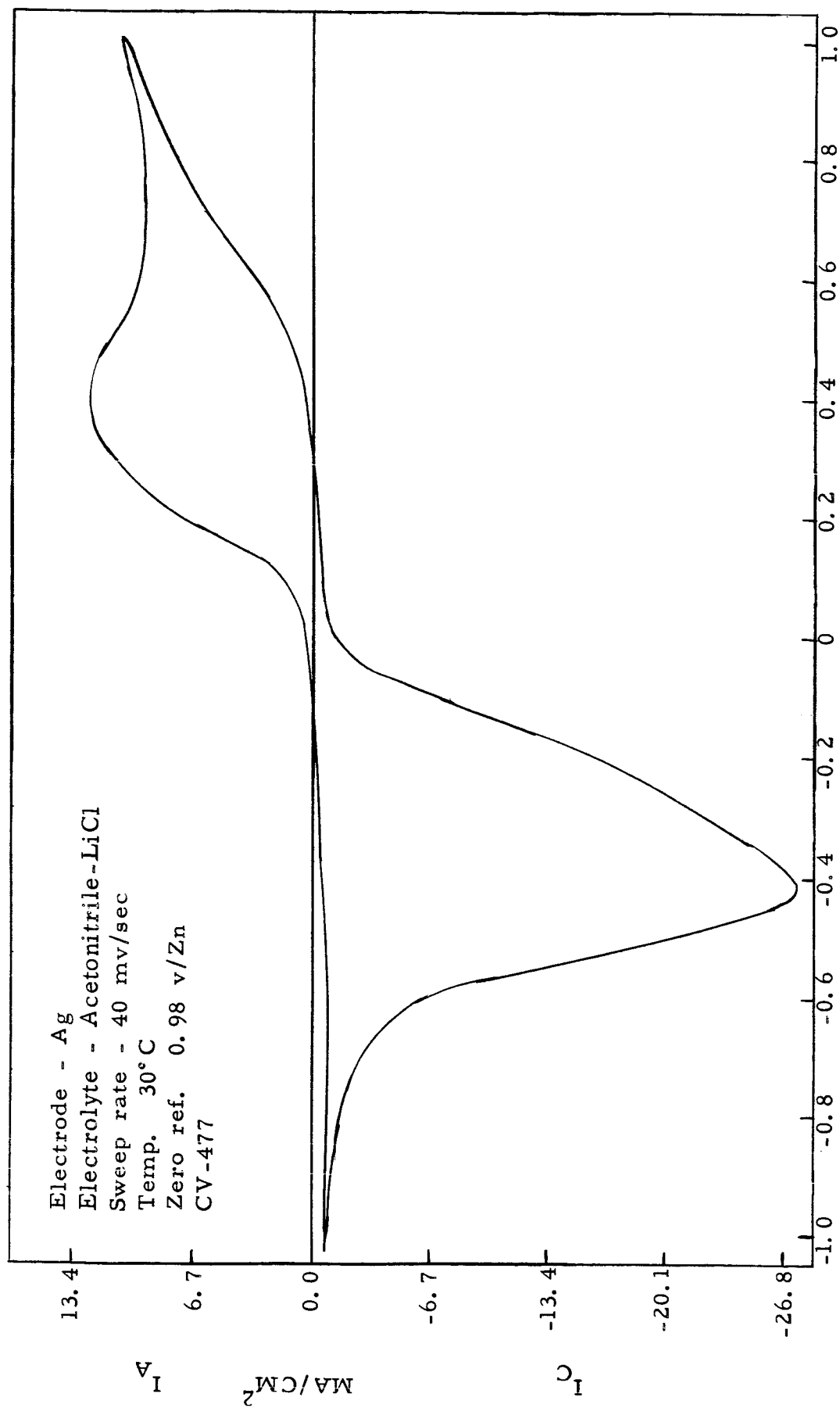
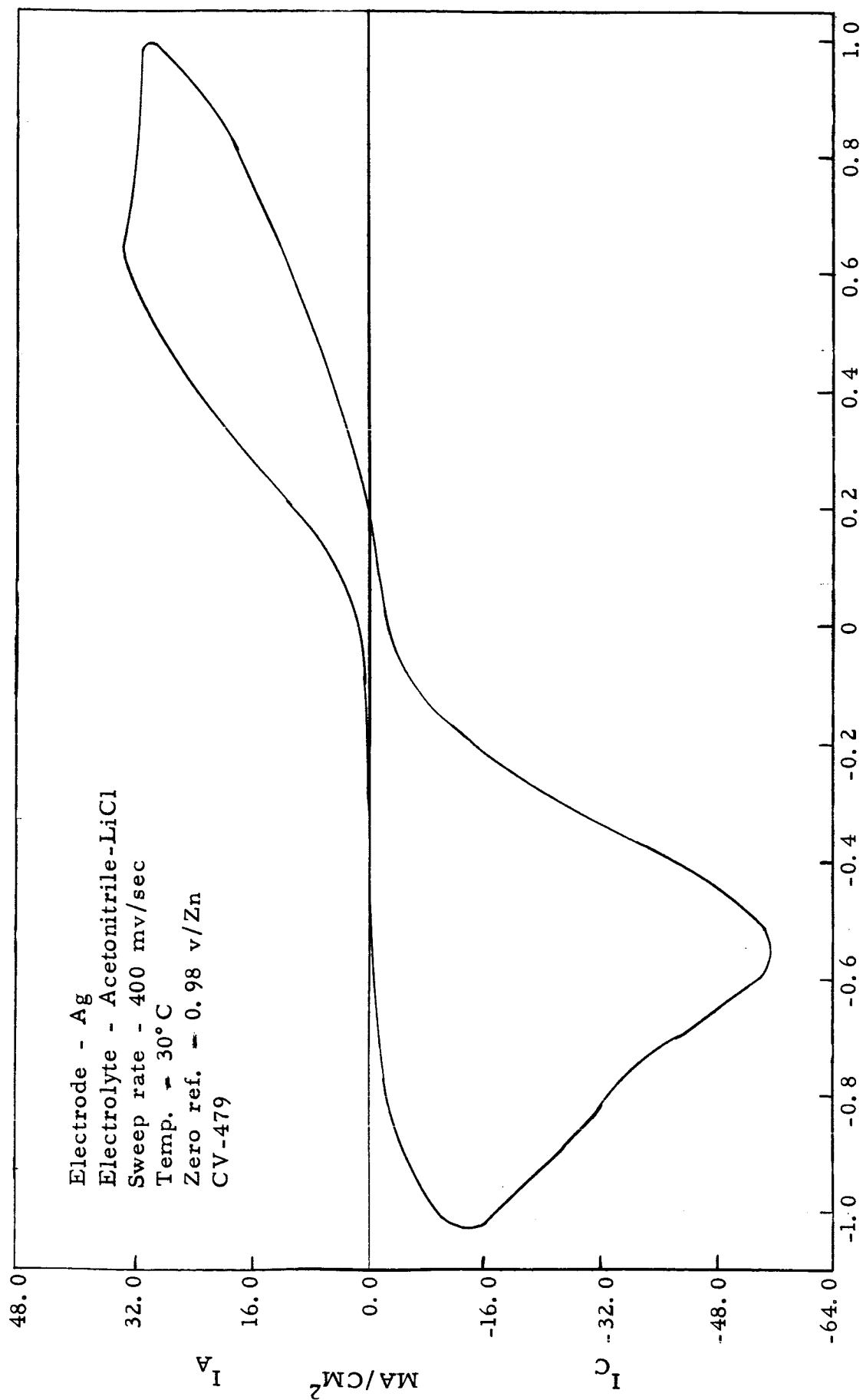


Figure 37



VOLTS POLARIZATION

Figure 38

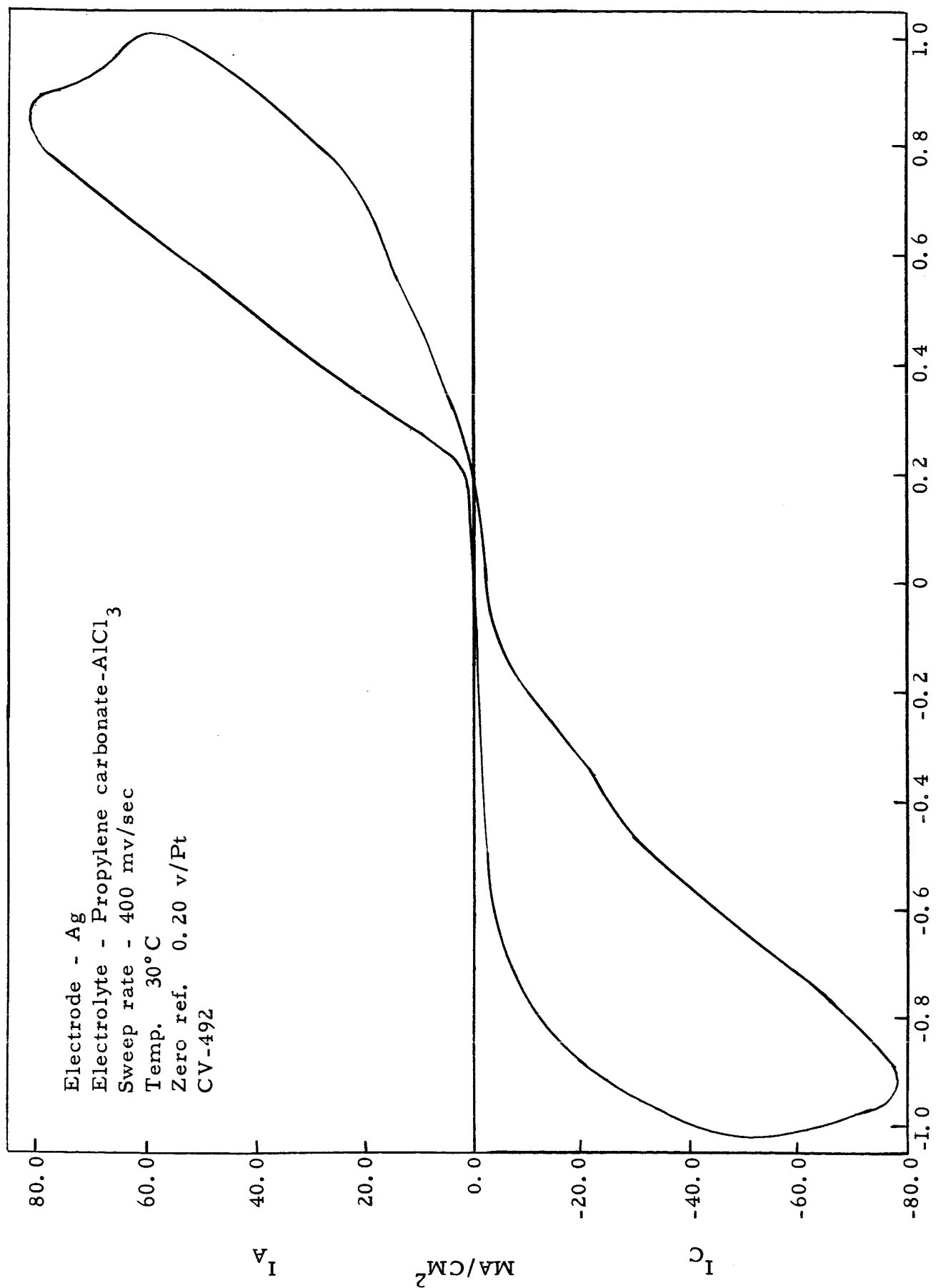
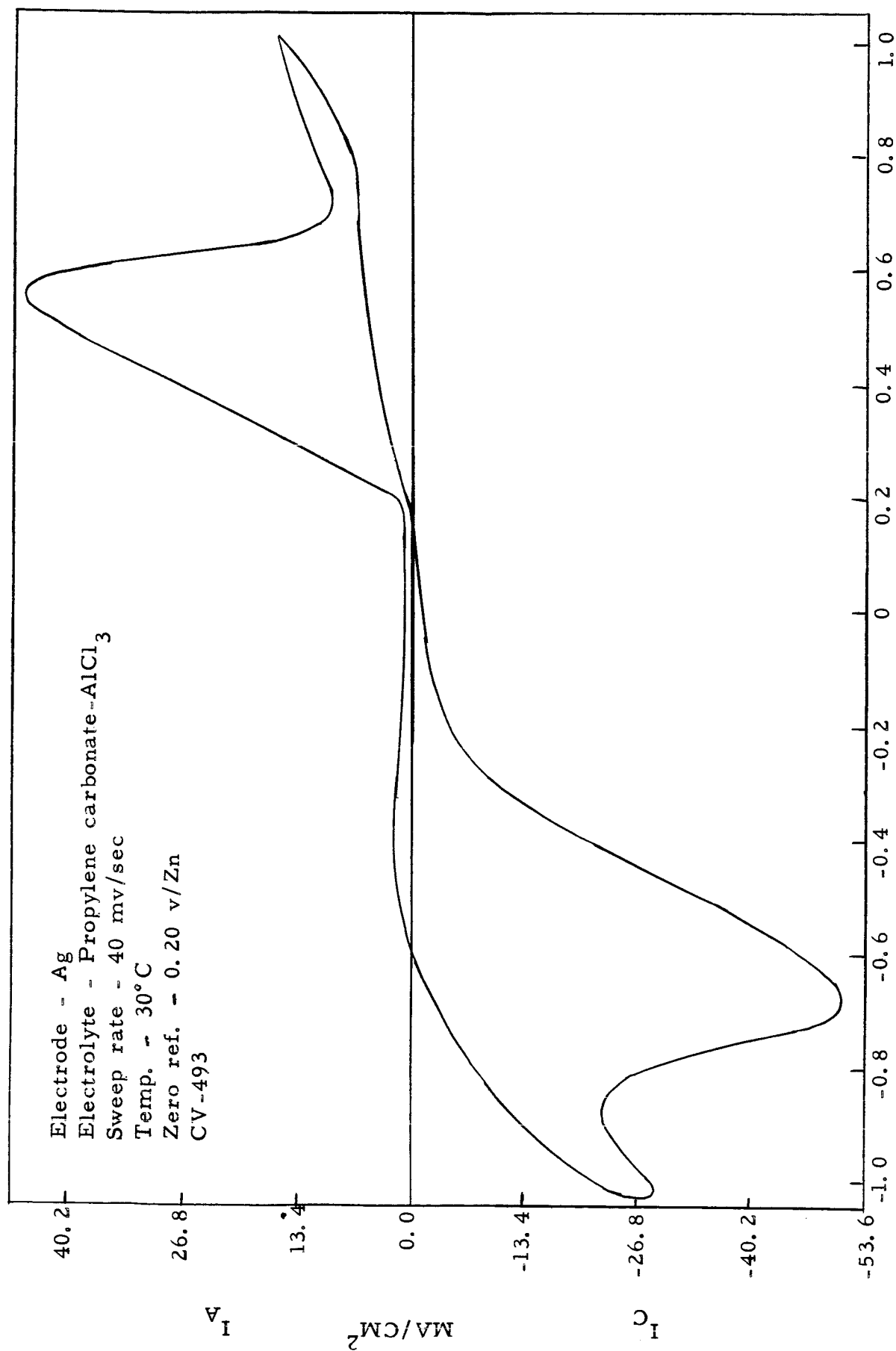


Figure 39



VOLTS POLARIZATION

Figure 40

Electrode - Cu  
 Electrolyte - Propylene carbonate-AlCl<sub>3</sub>  
 Sweep rate - 20 mv/sec  
 Temp. 30°C  
 Zero ref. 0.75 v/Zn  
 CV-125

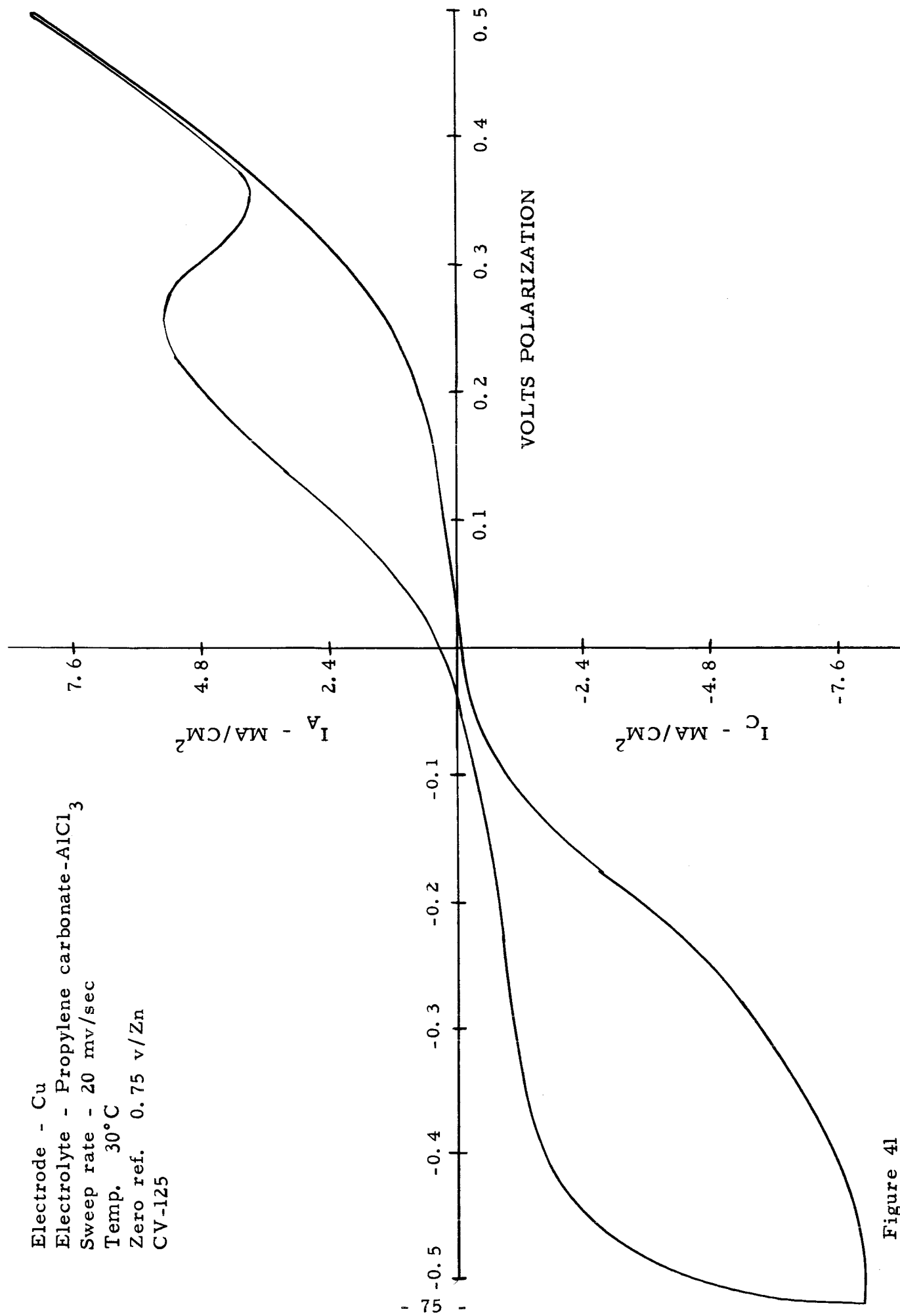


Figure 41

Electrode - Silver oxide  
 Electrolyte - Dimethylformamide-LiPF<sub>6</sub>  
 Sweep rate -200 mv/sec  
 Temp. 30°C  
 Zero ref. 1.56 v/Zn  
 CV-336

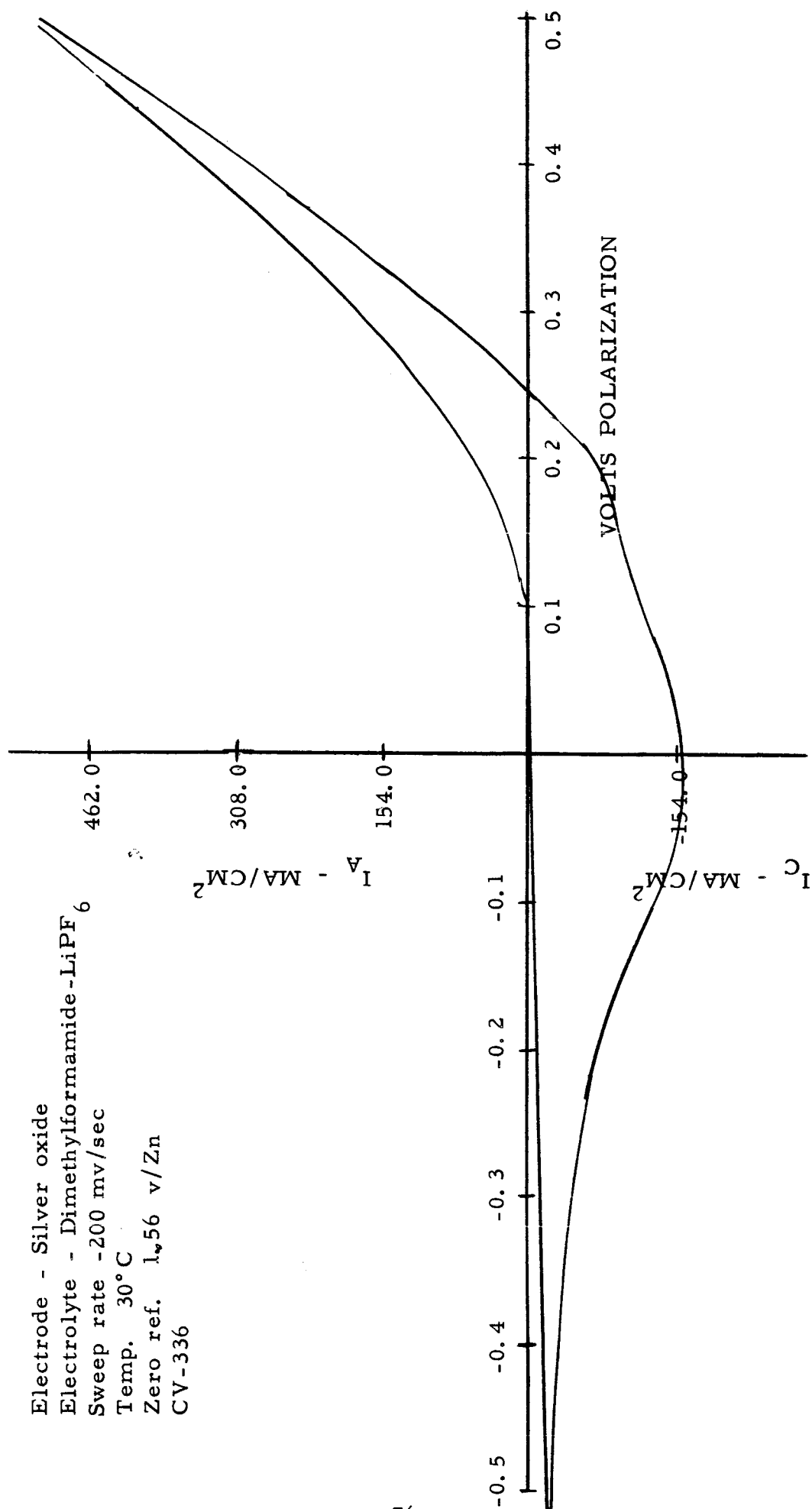


Figure 42

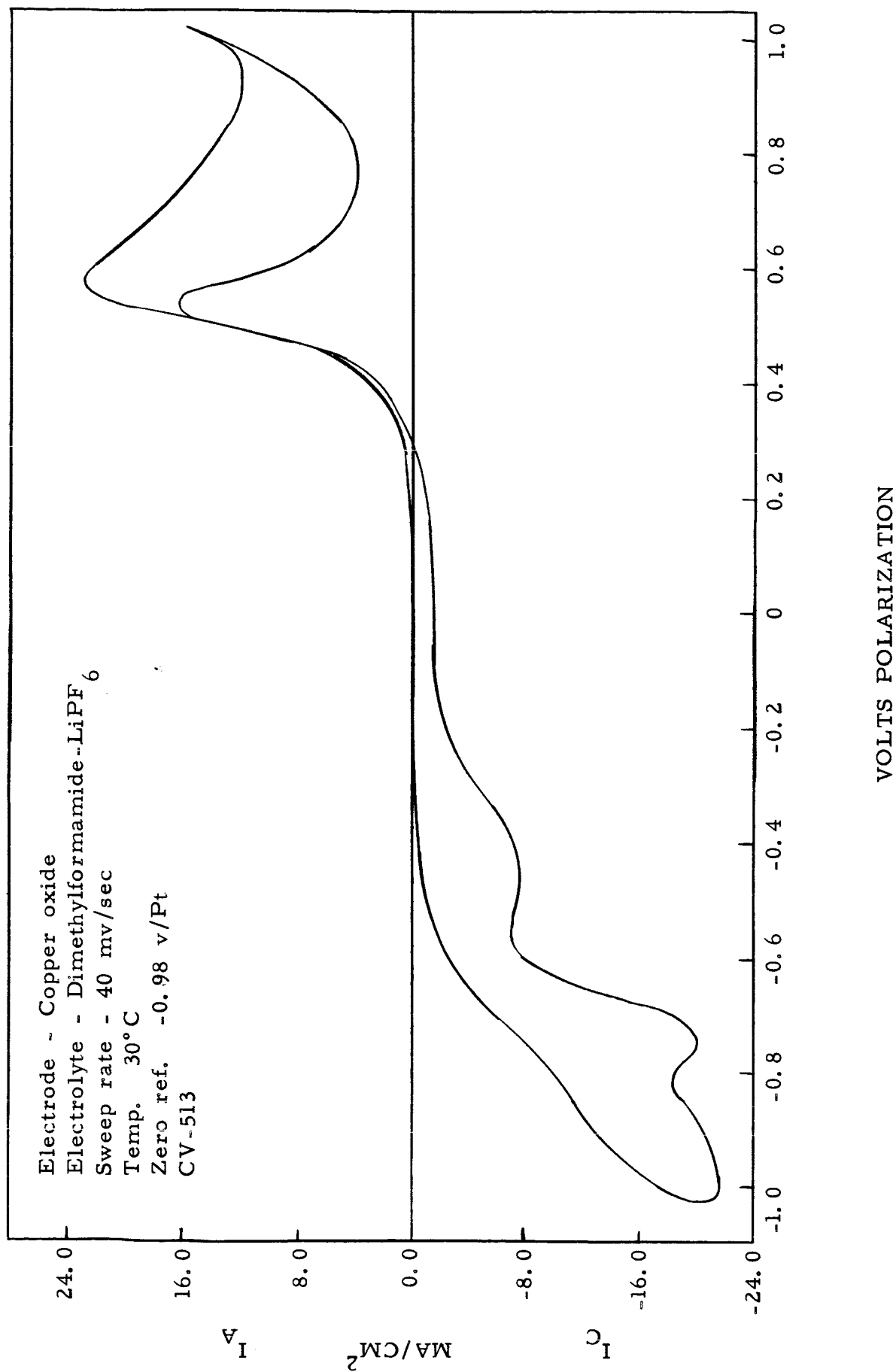


Figure 43

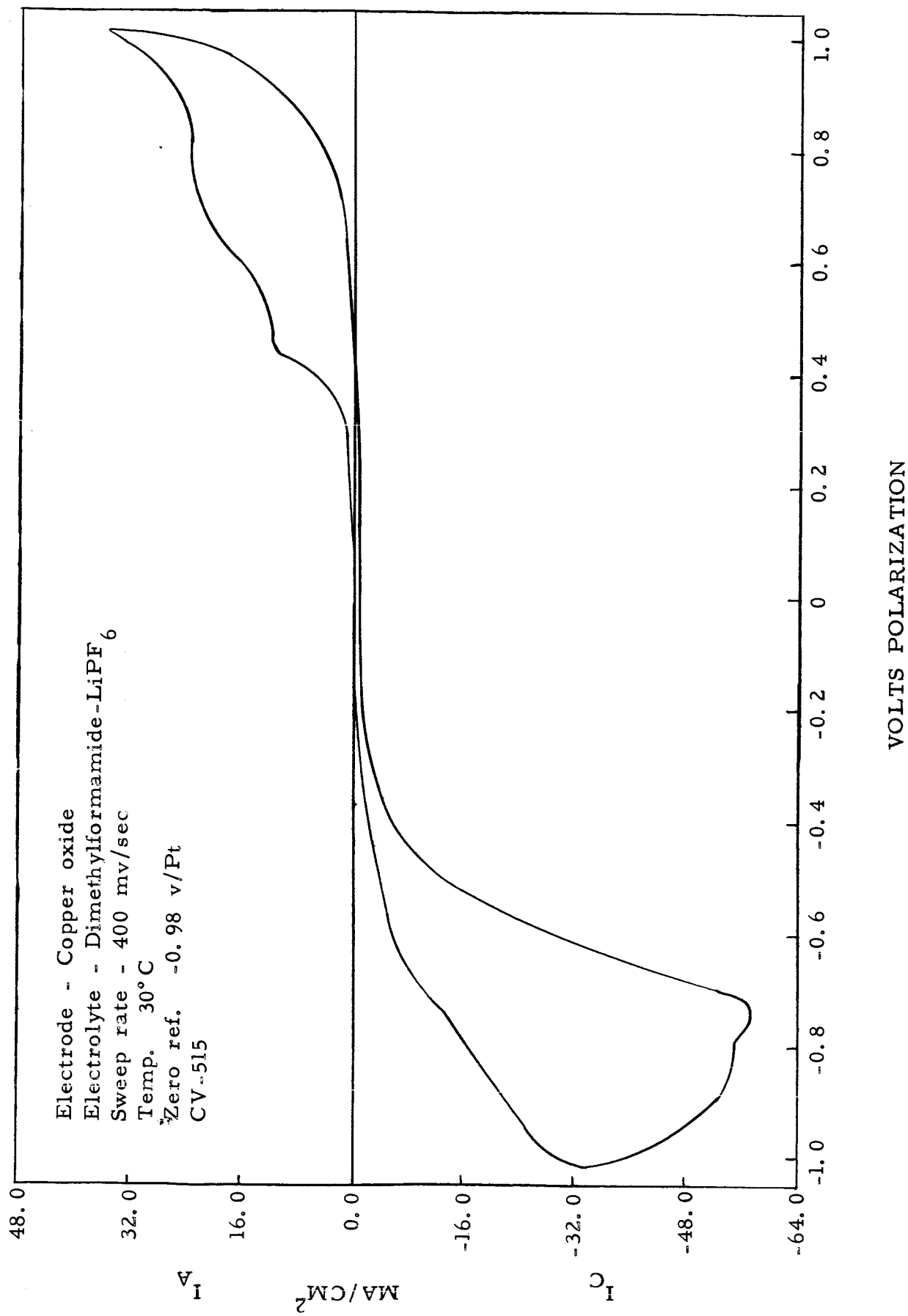


Figure 44

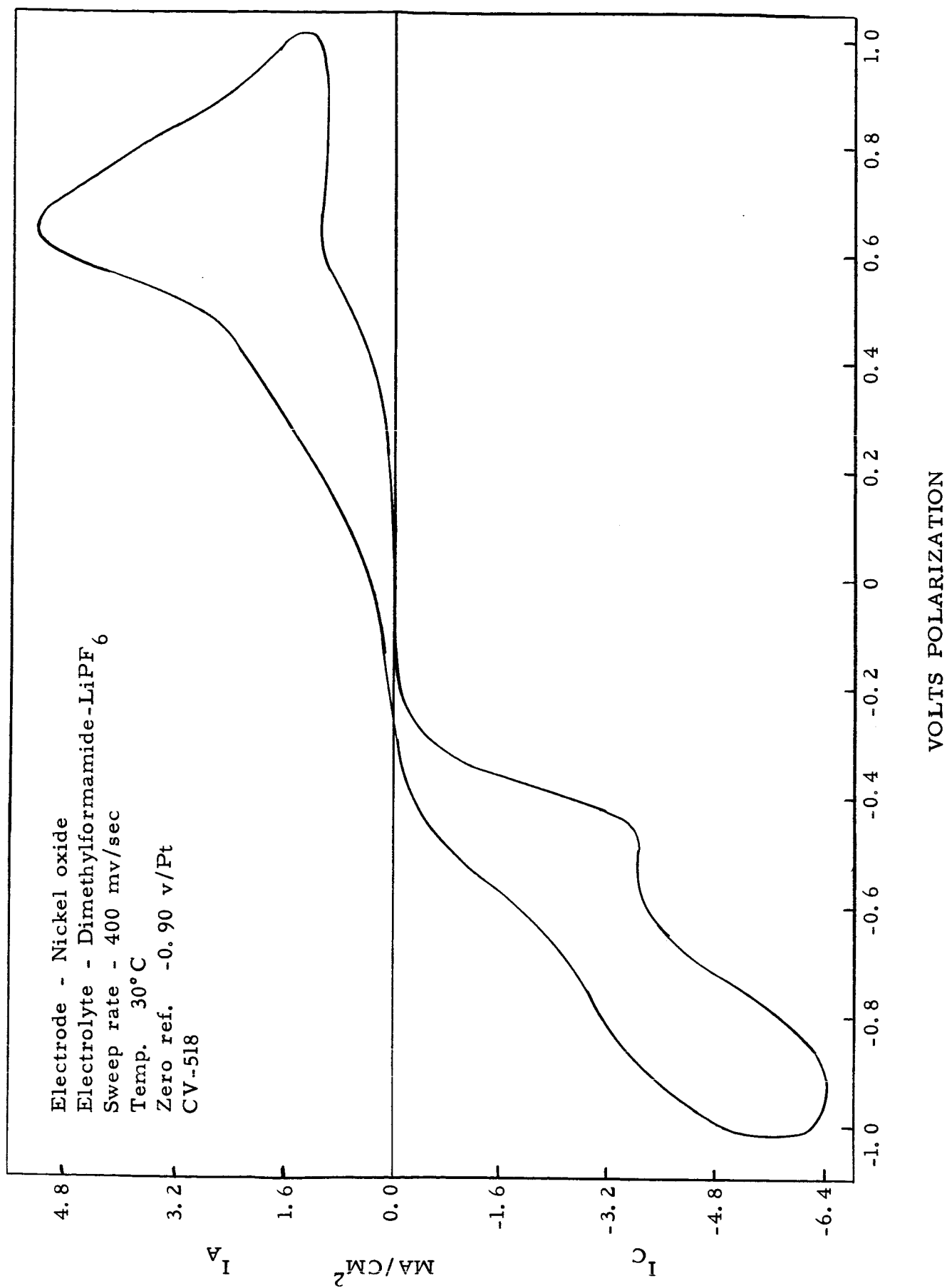


Figure 45

#### D. Sweep Index as a Relative Figure of Merit

As expected, the electrochemical systems screened to date demonstrate activation and concentration polarization, and electrochemical reactivity (peak height) to varying degrees. Visual examination of the cyclic voltammograms gives indication as to the magnitude of these parameters. In order to properly compare the extent of polarization among the different systems it would be necessary to record the peak heights, peak area, and the slope of the ascending portion of the peak. In addition these will be a function of sweep rate. A relative figure of merit would be desirable for the purpose of comparing the cyclic voltammograms, and might even serve as a threshold value to decide acceptance or elimination of any system in terms of further interest. The Sweep Index has been chosen for this purpose, and is defined as

$$\frac{(\text{Peak Current Density})^2}{\text{Sweep Rate} \times \text{Coulombs/cm}^2}$$

The dimensions of the Sweep Index are in  $\text{ohm}^{-1}\text{-cm}^{-2}$  units, or conductance per cm. It is intended only that Sweep Index be a semi-quantitative measure of the reaction rate and coulombic capacity for comparative purposes.

High Sweep Index values reflect higher reaction rates. Minimal activation polarization results in sharper peaks and lower peak areas leading to high index values. Solvent decomposition will result in larger areas, and therefore lower sweep indices. The sweep index values for a number of systems are presented in Tables III and IV for the anodic and cathodic peaks respectively.

TABLE III SWEEP INDEX - ANODIC

<u>System</u>	<u>Figure</u>	<u>Sweep Index</u>
Cu/Acetonitrile-LiClO <sub>4</sub>	4	590
Cu/Acetonitrile-LiF	21	193
Cu/Acetonitrile-LiPF <sub>6</sub>	18	162
Ag/Dimethylformamide-LiBF <sub>4</sub>	5	86.6
Ag/Butyrolactone-LiClO <sub>4</sub>	14	76.1
Cu/Butyrolactone-LiClO <sub>4</sub>	12	21.4
Ag/Butyrolactone-AlCl <sub>3</sub>	39	11.5
Ag/Propylene carbonate-LiAlCl <sub>4</sub>	25	10.1
Ag/Dimethylformamide-AlCl <sub>3</sub>	31	7.1
Ag/Acetonitrile-LiCl	38	3.2
Cu/Propylene carbonate-LiAlCl <sub>4</sub>	28	3.2
Cu/Propylene carbonate-AlCl <sub>3</sub>	41	0.9
Cu/Dimethylformamide-AlCl <sub>3</sub>	32	0.8

TABLE IV SWEEP INDEX - CATHODIC

<u>System</u>	<u>Figure</u>	<u>Sweep Index</u>
Ag/Dimethylformamide- $\text{AlCl}_3$	30	220
Cu/Butyrolactone- $\text{LiClO}_4$	12	144*
Ag/Acetonitrile- $\text{LiPF}_6$	17	75.0
Cu/Acetonitrile- $\text{LiClO}_4$	4	53.0
Ag/Dimethylformamide- $\text{LiBF}_4$	5	42.1
Cu/Propylene carbonate- $\text{LiBF}_4$	10	40.0
Cu/Butyrolactone- $\text{LiClO}_4$	11	29.6*
Ag/Butyrolactone- $\text{LiClO}_4$	14	26.3
Ag/Acetonitrile- $\text{LiBF}_4$	19	23.7
Ag/Acetonitrile- $\text{LiClO}_4$	3	16.6
Ag/Propylene carbonate- $\text{LiAlCl}_4$	25	15.7
Cu/Dimethylformamide- $\text{LiPF}_6$	9	15.1
Ag/Propylene carbonate- $\text{AlCl}_3$	39	13.2
Cu/Propylene carbonate- $\text{LiAlCl}_4$	28	8.4
Ag/Acetonitrile- $\text{LiCl}$	38	8.0
Cu/Propylene carbonate- $\text{AlCl}_3$	41	2.3
Ag/Butyrolactone- $\text{LiCl}$	33	2.1

\*Greatly differing sweep indices result for the same system because the cathodic reaction involves soluble copper species, and the peak changes rapidly due to dissolution of anodic product in the electrolyte.

#### E. Nature and Compatibility of Cathodes

In all systems except butyrolactone- $\text{LiClO}_4$  and dimethylformamide- $\text{AlCl}_3$  the cathodic reaction involved reduction of a solid product formed at the electrode during the anodic portion of the sweep. In many of these cases the cathode material dissolved in the electrolyte so that at low sweep rates, little or no cathodic reaction was evident. Tables V and VI list the nature and compatibility of the formed cathodic material for silver and copper in the various electrolytes.

TABLE V REACTIONS INVOLVING SILVER ELECTRODE

<u>System</u>	<u>Cathodic Reaction</u>	<u>Cathode Stability</u>
Acetonitrile-LiClO <sub>4</sub>	solid state	soluble
Butyrolactone-LiClO <sub>4</sub>	dissolved species	soluble
Propylene carbonate-AlCl <sub>3</sub>	solid state	insoluble
Dimethylformamide-LiAlCl <sub>4</sub>	solid state	soluble
Propylene carbonate-LiAlCl <sub>4</sub>	solid state	insoluble
Dimethylformamide-AlCl <sub>3</sub>	solid state	soluble
Butyrolactone-LiCl	solid state	insoluble
Acetonitrile-LiCl	solid state	insoluble
Dimethylformamide-LiCl	solid state	soluble
Dimethylformamide-LiBF <sub>4</sub>	solid state	soluble
Propylene carbonate-LiBF <sub>4</sub>	solid state	soluble
Dimethylformamide-LiPF <sub>6</sub>	solid state	soluble
Acetonitrile-LiPF <sub>6</sub>	solid state	soluble
Acetonitrile-LiBF <sub>4</sub>	solid state	soluble

TABLE VI REACTIONS INVOLVING COPPER ELECTRODE

<u>System</u>	<u>Cathodic Reaction</u>	<u>Cathode Stability</u>
Acetonitrile-LiClO <sub>4</sub>	solid state	insoluble
Butyrolactone-LiClO <sub>4</sub>	dissolved species	soluble
Propylene carbonate-AlCl <sub>3</sub>	solid state	insoluble
Dimethylformamide-LiAlCl <sub>4</sub>	solid state	soluble
Propylene carbonate-LiAlCl <sub>4</sub>	solid state	insoluble
Dimethylformamide-AlCl <sub>3</sub>	dissolved species	soluble
Butyrolactone-LiCl	solid state	insoluble
Acetonitrile-LiCl	no reaction	-
Dimethylformamide-LiCl	no reaction	-
Dimethylformamide-LiBF <sub>4</sub>	solid state	soluble
Propylene carbonate-LiBF <sub>4</sub>	solid state	soluble
Dimethylformamide-LiPF <sub>6</sub>	solid state	soluble
Acetonitrile-LiPF <sub>6</sub>	solid state	soluble
Acetonitrile-LiBF <sub>4</sub>	solid state	insoluble

## IV. EXPERIMENTAL

### A. Material Purification and Characterization

#### 1. Distillation of Solvents

The solvents used for the measurements were distilled at the indicated temperature and pressure in the same apparatus. Usually 1500 ml portions of solvent were distilled, with about 100 ml comprising the main cut and the remainder being divided between the head fraction and pot residue. Except for use in initial VPC work, only the main fraction was retained.

The distillation apparatus consisted of 1 inch by 3 feet vacuum jacketed (and silvered) column packed with 3/8" beryl saddles, and equipped with a total reflux return head. The head was connected to a revolving type multiple distillation receiver through a stopcock which was used to adjust the takeoff rate. The distillation head was also connected to the usual vacuum manifold consisting of rough and fine manometers connected in series with a Cartesian manostat, dry ice trap and vacuum pump.

After distillation startup and removal of low boiling impurities, the column was purposely flooded to insure proper wetting. It was then allowed to equilibrate over a 1-2 hour period and fractionation commenced. The main fractions were usually taken over a 48-hour period at reflux ratios of 20-25/1. Use of higher reflux ratios did not improve the fractionation characteristics.

## 2. Vapor Phase Chromatography

An Aerograph A-90-P vapor phase chromatograph equipped with a hot wire detector was used for the analysis under the conditions shown in Table VII. All analyses were obtained on a 1/4 inch by 6 feet s.s. column packed with 20% PEG 1540 on HMDS-treated 60/80 mesh chromosorb P. Use of a column packed with GE SF-96 silicone oil on 60/80 mesh firebrick afforded little or no resolution for the compounds investigated.

Usually 3-4  $\mu$ l samples were used in the order to reveal trace impurities without overloading the column. Stable baselines were obtained at maximum instrument sensitivity. No calibrations of the relative peak areas were made at this time.

## 3. Solution Preparation

All solutes, after drying under the conditions previously indicated, were stored in a desiccator over magnesium perchlorate. Physical manipulation of solvent and solute during electrolyte preparation was performed under a nitrogen mantle.

Most of the solutions were prepared in the following manner. 150 ml of solvent was placed in a 250 ml flask, equipped with a magnetic stirrer and thermometer. Small increments of solute were added with stirring (and cooling when necessary) until apparent saturation was reached. An additional amount (2-5g) of solute was then added and the solution allowed to stir overnight. If saturation was maintained during this period, the solution was filtered. An equal volume of solvent was added to the filtrate, and the conductance determined. If the solution did not maintain saturation, additional increments of the solute were added until

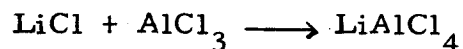
TABLE VII VAPOR PHASE CHROMATOGRAPHY CONDITIONS

<u>Solvent</u>	<u>Column Temp.</u> °C	<u>Injector Temp.</u> °C	<u>Detector Temp.</u> °C	<u>Helium Flow Rate</u> ml/min
Propylene carbonate	190	240	260	85
Dimethylformamide	160	238	260	40
Butyrolactone	171	235	250	120

saturation was maintained over a 24-hour period, and the solution was filtered and diluted as described above.

For the mixed salts, lithium fluoride - magnesium fluoride and lithium chloride - magnesium chloride, the period of stirring at saturation was extended to 48 hours.

Solutions of lithium chloride - aluminum chloride were prepared by initially saturating 150 ml of solvent with lithium chloride. An equimolar quantity of aluminum chloride was added to this solution over a 2-hour period, at 0° to 5°C. If saturation was maintained after stirring for 24 hours at room temperature, the solution was filtered and diluted as previously described. If saturation was not maintained, the saturation procedure was repeated. This method, in contrast to the fusion procedure described by other workers (Ref. 17), was used in order to facilitate the initial measurements. The initial results will be checked using fused material. However, because of the principle of microscopic reversibility, the solutions prepared by either method are expected to be the same as long as pure and dry materials are used. That is, if a true equilibrium exists for the reaction



then the same concentrations of each of the products and reactants will be reached at equilibrium, regardless of whether the solution is prepared from the individual salts or the complex salt. The possibility that a kinetic difference in the concentrations of the various species ( $\text{LiCl}$ ,  $\text{AlCl}_3$ ,  $\text{Al}_2\text{Cl}_6$ ,  $\text{AlCl}_4^-$ , etc.) affects side reactions with the solvent, cannot be eliminated at this time.

Conductivity measurements were obtained at 1000 cycles per second using an Industrial Instruments Inc. Model RC 16B2 conductivity bridge. A Tektronic Type 536 oscilloscope was placed in the detector arm for increased null sensitivity.

## B. Cyclic Voltammetric Measurements

### 1. Electrochemical Cell

Cyclic voltammetric measurements were made in a 3-electrode type shown in Figure 46. The reference electrode compartment and that of the main cell are filled with the same electrolyte to prevent solution junctions leading to voltage errors. The two compartments are attached to each other via an electrolyte bridge culminating in the main cell at a luggin capillary placed close to the surface of the working electrode, reducing ohmic losses to a minimum. The capillary tip is kept small in order to shield as little of the working electrode as possible to avoid localized polarization due to poor current distribution.

To facilitate handling, the working electrode was supported by a Teflon - glass holder designed to accommodate a 50-mil diameter wire as shown in Figure 47. The capillary tubing has one end pulled down slightly. The plug was machined from Teflon rod to a slightly undersized fit for the glass. The hole through the Teflon plug was also undersized. The cold flow property of Teflon resulted in a good seal. The wire was normally exposed to a 1 inch length, and was renewed by pulling it out further and cutting away the used portion. For those systems having high activity, it was necessary to expose a shorter length in order to reduce the current requirement.

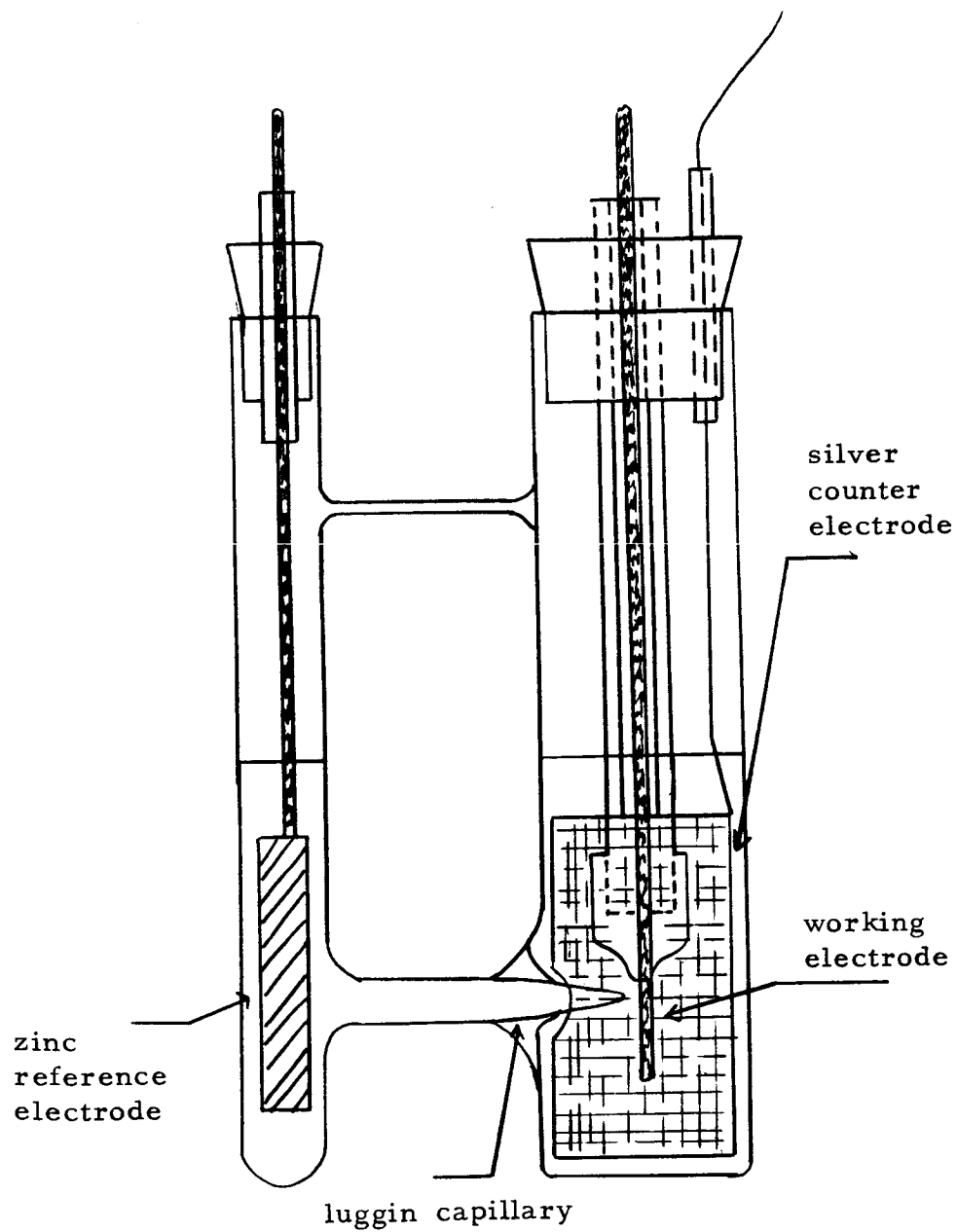


Figure 46 Measuring Cell for Cyclic Voltammetry

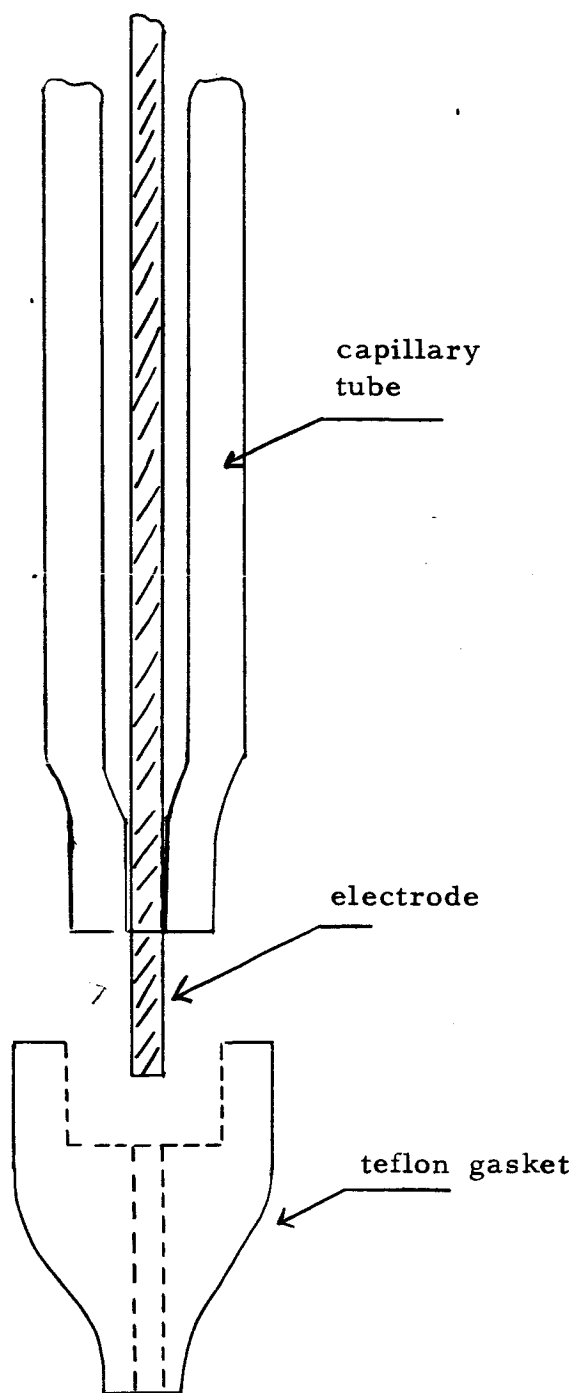


Figure 47 Working Electrode Detail

The counterelectrode consisted of a silver screen tube totally surrounding the working electrode in order to insure good current distribution.

## 2. Instrumentation

The instrumentation employed for the cyclic voltammetric measurements is schematically shown in Figure 48. Basic to the method is a potentiostat which maintains the voltage between the reference - working electrode couple at a value equal to the sum of the input reference voltages represented by the dc reference and function generator values. The potentiostat accomplishes this by controlling the current between the working and counterelectrodes. The potentiostat senses the difference between the reference - working electrode voltages and the sum of the reference input voltages by means of a high gain amplifier system, and feeds the output through the working electrode - counterelectrode couple. This amplifier has high input and low output impedance, and a rise-time less than  $10^{-4}$  sec. The system permits the measurement of current-voltage-time relationships under well-defined conditions. No voltage change is possible at the reference electrode, and the measurements reflect only the voltage changes at the working electrode - electrolyte interface independent of ohmic losses through the electrolyte and polarization at the counterelectrode.

Two types of potentiostats were employed. The Wenking TR61 was used for high currents and low voltages (less than 3 v). For higher voltages (up to  $\pm 100$  v) a laboratory constructed instrument employing operational amplifier modules was used. The modular circuit is limited to  $\pm 20$  ma, but was extended to higher values by use of a current amplifier. The use of

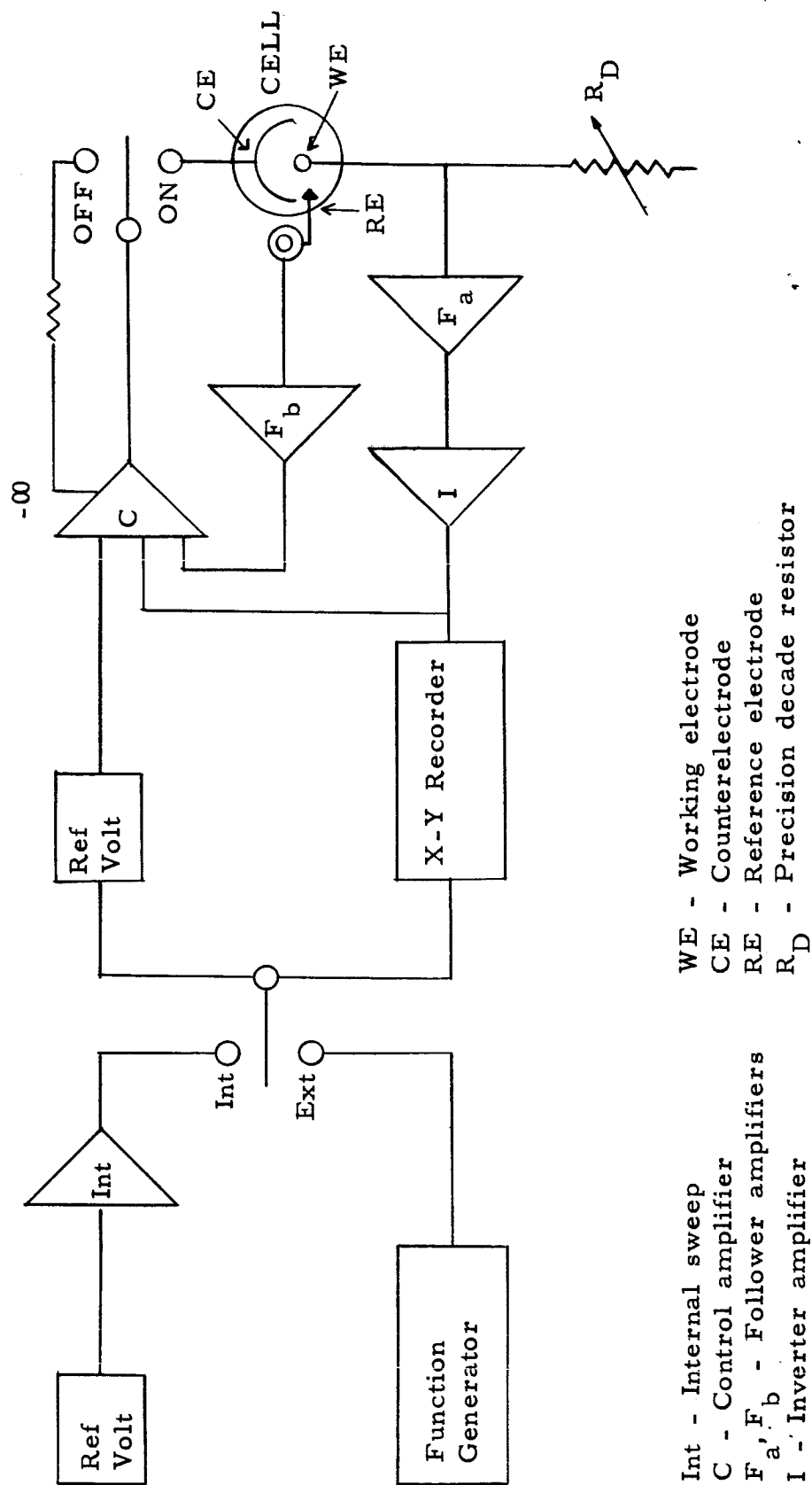


Figure 48 Block Diagram of Instrumentation

the Wenking potentiostat required that a buffer amplifier be used between the reference electrode and the potentiostat. This was necessary because the reference electrode input sensing circuit of the Wenking was too low for the type of reference electrodes employed in non-aqueous systems.

The function generator was the Hewlett-Packard Model 202A for cycle sweep repetition rates of 0.01 cps or greater. For frequencies less than this, an operational module consisting of an integrator circuit with a constant voltage input was used. The dc reference voltage was a simple circuit consisting of mercury cells in series with a 10-turn precision potentiometer and a voltage trim pot.

Voltammograms were recorded using the Moseley type 7035-A X-Y recorder.

### 3. Measurement Procedure

The dc reference voltage was set at the value of the open circuit voltage of the working electrode. The function generator was then set at the desired frequency with an output amplitude of 1 v peak-to-peak, causing the instrument to scan 0.5 volt anodic to 0.5 volt cathodic with respect to the open circuit potential. With the recorder at minimum sensitivity to prevent overloading, the instrument was switched to the cell just as the function generator voltage passed through zero. The cell was allowed to cycle at least 10 times at 200 mv/sec, during which time the current sensitivity was increased until the pattern covered a maximum area. During this time the pen was left in the "up" position. After 10 cycles had passed, the pen was switched to the "down"

position and a recording made, unless the voltammogram was still undergoing an obvious change, at which time further cycling was permitted prior to recording. Recordings were also made at 20 and 2 mv/sec respectively. The measurements were repeated at two other temperatures using a fresh electrode and fresh solution. A total of nine sweep curves were thus obtained for each system (three sweep rates and three temperatures, 30°, 40°, and 50°).

Measurements were made at three temperatures in the hope that the effect of temperature would be negligible so that triplication of data would be obtained. If temperature had an appreciable effect, this would serve as additional information, and triplication could then be obtained by repeating the measurements at a given temperature. When it later became apparent that too many systems showed a temperature effect, it was decided to screen the systems at a single temperature, 30° C.

Another procedural change was introduced at the same time, involving the range of voltage to be scanned. The original range of  $\pm 0.5$  volt relative to the zero reference, was based on the fact that if a system failed to exhibit an anodic or cathodic peak within 0.5 volt of the open-circuit voltage, then it would not be suitable for battery application, since extensive activation polarization would be indicated. Many sweep curves, however, failed to show a peak within this range, or indicated that the current rise was just approaching a peak, and would have done so if the voltage range had been only slightly extended. Since the occurrence of a peak would have permitted a more complete analysis, it was decided to scan 2.0 volts peak-to-peak, or  $\pm 1.0$  volt relative to the zero reference (open-circuit potential).

A third procedural change was to eliminate the very slow sweep (2 mv/sec). Although a number of systems showed excellent reproducibility at this slow sweep, many others gave erratic results owing to the much longer times required to complete a single cycle (over a half-hour), and therefore a longer duration for the electrode surface to change. The purpose of this program is to screen hundreds of electrochemical systems, and to study the more promising systems in more detail at a later date. In the interest of time, and because of the lack of reproducibility, the slow sweep rate was eliminated. The later sweep curves were therefore obtained at 400 and 40 mv/sec. (Since the function generator frequency was left unchanged, the sweep rates were doubled as a result of extending the voltage range from 1.0 to 2.0 volts peak-to-peak.)

Apart from a limited number of measurements on the oxides of silver, copper, and nickel, all sweep measurements were made with Ag, Cu, and Ni electrodes in the metal state. These metals were oxidized during the initial anodic sweep to some higher oxidation state involving reaction with the electroactive species in the electrolyte. The cathodic sweep then corresponds to the discharge of this electrolytically-formed cathode material. In some cases little or no anodic reaction occurred. By increasing both the Y-axis sensitivity of the recorder, and the resistance  $R_D$  in series with the working electrode, a pattern could be obtained. In a larger number of cases, however, the same results could be obtained in the absence of the solute, so that the resulting voltammogram represented only the background current of the solvent. In order to avoid this complication, a minimum threshold,  $0.1 \text{ ma/cm}^2$  per cm length measured along the Y-axis, was established. This figure was well-below the

unit divisional setting for the poorest systems containing an electroactive species, so there was no danger of eliminating any systems that might be of interest.

All cyclic voltammograms in this and subsequent reports are shown with the voltage scan in the clockwise direction, the voltage becoming more anodic to the right, and more cathodic to the left, so that the anodic reaction occurs above the X-axis (voltage axis), and the cathodic reaction below this axis. For the screening of cathodic materials, this corresponds to the charge reaction above the X-axis, and the discharge reaction below this axis. In subsequent screening of anodic materials, the anodic and cathodic reactions will be oriented as above, but these will now represent the discharge and charge reactions respectively.

## V. REFERENCES

1. Globe-Union Inc., Final Report, NASA Contract NAS3-2790  
NASA Report CR-54153, January 1965
2. Nicholson, R.S., Shain, I., Anal. Chem. 36, 706 (1964)
3. Nicholson, R.S., Shain, I., Ibid., 37, 178 (1965)
4. Polcyn, D.S., Shain, I., Ibid., 38, 370 (1966)
5. Nicholson, R.S., Ibid., 37, 1351 (1965)
6. Breiter, M.W., J. Electrochem. Soc., 109, 42 (1962)
7. Breiter, M.W., Gilman, S., Ibid., 109, 622 (1962)
8. Gilman, S., Breiter, M.W., Ibid., 109, 1099 (1962)
9. Breiter, M.W., Ibid., 110, 449 (1963)
10. Juliard, A.L., Shalit, H., Ibid., 110, 1002 (1963)
11. Buck, R.P., Griffith, L.R., Ibid., 109, 1005 (1962)
12. Mann, C.W., Anal. Chem., 36, 2424 (1964)
13. Rhodes, D.R., and Steigelmann, E.F., J. Electrochem. Soc.,  
112, 16 (1965)
14. Davis, D.G., and Orleron, D.J., Anal. Chem., 38, 179 (1966)
15. P. R. Mallory and Co., Inc., Third Quarterly Report,  
NASA Contract NAS3-6017, NASA Report CR-54732, Aug. 1965, p.8
16. Livingston Electronic Corp., Third Quarterly Report,  
NASA Contract NAS3-6004, NASA Report CR-54659, December 1964-  
March 1965, p. 30
17. P. R. Mallory and Co., Inc., Second Quarterly Report,  
NASA Contract NAS3-6017, NASA Report CR-54407, p. 28